August 2015

Oceanographic Controls on the Expression of Cretaceous Oceanic Anoxic Events in the Western Interior Sea

Christopher M. Lowery
University of Massachusetts Amherst

OCEANOGRAPHIC CONTROLS ON THE EXPRESSION OF LATE CRETACEOUS OCEANIC ANOXIC EVENTS IN THE US WESTERN INTERIOR SEA

A Dissertation Presented

by

CHRISTOPHER M. LOWERY

Submitted to the Graduate School of the
University of Massachusetts, Amherst in partial fulfillment
of the requirements for the degree of

DOCTOR OF PHILOSOPHY

May 2015

Geosciences

OCEANOGRAPHIC CONTROLS ON THE EXPRESSION OF CRETACEOUS OCEANIC ANOXIC EVENTS IN THE US WESTERN INTERIOR SEA

A Dissertation Presented

By

CHRISTOPHER M. LOWERY

Approved as to style and content by:

____
R. Mark Leckie, Chair

____
Robert DeConto, Member

____
Steven Petsch, Member

____
Justin Fermann, Outside Member

____
Steven Petsch, Graduate Program Director
Department of Geosciences

DEDICATION

To my patient and loving wife

ACKNOWLEDGEMENTS

I would like to thank my advisor, Mark Leckie, for his years of mentorship and support, and for the myriad of opportunities he has opened up for me. I would also like to extend thanks to the members of my committee – Rob DeConto, Steve Petsch, and Justin Fermann – for their guidance and support, and the many helpful suggestions they've provided throughout this project.

I am very grateful to BP and the American Chemical Society Petroleum Research Fund for their grants supporting this project, and for the smaller grants I received for travel and field work from the GCS-SEPM Ed Picou Fellowship, the Geological Society of America, The Cushman Foundation for Foraminiferal Research, Ocean Leadership, and the National Science Foundation.

Like all (hopefully) worthwhile scientific endeavors, this project involved a lot of collaboration, and I am especially grateful Matt Corbett, Andy Fraass, Amanda Parker, Zack Kita, and Allie Tessin for their friendship, assistance in the field, and fruitful discussions, as well as Art Donovan, Scott Staerker, Aris Pradmudio, Weiguo Li, Andrea Miceli Romero, David Watkins, Brad Sageman, for their assistance in the field, mentorship, and/or encouragement, as the case may be. Thanks as well to BP, Swift Energy, Encana Energy, the US Geologic Survey, Billy and Andrea Scott, and Billy Foster, for access to cores and outcrops.

Finally, I would like to thank my parents, Mike and Ruth, for, well, everything, and I am eternally grateful to my patient and loving wife, Lindsey, for her support and her help in the field.

ABSTRACT

OCEANOGRAPHIC CONTROLS ON THE EXPRESSION OF LATE CRETACEOUS OCEANIC ANOXIC EVENTS IN THE US WESTERN INTERIOR SEA

MAY 2015

CHRISTOPHER M. LOWERY, B.S., UNIVERSITY OF MARY WASHINGTON

M.S., UNIVERSITY OF MASSACHUSETTS, AMHERST

Ph.D., UNIVERSITY OF MASSACHUSETTS, AMHERST

Directed by: Prof. R. Mark Leckie

The Cretaceous Period (145-66 Ma) was a time of elevated global temperatures superimposed on fluctuating climate regimes and repeated biotic turnover. It recorded several major perturbations of the carbon cycle, characterized by widespread deposition of organic-rich black shale and benthic and photic zone dysoxia to euxinia, termed oceanic anoxic events (OAEs). The Cenomanian-Turonian OAE2 and the enigmatic Coniacian-Santonian OAE3 are well-preserved in the Western Interior Sea (WIS) of North America. The expression of these OAEs in the WIS differs both from each other and from contemporaneous open-ocean sections. Despite decades of research, questions remain about the role of oceanographic parameters (sea level, water mass source and character, terrestrial runoff, stratification, productivity, circulation) on the development of organic-rich shales and anoxic to dysoxic conditions in the WIS. This study utilizes foraminiferal paleoecology and bulk rock geochemical data to address the question "How did oceanographic changes effect the development of OAEs in the Western Interior?"

A transect of sites in Texas is used to understand the connection between the well-studied OAE2 interval of the WIS (Greenhorn Formation) and the open ocean, which appears to have been controlled by a sill at the SE aperture of the WIS that was overcome by rising sea level in the late Cenomanian, ventilating the sea. The poorly understood development of OAE3 in the central Western Interior is studied in the Niobrara Formation in Colorado, Kansas, and New Mexico and equivalent rocks further west. Foraminiferal trends through this interval show a slow increase in dysoxia prior to the "onset" of OAE3 recorded by other proxies. Above this level, benthic foraminifera disappear and a stressed planktic assemblage remains unchanged for ~3 million years. This suggests a threshold for anoxia that, once exceeded, pushed the WIS into a new equilibrium. Sea level change is the principle control on the redox state of the sea: transgressions are associated with improving oxygenation due to increasing ventilation, and regressions are associated with deteriorating oxygenation and the deposition of organic carbon due to greater stratification. Though anoxic, OAE3 is not an event and should not be regarded as such.

CONTENTS

Page

ACKNOWLEDGEMENTS v

ABSTRACT vi

LIST OF FIGURES xi

INTRODUCTION 1

CHAPTER

I: THE EXPRESSION OF OAE2 IN TEXAS 16

1.1 Abstract 16

1.2 Introduction 18

1.3 Geologic Setting 20

1.3.1 Stratigraphy and Micropaleontology of the Western Interior Sea 20

1.3.2 Stratigraphy and Micropaleontology of Texas 25

1.3.3 Sequence Stratigraphy 27

1.4 Locations and methods 30

1.4.1 Study Sites 30

1.4.1.1 Lozier Canyon 30

1.4.1.2 Bouldin Creek 32

1.4.1.3 Fasken Core 35

1.4.2 Foraminiferal Methods 36

1.4.3 Calcareous Nannofossil Methods 37

1.4.4 Geochemistry Methods 37

1.5 Results 38

1.5.1 Geochemistry 38

1.5.1.1 Stable Isotopes 38

1.5.1.2 TOC 41

1.5.2 Foraminifera 44

1.5.2.1 Planktic Foraminifera 44

1.5.2.2 Benthic Foraminifera 51

1.5.3 Calcareous Nannofossils 53

1.6 Discussion..55
1.6.1 Affinity with the Western Interior and Oceanographic Front..................................55
1.6.2 TOC Trends, Oxygenation, and Productivity 57
1.6.3 Sea Level Variablity/Sequence Stratigraphy 63
1.7 Conclusions..66
II: REDOX CHANGES ASSOCIATED WITH OAE3 IN COLORADO AND KANSAS..........68
2.1 Abstract..68
2.2 Introduction..69
2.3 Locations..71
2.3.1 Portland Core 72
2.3.2 Aristocrat Angus Core 72
2.3.3 Kansas Outcrops 74
2.4 Methods 74
2.5 Results..75
2.5.1 Aristocrat Angus Core 75
2.5.2 Portland Core 75
2.5.3 Kansas Outcrops 77
2.6 Discussion..78
2.7 Conclusions..81
III: PALEOCEANOGRAPHIC CONTROLS ON THE DEVELOPMENT OF ANOXIA IN THE NIOBRARA SEA 83
3.1 Abstract..83
3.2 Introduction..85
3.3 Background..89
3.3.1 Tectonics..89
3.3.2 Sea Level and Lithology 91
3.3.3 Climate and Circulation 93
3.3.4 Niobrara Cycle...96
3.3.5 Oceanic Anoxic Event 3 100
3.4 Location and Methods..102

3.4.1 Central and Eastern Sea 102
3.4.1.1 Portland Core 102
3.4.1.2 Bounds Core 104
3.4.1.3 Kansas Outcrops 105
3.4.2 Western Sea 105
3.4.2.1 Mesa Verde, CO 105
3.4.2.2 Vermillion Creek, CO 106
3.4.2.3 Elk Creek, CO 107
3.4.3 Northern Sea 107
3.4.3.1 Centennial Valley, WY 107
3.4.4 Southern Sea 109
3.4.4.1 Wagon Mound, NM 109
3.4.4.2 Lozier Canyon, TX 110
3.5 Discussion/Interpretation 111
3.5.1 Central and Eastern Sea 111
3.5.2 Western Sea 121
3.5.3 Northern Sea 126
3.5.4 Southern Sea 128
3.6 Discussion/Interpretation 131
3.6.1 Middle Turonian *(Prionocyclus macombi to Scaphites whitfieldi)* 131
3.6.2 Upper Turonian *(Scaphites nigricollensis to Scaphites mariasensis)* 132
3.6.3 Lower Coniacian *(Scaphites preventricosus)* 133
3.6.4 Middle Coniacian (*Scaphites ventricosus*) 134
3.6.5 Upper Coniacian (*Scaphites depressus*) 138
3.6.6 Lower Santonian – lower Campanian (*Clioscaphites vermiformis – S. leei III* 138
3.6.7 Lower Campanian (*Scaphites hippocreppis I-III*) 140
3.6.8 Role of Sea Level 140
3.7 Conclusions 141
CONCLUSION 146
WORKS CITED 151

LIST OF FIGURES

Figure Page

I.1 Maximum extent of the Western Interior Seaway, which was during the middle Turonian highstand of the Greenhorn cycle, in the *Colignoceras woollgari* ammonite zone (Blakey, 2015) 2

I.2 West-east cross section of the Western Interior Seaway 4

I.3 Major sea level cycles of the Western Interior Sea. Also plotted are general global temperature trends, seafloor spreading rates, stratigraphic density of ash layers in the Western Interior, and major thrusting events 4

I.4 Expected distribution of planktic and benthic groups for various redox regimes 8

1.1 Map of Texas showing modern Eagle Ford outcrop belt (light gray), extent of the Comanche Platform, relevant paleobathymetric features, and location of study sites (stars) 21

1.2 Photograph of Lozier Canyon locality 28

1.3 Chronostratigraphic correlation between south Texas and the Cenomanian-Turonian GSSP in Pueblo, Colorado 34

1.4 Comparison of bulk carbonate (black line) and organic (gray line) carbon isotope values during OAE2 from Eastbourne, England (carbonates: Paul et al., 1999; organics: Gale et al., 2005), the C-T GSSP at Rock Canyon, CO (carbonates: Caron et al., 2006; organics: Pratt and Threlkeld, 1984), Lozier Canyon, TX (this study) and the Fasken Core in Webb CO, TX (this study) 39

1.5 Geochemical and foraminiferal assemblage data from the Lozier Canyon outcrop in Terrell Co., TX 42

1.6 Geochemical and foraminiferal assemblage data from the Bouldin Creek outcrop in Travis Co., TX 45

1.7 Geochemical and foraminiferal assemblage data from Swift Energy's Fasken A #1H core in Webb Co., TX 47

1.8 Nannoplankton assemblage data from the Lozier Canyon outcrops in Terrell County (A), ACC #1 Core in Travis County, 11 miles SE of the Bouldin Creek outcrop (B), and from the Fasken A #1H Core in Webb County (C) 54

1.9 Benthic foraminifera abundance vs. TOC cross plots for Lozier Canyon (A) and Bouldin Creek (B) 60

2.1 Location map and geochemical and benthic foraminiferal data for the Aristorcrat Angus Core 73

2.2 TOC and foraminiferal abundance data for USGS Portland #1 Core and foraminiferal abundance data for Kansas outcrop composite section 76

3.1 Location Map showing the early Coniacian maximum transgression of the Niobrara Sea.. 90

3.2 West-to-east summary of stratigraphy, sea level change, and biostratigraphy during the Greenhorn and Niobrara Cycles 92

3.3 Stratigraphic correlations between main study sites 97

3.4 Stratigraphic column for idealized Front Range Composite Section, based of description of Pueblo outcrops by Scott and Cobban, 1964 103

3.5 Summary of %Benthic foraminifera (vs. total foraminifera), %Biserial planktic foraminifera (vs. total planktics) and the simple diversity of keeled planktic foraminifera from the USGS #1 Portland Core 112

3.6 Summary of foraminiferal assemblages and geochemical trends for the Amoco Rebecca Bounds #1 Core 114

3.7a Location map showing position of outcrops used to construct composite Section.. 115

3.7b. Summary of %Benthic foraminifera (vs. total foraminifera), %Biserial planktic foraminifera (vs. total planktics) and the simple diversity of keeled planktic foraminifera from the Kansas outcrop composite section 116

3.8 Major and trace element data from the Coquina Oil Berthoud State #4 Core, replotted from Dean and Arthur (1998b) 119

3.9 Summary of foraminiferal assemblages (Sterzinar, 2005) and clay mineralogy (Hayden Scott, 1992) at Mesa Verde 122

3.10 Summary of benthic foraminiferal abundance and the ranges of key species at Vermillion Creek, CO, after Kent (1968) 124

3.11 Summary of benthic foraminiferal abundance and the ranges of key species at Elk Creek, CO, after Kent (1968) 125

3.12 Summary of foraminiferal trends at Centennial Valley, WY, after Frerichs et al. (1975) and Frerichs, (1979) 127

3.13 Summary of foraminiferal trends at Wagon Mound, NM 129

3.14 Cross plots of benthic and biserial foraminifera abundances against TOC and %$CaCO_3$ 137

3.15 Diagram showing the effect of sea level on circulation in the WIS 142

3.15 Simplified relationship between sea level and oxygen in the WIS 143

INTRODUCTION

The Cretaceous Period (145-66 Ma) was a time of elevated global temperatures superimposed on fluctuating climate regimes and repeated biotic turnover. It recorded large swings in atmospheric carbon dioxide concentrations and global temperatures; the climatic and biotic response to these events have the potential to provide an illuminating analog for future climate change. Global perturbations of the carbon cycle, characterized by widespread deposition of organic-rich black shale, benthic and photic zone dysoxia to euxinia, and positive excursions in carbon isotopes, occurred intermittently throughout the Cretaceous (Schlanger and Jenkyns, 1976). The last two of these Oceanic Anoxic Events (OAEs), the Cenomanian-Turonian OAE2 (~94-93 Ma) and the Coniacian-Santonian OAE3 (~89-85 Ma), are well-preserved in the Western Interior Sea (WIS) of North America (Figure 1). A myriad of causal mechanisms, usually invoking some combination of global warming, enhanced primary productivity, and increased nutrient flux, have been proposed for these events and, as van Helmond et al. (2015) succinctly put it, "disentangling these factors on a regional scale has remained problematic." The Western Interior Sea (WIS) of North America was a relatively shallow, restricted sea that connected the Gulf of Mexico/western Tethys and Canadian Arctic, over 3000 miles (4800 km) north to south; at its widest, it ranged over 1000 miles (1600 km) from western Utah to central Minnesota (Kauffman, 1984). The purpose of this dissertation is to disentangle the regional factors leading to enhanced carbon burial in the WIS, in order to better understand how these global events are filtered through local climatic, oceanographic, and tectonic controls, what remains of the primary, "global" signal, and what this tells us about the evolution of Cretaceous climate.

Figure I.1. Maximum extent of the Western Interior Seaway, which was during the middle Turonian highstand of the Greenhorn cycle, in the *Colignoceras woollgari* ammonite zone (Blakey, 2015).

I. 1 The Cretaceous Western Interior Sea

The development of the Western Interior Basin was tectonically controlled. Accommodation was created through a combination of thrust-induced subsidence, which caused the formation of a narrow foreland basin along the western margin adjacent to the Sevier Highlands (e.g., Armstrong, 1968; Schwartz and DeCelles, 1988), and more broadly through drag-induced subsidence driven by the subduction of the Farallon Plate beneath North America (Pang and Nummendal, 1995; Liu and Nummendal, 2004; Liu et al., 2005, 2008, 2011, 2014). Periods of high sea level in the WIS are tied to increased volcanic activity in the thrust zone (Kauffman, 1985), suggesting a tectonic driver for local sea level or accommodation change. However, overall high rates of seafloor spreading and subduction in the Cretaceous drove global sea level variations (e.g., Larson, 1991) and sea level cycles in the WIS are generally synchronous with eustatic sea level changes (Hancock and Kauffman, 1979), making it difficult to separate a local tectonic driver from the global one. The tectonically active western margin of the WIS was contrasted by a stable eastern "hinge" zone connected to the North American Craton, creating an asymmetric basin profile (Figure 2). Thrusting induced subsidence resulted in the largest accommodation in the sea in the western foreland basin, which, along with proximity to the Sevier Highlands, lead to the thickest accumulation of sediments in this area (Kauffman, 1984). Meanwhile, mantle-flow induced subsidence of the Farallon Plate in the middle of the basin resulted in the deepest water depths in a central axis that runs roughly parallel to the modern Colorado Front Range (Sageman and Arthur, 1994). Hemi-pelagic carbonate sedimentation occurred in the central axis of the sea during sea level highstands.

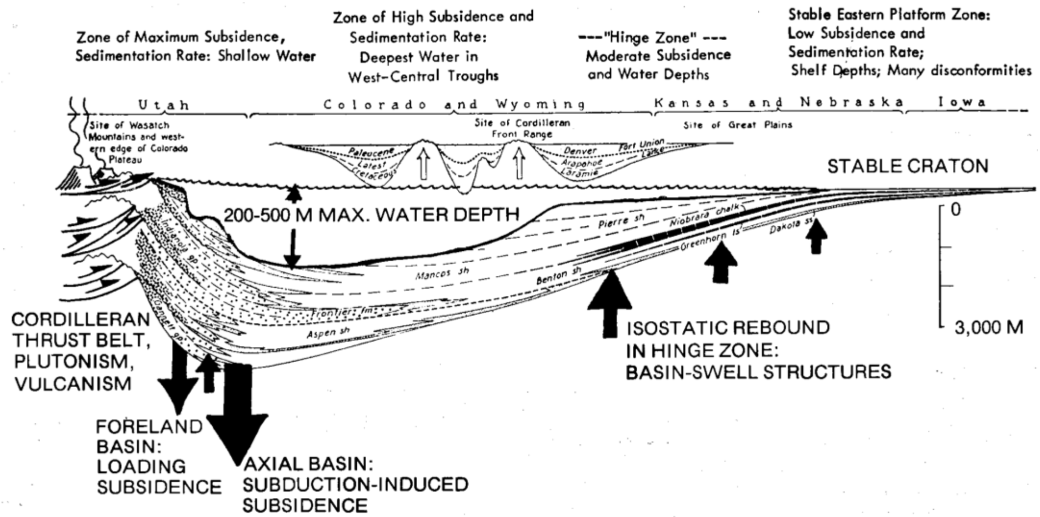

Figure I.2. West-east cross section of the Western Interior Seaway. Maximum water depths were probably <200 m. From Kuaffman (1984).

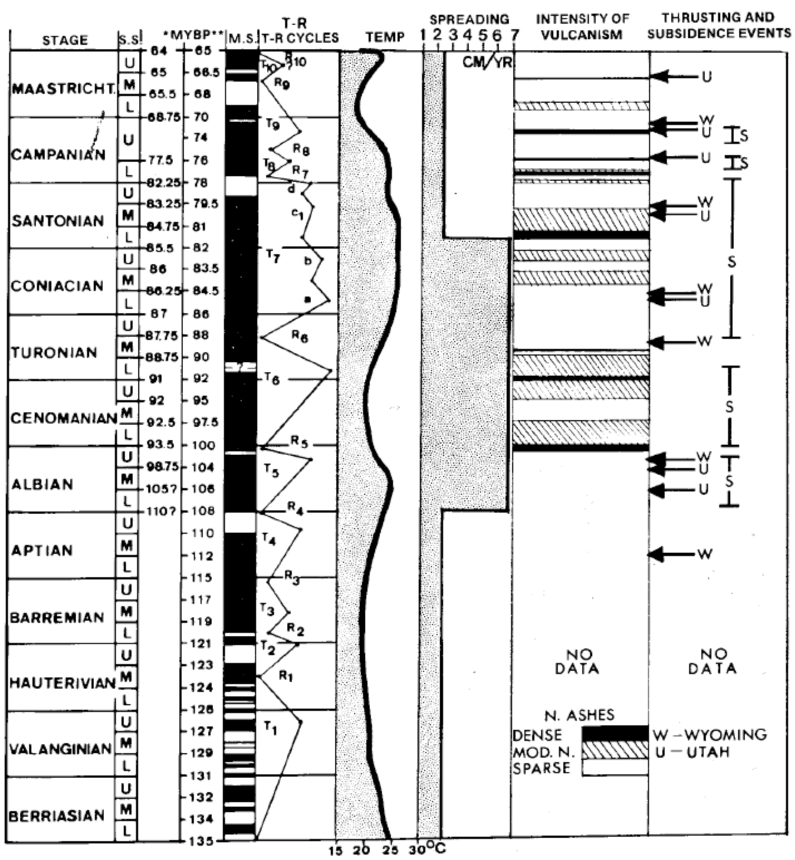

Figure I.3. Major sea level cycles of the Western Interior Sea. Also plotted are general global temperature trends, seafloor spreading rates, stratigraphic density of ash layers in the Western Interior, and major thrusting events. T6 is the Cenomanian-Turonian Greenhorn Cycle; T7 is the Turonian-Campanian Niobrara Cycle. From Kauffman, 1984.

The WIS was flooded for approximately 38 million years, during which time five 3rd-order sea level cycles are recognized (Figure 3; Kauffman, 1984). The two largest, the Cenomanian-Turonian Greenhorn Cycle and the Turonian-Campanian Niobrara Cycle, record the last two OAEs of the Cretaceous.

OAE development and expression in the WIS differs from the open ocean and marginal basins. OAE2 was characterized by water column anoxia and widespread deposition of black shales in many places around the world, but fossils and geochemical data in the WIS suggest improving conditions, with increasing oxygen and decreasing organic matter preservation at the onset of the event. In contrast, data from OAE3 in the WIS suggest sustained anoxia and organic matter preservation at a time when large swaths of the global ocean were becoming increasingly oxygenated. Despite decades of research in this region, questions remain about the role of oceanographic parameters (e.g., sea level, water mass, terrestrial runoff, stratification, productivity, circulation) on the development (or not) of organic-rich shales and anoxic to dysoxic conditions in the WIS.

This dissertation aims to address the broad question "How did oceanographic changes effect the development of OAEs in the Western Interior?" by utilizing foraminiferal assemblage and biostratigraphic data, in conjunction with geochemical proxies, to understand the nature of dissolved oxygen, water depth, and water mass changes prior to and during OAE2 and OAE3 in the WIS. Foraminifera are powerful paleoceanographic proxies that yield a variety of important data, including a primary biostratigraphic framework, surface ocean and seafloor paleoenvironmental parameters from the variations in the population of environmentally sensitive species and groups, and geochemical data from their calcium carbonate tests. Unfortunately, post-burial

diagenesis is common due to high heat and pressure in many Western Interior formations, and is often exacerbated by alteration by meteoric water in many outcrops, completely obscuring any primary species-specific geochemical signal that might be recovered from foraminifera. For this reason, basic bulk-rock geochemical analyses supplement the paleoecological data developed from foraminiferal populations.

I. 2 Planktic and Benthic Foraminiferal Proxies of Paleoenvironment

Foraminiferal populations respond to a number of environmental pressures, including water depth, food supply, dissolved oxygen, salinity, and pH, and are often used as environmental proxies in the WIS (e.g., Eicher and Worstell, 1970; Eicher and Diner, 1985; Leckie, 1985; Leckie et al., 1991, 1998; West et al., 1998; DaGama et al., 2014; Elderbak et al., 2014; Lowery et al., 2014). Careful analysis of foraminiferal data can deconvolve these often overlapping signals to understand their relative contributions to the paleoceanography of the environment of deposition. At the most basic level, foraminifera can be divided into two major groups: planktic foraminfera, which live suspended in the water column, and benthic foraminifera, which live on or in the uppermost centimeters of seafloor. The ratio of planktic to benthic foraminifera ("P:B ratio," herein reported as %benthics), is a commonly used measure of foraminiferal populations. In open shelf environments, the P:B ratio is strongly correlated to water depth, with a decreasing percentage of benthics in the offshore direction (Murray, 1976; Culver, 1988; Gibson, 1989; Hayward, 1990; Van der Zwaan et al., 1990; Leckie and Olson, 2003). However, the abundance of benthic foraminifera is strongly controlled by food supply and available oxygen; water depth moderates these parameters as well as the diluting flux of planktic foraminifera to the seafloor (Jorissen, 1996; 2007). In

environments prone to anoxia, like the WIS, P:B (%benthics) can be used as a proxy for bottom water oxygenation (e.g., Van Hinsbergen et al., 2005). Benthic foraminifera fill different ecological niches, with some living on or attached slightly above the seafloor (epifaunal) and others living below the sediment water interface (infaunal). Infaunal benthics in the Cretaceous are generally assumed to be low-oxygen tolerant, an adaptation that would allow them to colonize dysoxic intervals below the sediment-water interface (e.g., Leckie et al., 1998). Planktic foraminifera can also be broadly divided into morphogroups: keeled planktic foraminifera, so named for their raised, imperforate equatorial regions, tend to live deeper in the seasonal thermocline (e.g., Ando et al., 2010), and their absence may indicate the lack of suitable habitat, whether because of shallow water depth, well-mixed upper water column, or an impinging oxygen minimum zone. Among mixed-layer dwelling planktics, the Cretaceous biserial planktics are particularly ecologically sensitive. Or, perhaps more accurately, they are hardly sensitive at all, being commonly characterized as an opportunistic group that thrives in stressed conditions, particularly non-normal marine environments (brackish or hypersaline; e.g., Leckie et al., 1998). Changes in the abundance of biserial taxa suggests environmental changes in the upper water column. Figure 4 contains a broad summary of foraminiferal life positions and ecological trends related to changing redox conditions; taxon-specific responses to different parameters are discussed in detail where appropriate in subsequent chapters.

I.3 The Eagle Ford Shale and OAE2

The Cenomanian-Turonian OAE2 was a global event that corresponded to widespread burial of organic matter (expressed as black shales) and localized bottom

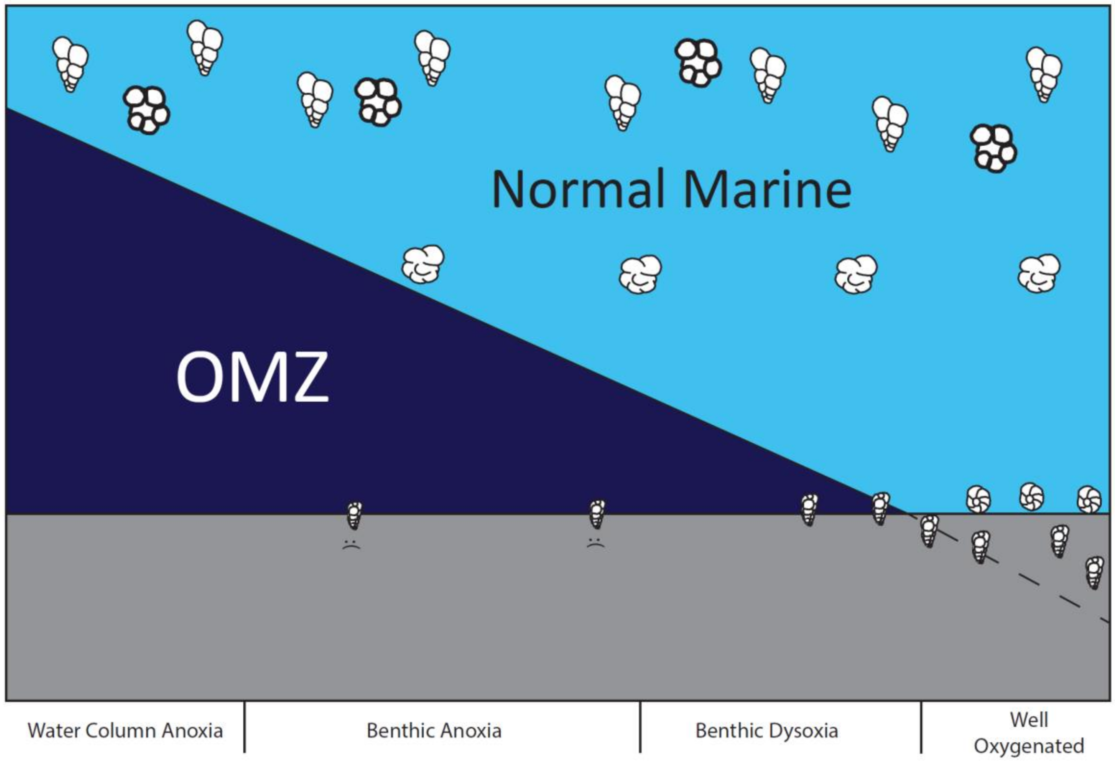

Figure I.4. Expected distribution of planktic and benthic groups for various redox regimes. In well oxygenated conditions, and with all other parameters being equal, benthic foraminifera can be expected to be relatively common and diverse. Benthic anoxia can be expected to cause the disappearance of all or nearly all benthic taxa, with infaunal taxa being the most adaptable to low oxygen conditions, while anoxia in the middle water depths (e.g., an oxygen minimum zone, OMZ) would cause the disappearance of keeled planktic foraminifera.

water and photic zone dysoxia or anoxia (Schlanger and Jenkyns, 1976; Jenkyns, 1980; Arthur et al., 1990; Jenkyns, 2010; Owens et al., 2012), tied to a positive 2‰ excursion in carbon isotopes caused by the enhanced burial of isotopically light organic carbon (Scholle and Arthur, 1980; Pratt and Threlkeld, 1984; Jarvis et al., 2006, 2011; Sageman et al., 2006; Gale et al., 2008; Barclay et al., 2010). Globally, OAE2 was caused by increased productivity driven by a rapid influx of micronutrients, likely from seafloor hydrothermal activity related to the emplacement of the Caribbean Large Igneous Province, increased rates of ocean crust production, or increased volcanic CO_2 emissions resulting in global warming and a strengthening of the hydrologic cycle (Leckie et al., 2002; Snow et al., 2005; Barclay et al., 2010; Jenkyns, 2010; van Bentum et al., 2012; Monteiro et al., 2012).

Productivity and enhanced carbon burial associated with this nutrient increase were widespread but not global. In the Western Interior Sea, the onset of OAE2 (based on carbon isotope enrichment) is associated with a transition from dark-gray, organic rich shale to light-gray shale interbedded with limestone (e.g., Kauffman, 1984), a decrease in total organic carbon (e.g., Pratt, 1985), and an increase in planktic and benthic foraminiferal abundance and diversity (Eicher and Worstell, 1970; Eicher and Diner, 1985; Leckie, 1985) suggesting a local increase in oxygen at a time when large areas of the open ocean were experiencing anoxia (e.g., Jenkyns, 2010).

Multiple incursions of warm, normal-marine waters from the Tethys made their way into the WIS during its history, coinciding with eustatic transgressions. The largest of these, the transgression of the 3rd-order Greenhorn Cycle, coincides with the onset of OAE2 and a coeval increase in marine macrofossil and microfossil diversity (e.g., Eicher

and Worstell, 1970; Cobban and Scott, 1972; Frush and Eicher, 1975; Kauffman, 1984; Eicher and Diner, 1985; Elder, 1985, 1989; Watkins, 1985; Bralower, 1988; Leckie et al., 1998; Elderbak et al., 2014; Lowery et al., 2014). This correlation suggests that a sill at the southern aperture of the WIS isolated the sea during low sea level, causing stagnation and organic matter preservation (e.g., Arthur and Sageman, 2005). If this is the mechanism causing the WIS to behave differently than the global ocean during OAE2, there should be evidence of a clear transition between the WIS and the Tethys across the southern aperture of the sea.

The Eagle Ford Shale of Texas (Figure 1), a calcareous shale draped over the Aptian-Albian reef buildups that comprise the Comanche Platform of central Texas, is equivalent to the Greenhorn Limestone of the WIS and contains OAE2 (e.g., Donovan et al., 2012). Geologists were working on the Eagle Ford of west Texas, where it crops out along road cuts and stream embankments, as early as 1907 (Udden), although Hazzard (1959) was the first to describe it in detail. The recent boom in drilling activity in the Eagle Ford unconventional gas play in south and east Texas has driven an increase in petroleum-oriented research of the west Texas outcrops (e.g., Donovan and Staerker, 2010; Hentz and Ruppel, 2010; Lock et al., 2010; Donovan et al., 2012; Eldrett et al., 2014), but most micropaleontological work is decades old.

Chapter 1 attempts to geographically locate the transition between the Western Interior Sea and the Tethys by quantifying organic matter content (total organic carbon), bottom water and water column oxygenation (as defined by benthic and planktic foraminiferal assemblages), and water mass changes (as defined by planktic foraminifera) before and during OAE2 (as defined by carbon isotopes) along a transect of sites in

central and southern Texas. These include Lozier Canyon in Terrell Co., TX, on the western part of the Comanche Platform; Bouldin Creek, in Travis Co., TX, adjacent to a structural high called the San Marcos Arch; and Swift Energy Company's Fasken A #1H Core, off the southeastern edge of the Comanche Platform on the Rio Grande Submarine Plateau, a deeper water site between two Early Cretaceous reef margins. This transect will test the hypothesis that the edge of Western Interior affinity waters is on the edge of the Comanche Platform. If this sill marks the edge of the Western Interior sea, it suggests that sill depth, and therefore sea level, plays an important role in controlling the paleoceanography of the WIS.

I.4 The Niobrara Formation and OAE3

If it is true that sill depth was an important control on the paleoceanography of the Western Interior Sea during OAE2, then it is likely that sea level was also an important forcing function during the subsequent OAE3 when organic carbon burial in the WIS was focused during a period of general regression in the sea. OAE3 was more geographically restricted (e.g., Wagerich, 2009) and is marked by a smaller carbon isotope excursion (e.g., Jarvis et al., 2006) than OAE2, although it is also associated with increased carbonate burial, which would shift carbon isotope curves in a negative direction and therefore may mask the "true" excursion (e.g., Locklair et al., 2011). Within the WIS, OAE3 represents a period of organic carbon burial, and apparent anoxia (e.g., Locklair et al., 2011), while OAE2, regionally, begins with relatively little organic carbon burial and displays peak burial after OAE2 (e.g., Pratt et al., 1993; Sageman et al., 1997, 1998, 2006).

Though not as exhaustively studied as the Greenhorn, multiple facets of the Turonian-Santonian Niobrara Formation have been investigated, including stratigraphy and molluscan biostratigraphy (e.g., Scott and Cobban, 1964; Hattin, 1982; Walaszczyk and Cobban, 1998; Walaszczyk and Cobban, 2007), organic carbon deposition (e.g., Pratt et al., 1993; Locklair et al., 2011), orbital cyclicity (e.g., Gilbert, 1895; Hattin, 1982; Locklair and Sageman, 2008; Sageman et al., 2014), and nannofossil biostratigraphy and paleoecology (Watkins et al., 1993). A number of foraminiferal studies have provided some basic insights into the variable nature of the Niobrara depositional environment, including the influences of low oxygen conditions, relative sea level change, and tectonics in the Western Interior foreland basin (Kent, 1967, 1968; Frerichs et al., 1975, 1977; Frerichs and Dring, 1981; McNeil and Caldwell, 1981; Fisher et al., 1985; Caldwell et al., 1993; Martinson et al., 1998; Schröder-Adams et al., 2001; Sikora et al., 2004; Da Gama et al., 2014). However, there have been very few detailed studies of Niobrara foraminiferal assemblages as paleoenvironmental proxies, and all are geographically limited in scope. It is still unclear, from the established literature, whether parts or all of the WIS experienced dysoxic to anoxic conditions during OAE3 (with redox-sensitive trace metal data from the central axis of the sea, Locklair et al., 2011 only venture that the WIS "appears to record…elevated concentrations of geochemical proxies for anoxia"), whether the planktic community was affected, and what role geography, bathymetry, and circulation may have played in these changes.

Chapter 2 will focus on whether or not there is foraminiferal evidence for dysoxia/anoxia during OAE3 in the WIS. To address these questions, the study area is focused on the central axis of the sea, anchored by two cores in the Colorado Front

Range: ~75 samples from the USGS Portland #1 core in Fremont (which only contains the lower half of the Niobrara Fm.), and ~50 samples from the Encana Energy Aristrocrat-Angus Core in the Denver Basin. Both of these cores have been the focus of intensive geochemical and cyclostratigraphic study (e.g., Locklair and Sageman, 2008; Locklair et al., 2011) that allow correlation to a robust existing dataset. To augment these Front Range cores, this study also incorporates a composite outcrop section, with ~200 samples from western Kansas along the Smoky Hill River in a series of outcrops described by Hattin (1982).

I.5 Comparison of OAE2 and OAE3 in the Western Interior Sea

Building on the investigation of the presence or absence of anoxia during OAE3 in the Western Interior, Chapter 3 attempts to understand the paleoceanographic mechanisms that allow for the development of anoxia during OAE3 but not OAE2. Is there a common mechanism that controls oxygenation and organic matter deposition in the WIS during OAEs? Answering this question will improve understanding of the underlying forcings of Cretaceous anoxic events, North American climate during the Cretaceous, and the mechanisms controlling oxygenation in restricted seas in both ancient and modern environments. This third chapter attempts to synthesize the new data presented above with the balance of published data on the WIS in an attempt to answer that question.

Circulation in the WIS has been a topic of scientific investigation for decades (e.g., Hay, 1993; Jewell, 1993; Fisher, 1995). The authoritative work to which everyone compares is that of Slingerland (1996), who proposed an estuarine circulation model for the WIS, with a cyclonic gyre in the center of the sea driven by warm Tethyan water

moving north along the eastern margin and cool boreal water moving south along the western margin. Leckie et al. (1998) suggested a modification to this model, arguing that a bathymetric high created by a forebulge of the Sevier highlands (see Kaufmann, 1984) would have caused bathymetrically-induced upwelling. Similarly, the relative importance of freshwater runoff and associated terrigenous clays in water-column stratification and lithology has been debated.

The hemi-pelagic limestones of the Bridge Creek and Niobrara Formations are well known for displaying cyclic patterns of sedimentation, which was recognized as far back as 1895 by G.K. Gilbert, who attributed them to orbitally-driven changes in insolation, a hypothesis that was greatly expanded upon by Fischer (1980), Fischer et al. (1985) and Fischer and Bottjer (1991). More recent orbital tuning by Locklair and Sageman (2008) found that the variation between limestone and marl in the Ft. Hays Limestone and Smoky Hill Shale members of the Niobrara Formation averages 1.7 myr; this does not fit the expected 2.3 myr long eccentricity cycle, although the authors note that this frequency has been observed in other Cretaceous records and may be orbitally-driven. The mechanism through which orbital cyclicity may have driven sedimentation changes is unclear, and revolves around wet/dry climate cycles and the relative contributions of detrital sediments and carbonate productivity. Increased precipitation may have resulted in increased terrigenous flux to the sea, resulting in dilution of carbonates and increased stratification of the water column. Conversely, this same increased precipitation (and increased freshwater input) may have strengthened circulation in the sea, preventing clay particles from reaching the center of the gyre and perhaps increasing carbonate productivity as well (Slingerland et al., 1996). Of course, as

Locklair and Sageman note, these ~1.7 myr cycles may not be orbitally driven at all, but rather driven by tectonic processes changing rates of subduction and thrusting, changing relative sea level within the sea (Dean and Arthur, 1998).

As discussed above, foraminiferal assemblages provide a wealth of information on various oceanographic parameters, and are useful tracers of water mass changes; Chapter 2 will show that they are also excellent indicators of anoxia during deposition of the Niobrara Formation. Mapping the geographic and temporal changes in the distribution of foraminifera from east to west and south to north across the WIS should allow the determination of the distribution and timing of anoxia and its relationship to water mass, sediment flux, and sea level changes. Chapter 3 will utilize the data developed from the Portland Core, Angus Core, and Kansas outcrops along with new data from an outcrop in Wagon Mound, NM, and from the Austin Chalk exposed along Hwy 90 near Lozier Canyon, TX, as well as a wealth of existing datasets in published papers and unpublished masters theses.

Understanding the underlying mechanisms that lead to the development of anoxia during OAE3 in the Western Interior Sea should also help understand why anoxia was delayed during the more globally severe OAE2. The discovery of these mechanisms in the WIS will enhance our understanding of the development of anoxia in shallow, restricted seas and in general.

CHAPTER I

THE EXPRESSION OF OAE2 IN TEXAS

1.1 Abstract

The Upper Cretaceous of central Texas is dominated by a broad, shallow carbonate platform called the Comanche Platform that occupies an important gateway between the epeiric Western Interior Sea (WIS) of North America to the open-marine Gulf of Mexico/Tethys. We investigated the Cenomanian-Turonian Eagle Ford Shale on and adjacent to the Comanche Platform to determine whether the Eagle Ford Shale has an affinity with the Western Interior, and if so, determine where the transition from Western Interior to open ocean is located. We were also interested in the relationship, if any, between the organic-rich facies of the Eagle Ford and Oceanic Anoxic Event 2 (OAE2). Our work is based on quantitative foraminiferal population counts and associated sedimentary particles (including inoceramid prisms, sand, glauconite, and pyrite grains), calcareous nannofossil assemblages, carbon isotopes, and total organic carbon (TOC) from three sites across a range of paleo water depths: an outcrop in Lozier Canyon in Terrell County, west of Langtry, TX, an outcrop at Bouldin Creek outside of Austin, TX, and Swift Energy's Fasken A #1H core in Webb County, TX.

The highest TOC in the Eagle Ford occurs before the onset of OAE2 (6% at Lozier Canyon, 7% at both Bouldin Creek and the Fasken Core) and then declines steadily through the rest of the section (except for a small increase at the end of OAE2 at Lozier and a fairly large post-OAE2 increase at Bouldin Creek). Nannofossil paleoproductivity indicators (%*Zeugrhabdotus* and %*Biscutum*) track TOC at Bouldin Creek and in the Fasken Core and display similar trends to those observed in the Western

Interior Sea to the north. Benthic foraminiferal abundances increase as TOC decreases and the lithology shifts from laminated black shale to bioturbated light gray shale; low-oxygen-tolerant infaunal *Neobulimina* spp. appear first and gradually increase in abundance; epifaunal benthics appear soon after. This oxygenation trend continues through the OAE2 interval and the upper Eagle Ford contains a diverse epi- and infaunal benthic foraminiferal assemblage and macrofossil assemblage. This trend of decreasing TOC and nannofossil paleoproductivity indicators coupled with increasing benthic foraminiferal abundance and diversity (and seafloor oxygenation) corresponds to rising sea level.

Based on foraminiferal and nannofossil events, TOC trends, and changes in lithology, both platform sites have a strong affinity with the Western Interior, with Lozier Canyon being the most similar; the Fasken Core bears all the characteristics of an open ocean site, except for the fact that peak TOC occurs before OAE2. This suggests that the oceanographic boundary between WIS and Tethys can be placed on the edge of the Comanche Platform.

Productivity was likely driven by bathymetry-induced upwelling caused by restriction between the WIS and Tethys during times of low sea level; as sea level rose, upwelling diminished and productivity decreased. This explains why the Fasken Core, adjacent to the platform margin and in the center of this upwelling zone, displays the same TOC trends as the platform sites. Organic carbon content in the sea was controlled by stratification and enhanced preservation, but this was also reduced by rising sea level, which is why the two areas show parallel trends.

1.2 Introduction

The Cenomanian and Turonian Stages of the Cretaceous (~100-90 Ma) were a time of elevated tectonic activity, global warmth, high sea level, biotic turnover, and burial of vast amounts of organic carbon in the deep-sea, along continental margins, and in epicontinental seas (e.g., Schlanger and Jenkyns, 1976; Kauffman, 1977a; Scholle and Arthur, 1980 Arthur et al., 1987; Schlanger et al., 1987; Voigt, 2000; Leckie et al., 2002; Arthur and Sageman, 2005; Jenkyns, 2010; Friedrich et al., 2012).

Changes in biota across the Cenomanian-Turonian boundary are linked to environmental perturbations associated with Oceanic Anoxic Event 2 (OAE2), which caused the evolutionary turnover of, among other things, molluscs (Elder, 1985, 1991), calcareous nannofossils (e.g., Bralower, 1988; Erba, 2004), radiolarians (Erbacher et al., 1996; Erbacher and Thurow, 1997), and benthic and planktic foraminifera (e.g., Leckie, 1985; Kaiho and Hasegawa, 1994; Premoli Silva and Sliter, 1999; Leckie et al., 2002). OAE2 was a global event that corresponded to widespread burial of organic matter (expressed as black shales) and localized bottom water and photic zone dysoxia or anoxia (e.g., Schlanger and Jenkyns, 1976; Jenkyns, 1980; Arthur et al., 1990; Jenkyns, 2010; Owens et al., 2012), tied to a positive 2‰ excursion in carbon isotopes caused by the enhanced burial of isotopically light organic carbon (e.g., Scholle and Arthur, 1980; Pratt and Threkeld, 1984; Arthur et al., 1987; Pratt et al., 1993; Tsikos et al., 2004; Jarvis et al., 2006, 2011; Sageman et al., 2006; Gale et al., 2008; Barclay et al., 2010).

Current research suggests that OAE2 was caused by increased productivity driven by a rapid influx of micronutrients, likely from seafloor hydrothermal activity related to LIP emplacement (i.e., the Caribbean Large Igneous Province), increased rates of ocean

crust production, or increased volcanic CO_2 emissions resulting in global warming and strengthening of the hydrologic cycle, increasing continental weathering and nutrient influx to the oceans (e.g., Leckie et al., 2002; Snow et al., 2005; Barclay et al., 2010; Jenkyns, 2010; van Bentum et al., 2012; Monteiro et al., 2012).

Productivity and enhanced carbon burial associated with this nutrient increase were widespread but not global. A notable exception is the Western Interior Sea of North America, a shallow epicontinental sea that extended from the Canadian Arctic to the Gulf of Mexico, where the onset of OAE2 (based on carbon isotope enrichment) is associated with a transition from dark-gray, organic rich shale to light-gray shale interbedded with limestone (e.g., Kauffman, 1984), a decrease in total organic carbon (e.g., Pratt, 1985), and an increase in planktic and benthic foraminiferal abundance and diversity (e.g., Eicher and Worstell, 1970; Eicher and Diner, 1985; Leckie, 1985) suggesting a local increase in oxygen at a time when large areas of the open ocean were experiencing anoxia and even photic zone euxinia (e.g., Jenkyns, 2010).

Multiple incursions of warm, normal-marine waters from the Tethys made their way into the WIS during its history, coinciding with eustatic transgressions. The largest of these, the transgression of the 3rd-order Greenhorn Cycle, coincides with the onset of OAE2 and a coeval increase in marine macrofossil and microfossil diversity (e.g., Kauffman, 1984; Eicher and Diner, 1985; Elder, 1985, 1989; Leckie et al., 1998). This correlation hints at a sill at the southern aperture of the WIS that isolates the sea during low sea level, causing stagnation and organic matter preservation. If this is the mechanism causing the WIS to behave differently than the global ocean during OAE2,

there should be evidence of a clear transition between the WIS and the open ocean (Gulf of Mexico/Tethys).

The Comanche Platform of Texas may have represented such a sill at the mouth of the Western Interior Sea. The Cenomanian-Turonian Eagle Ford Shale was draped across this shallow platform and thickens in adjacent basinal and deepwater sections, where it evolved into a major petroleum source rock (Figure 1). Unlike its well-studied cousin to the north, the Greenhorn Limestone, and in spite of its unique location in the mouth of the Western Interior Sea, the micropaleontology of the Eagle Ford in Texas has been the focus of surprisingly little research in recent decades (e.g., Pessagno, 1969; Frush and Eicher, 1975; Smith, 1981; Jiang, 1989; Lundquist, 2000; Denne et al., 2014). We investigated carbon isotopes, total organic carbon, and foraminiferal and calcareous nannofossil assemblages in the Eagle Ford Shale from a transect across the Comanche Platform in order to determine 1) whether any part of the Eagle Ford has an affinity with the central Western Interior; 2) where the oceanographic transition from the Western Interior to the Gulf of Mexico is located; 3) what that position may tell us about the influence of sea level in controlling organic matter content in the Western Interior Sea; and 4) if there is a relationship between the organic-rich facies of the Eagle Ford and OAE2.

1.3 Geologic Setting

1.3.1 Stratigraphy and Micropaleontology of the Western Interior Sea

The Cenomanian-Turonian interval of the Cretaceous Western Interior Sea of North America has been the focus of paleoceanographic research for decades (e.g., Eicher and Worstell, 1970; Hattin 1971; Kauffmann, 1977a,b; Pratt and Threlkeld, 1984;

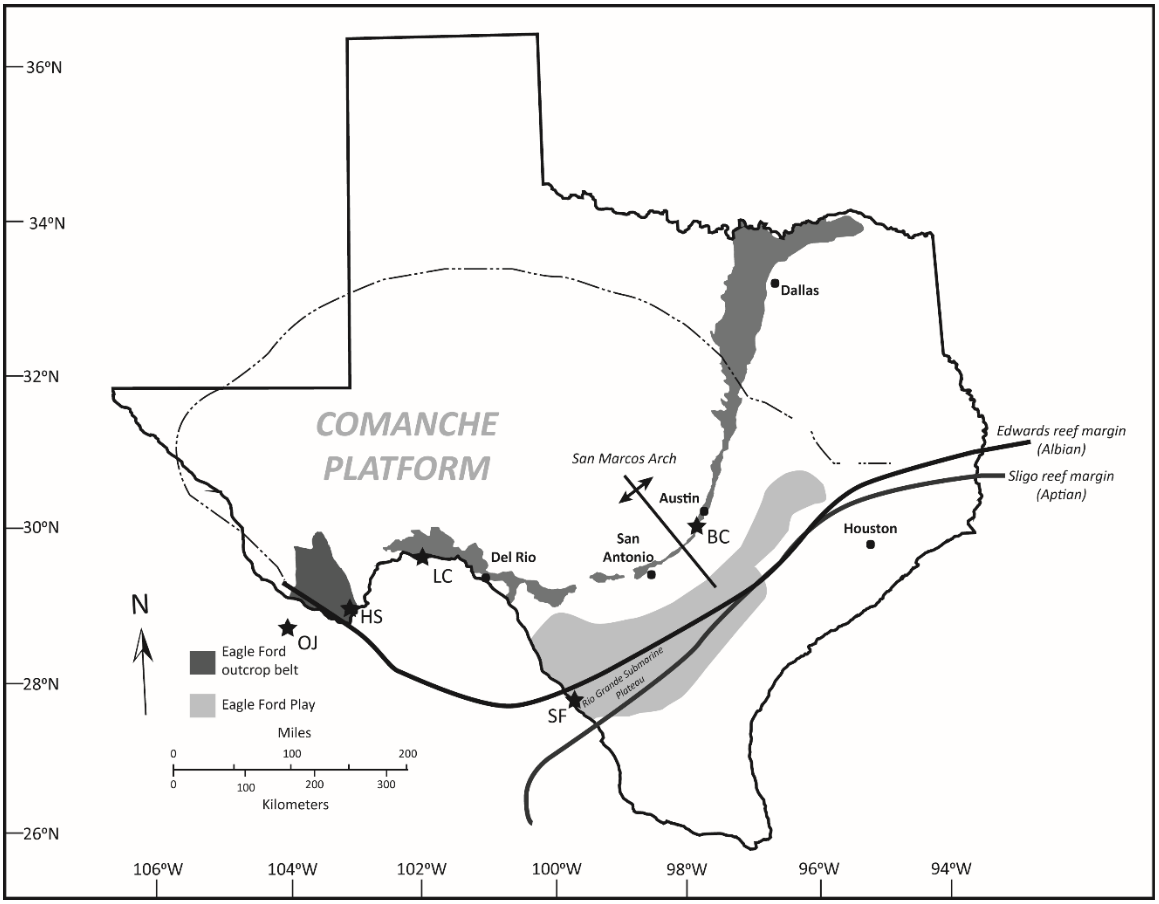

Figure 1.1. Map of Texas showing modern Eagle Ford outcrop belt (light gray), extent of the Comanche Platform, relevant paleobathymetric features, and location of study sites (stars). OJ: Ojinaga, Mexico, from Frush and Eicher, 1975; HS: Hot Springs locality in Big Bend National Park, from Frush and Eicher, 1975; LC: Lozier Canyon; BC: Bouldin Creek; SF: Swift Energy's Fasken Core. Modified from Donovan et al., 2012.

Eicher and Diner, 1989; Elder and Kirkland, 1994; Sageman and Arthur, 1994; Leckie et al., 1998; Sageman et al., 1998, 2006; West et al., 1998; Meyers et al., 2001; Meyers et al., 2005; and others). The Global Stratotype Section and Point (GSSP) for the Cenomanian-Turonian Boundary has been placed at the classic exposure at the Rock Canyon Anticline, near Pueblo, CO (Kennedy et al., 2005). Located in the central axial basin of the sea, the Rock Canyon section occupied a favorable zone where it was not inundated with siliciclastic sediments pouring off the Sevier Highlands to the west or the cratonic interior to the east, and was deeper than the gently sloping hinge-zone of the stable craton to the east (Kauffman, 1984; Sageman and Arthur, 1994; Elderbak et al., in press). Its depth and central location meant that it was more likely to be colonized by marine organisms from the Tethyan realm during transgressions and high stands of sea level; Tethyan fauna invaded there first and lingered there the longest, allowing for correlation to other sites ringing the North Atlantic in Europe and North Africa. Foraminiferal studies at Rock Canyon date back to the 1960s (Eicher, 1965, 1966, 1969; Eicher and Worstell, 1970) and have helped form some of our basic notions about foraminiferal trends across the Cenomanian-Turonian boundary (Eicher and Diner, 1985; Leckie, 1985; Fisher et al., 1994; Leckie et al., 1998; Caron et al., 2006). To summarize decades of work, the basic foraminiferal trends at Rock Canyon (and by extension, the southern part of the WIS) are as follows:

The upper Cenomanian Hartland Shale Member of the Greenhorn Limestone, a dark-gray, organic-rich shale, contains an abundant, moderate diversity assemblage of planktic foraminifera, is barren of benthic forams, and corresponds to a time of relative restriction when the sea was brackish due to poor communication with the Tethys

(because of the Comanche Platform in Texas) and freshwater input from the surrounding continent (Kauffman, 1984; Eicher and Diner, 1985; Sageman, 1985; Elderbak et al., in press). The contact with the overlying Bridge Creek Limestone Member (commonly known as Bed 63 in Colorado and Marker Bed HL-1 in Kansas; Cobban and Scott, 1972; Hattin, 1975; Elder and Kirkland, 1985) shows a marked increase in planktic foraminifer diversity, including an increase in keeled planktic foraminifera, which characterize normal marine conditions and tend to live in deeper waters (Eicher and Diner, 1985; Leckie, 1985; Leckie et al., 1998; Norris and Wilson, 1998; Petrizzo and Huber, 2008; Ando et al., 2010). This level also represents an acme of benthic foraminiferal abundance and diversity, labeled the "Benthonic Zone" by Eicher and Worstell (1970). The rapid increase in diversity has traditionally been linked to an incursion of a warm, normal saline, and well-oxygenated water mass from the south associated with the transgressive phase of the Greenhorn Cycle (Eicher and Worstell, 1970; Eicher and Diner, 1985; Elder, 1985; Elder and Kirkland, 1985; Leckie, 1985; Watkins, 1985; Savrda and Bottjer, 1993 Fisher et al., 1994; Leckie et al., 1998). Directly above this interval, benthic foraminifera become scarcer and assemblages are dominated by two species of calcareous taxa: *Neobulimina albertensis* and *Gavelinella dakotaensis*. The planktic keeled genus *Rotalipora* goes extinct, and the assemblages are dominated by surface-dwelling planktics, notably the biserial genus *Heterohelix*, an opportunistic taxon that thrives in environments in which other foraminifera struggle (Leckie et al., 1998). These events have been interpreted as the result of the incursion of a low-oxygen water mass from Tethys, where OAE2 was taking hold; this incursion resulted in stratification and deep dysoxia or anoxia in the Western Interior Basin (e.g., Eicher and Diner, 1985; Leckie,

1985; Leckie et al., 1998; Caron et al., 2006). This interval also corresponds to the Cenomanian-Turonian boundary (base of Bed 86 of the Bridge Creek Limestone), which is defined by the first occurrence of the ammonite *Watinoceras devonense* (Kennedy et al., 2005). Above Bed 86, in the lower Turonian, benthic foraminifera remain sparse and of very low diversity while keeled planktics reappear as the low oxygen conditions of OAE2 abate, a trend that continues into the lower part of the middle Turonian Fairport Member of the Carlile Shale (Eicher, 1966; Eicher and Diner, 1985; Leckie et al., 1998; West et al., 1998; Caron et al., 2006).

Calcareous nannofossils are more poorly constrained at Rock Canyon, as important marker species for the Cenomanian-Turonian boundary are reported at many different stratigraphic levels across the boundary interval, possibly reflecting diachroneity of extinctions or problems with rare/poorly preserved specimens (Bralower and Bergen, 1998; Desmares et al., 2007). Biostratigraphic analyses of the exposures at Rock Canyon have been published by Watkins (1985), Bralower (1988), and Corbett et al. (2014). Corbett and colleagues analyzed fifty-eight samples from the Bridge Creek Limestone at Rock Canyon and identified six datums within the OAE2 interval, including the lowest occurrences of *Eprolithus moratus*, *Ahmuerllerella octoradiata*, and the highest occurrence of *Corollithion kennedyi,* which are found in the OAE2 interval of the lower Bridge Creek, while the highest occurrence of *Helena chiastia* and the lowest occurrence of *Quadrum gartneri* bracket the Cenomanian-Turonian Boundary at Bed 86.

The only detailed analysis of calcareous nannofossil assemblages comes from the nearby USGS Portland Core, about 20 miles to the west of Rock Canyon, and has been deemed unreliable for paleoecological interpretation (Burns and Bralower, 1998).

Evidence of poor preservation, particularly the dominance of the dissolution resistant species *Watznaueria* (between 40-70% of the assemblage), suggests the more delicate high fertility species may have been preferentially removed. Despite this possible limitation, high fertility species *Zeugrhabdotus* is relatively abundant (~20%) through the middle of the OAE2, suggesting an increase in local productivity. Above this level, organic carbon content increases somewhat in the interbedded shales of the upper Bridge Creek Limestone, at and above the termination of OAE2, but does not return to the levels seen in the Hartland Shale (Pratt, 1985).

1.3.2 Stratigraphy and Micropaleontology of Texas

The Comanche Platform covers a large portion of west Texas and is rimmed by reef buildups; it is bounded to the southeast by the Aptian and Albian Edwards and Sligo reef margins (sometimes collectively called the Stuart City Reef Trend), to the southwest by the Maverick and Sabinas Basins (Donovan and Staerker, 2010), and to the west by the Chihuahua Trough in Mexico (Figure 1). The Edwards and Sligo reef buildups diverge in southeast Texas, and the deep platform between them is called the Rio Grande Submarine Plateau. The organic-rich mudstones of the Eagle Ford Shale cover the Comanche Platform and form thick deposits in the adjacent basins, which are the centers of the current Eagle Ford oil and gas play. The Eagle Ford is regionally underlain by the lower Cenomanian Buda Limestone (in east Texas the Cenomanian Woodbine Sandstone can be found between the Buda and Eagle Ford) and overlain by the Austin Group.

Geologists were working on the Eagle Ford of west Texas as early as 1907 (Udden), and was first described in detail here by Hazzard (1959). A recent boom in drilling activity in the Eagle Ford unconventional gas play in south and east Texas has

driven an increase petroleum-oriented research of the west Texas outcrops (e.g., Donovan and Staerker, 2010; Hentz and Ruppel, 2010; Lock et al., 2010; Donovan et al., 2012; Slatt et al., 2012; Eldrett et al., 2014), but most micropaleontological work is decades old.

Pessagno (1969) conducted a regional foraminiferal biostratigraphic study of mid-Cretaceous rocks that defined the Cretaceous planktic foraminiferal zones of the Gulf Coastal Plain. Pessagno sampled a large number of sites in the Eagle Ford outcrop belt, including our study sites at Lozier Canyon and Bouldin Creek; the paper reports mostly marker taxa and no abundance data were recorded, preventing paleoecological interpretation. In far west Texas, Frush and Eicher (1975) studied a series of outcrops in the Big Bend region of Texas and Mexico, on the western flank of the Comanche Platform, where they found an assemblage of foraminifera remarkably similar to what had been described from the U.S. Western Interior, including the “Benthonic Zone.” This indicates that assemblages of foraminifera with a Western Interior affinity extend at least as far as the western margin of the Comanche Platform.

Recently published foraminiferal data from Denne et al. (2014) from the Eagle Ford play area on eastern margin of the Comanche Platform, east of our study sites, shows low benthic abundances in the lower Eagle Ford, during intervals of high TOC, and higher abundance and diversity of benthics during the OAE2 interval, which records low TOC.

Smith (1981) published nannofossil data from several roadside outcrops of the Eagle Ford in the vicinity of Del Rio, TX. The biostratigraphic results, however, do not reflect zonal schemes that are now commonly used and many key marker species were not recorded in his study. Nannofossils were only recorded qualitatively and so cannot

be used to interpret paleoecological changes. Jiang (1989) performed additional analysis of the Eagle Ford and Austin Chalk at fifteen sites through central and northern Texas around Austin and Dallas, including the West Bouldin Creek site sampled in this paper. No detailed assemblage data were collected in Jiang's study, and while it provides more detailed biostratigraphic information than Smith's earlier work, several key marker taxa were not reported (e.g. *Eprolithus octopetalus*).

1.3.3 Sequence Stratigraphy

The Cretaceous stratigraphy of Texas can be divided into two 2nd-order cycles based on Hill (1887a,b): the Lower Cretaceous Comanchean Sequence, which records the deposition of the carbonate systems that formed the Comanche Platform and includes the Sligo, Pearsall, Glen Rose, Edwards, Georgetown, Del Rio, and Buda formations, and the Upper Cretaceous Gulfian Sequence, a siliceous-dominated sequence that begins with the Eagle Ford and includes the Austin, Anacacho, San Miguel, Olmos, and Escondido formations. The Eagle Ford contains the maximum flooding of the Gulfian sequence, and in fact, represents the maximum flooding of the 1st-order Zuni sequence, which corresponds to the latter half of the Mesozoic (Sloss, 1963). The Eagle Ford itself represents a 3rd-order cycle (called the "Eagle Fordian;" e.g., Pessagno, 1969), which is equivalent to the 3rd-order Greenhorn Cycle in the WIS (Kaufmann, 1984), making it coeval with the Greenhorn Limestone described above. Donovan and colleagues (2012), working primarily from Lozier Canyon and correlating to surrounding sites and the east Texas subsurface, divided the Eagle Ford into four members (Lozier Canyon Member, Antonio Creek Member, Scott Ranch Member and Langtry Member; Figure 2), each of which corresponds to a 4th-order sequence. The definitions and rational for these

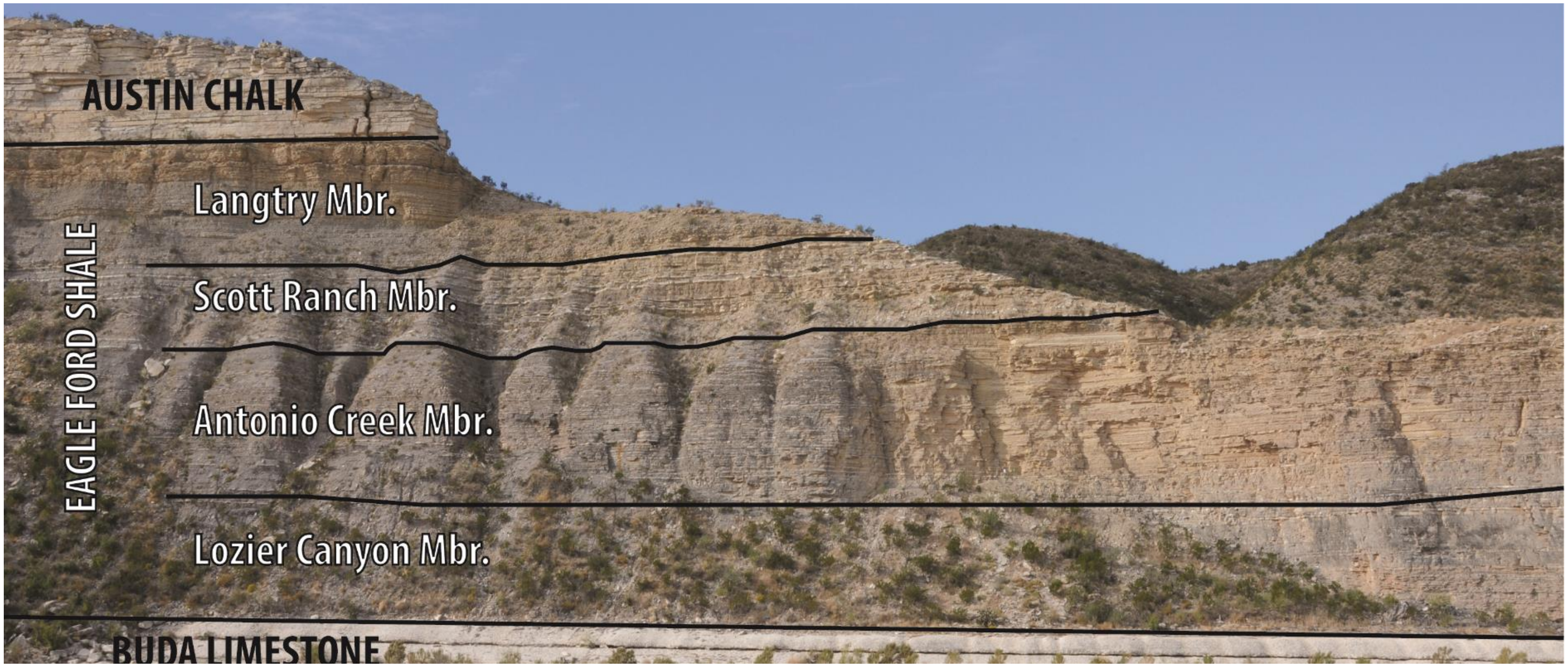

Figure 1.2. Photograph of Lozier Canyon locality. This shows typical stratigraphy of the Eagle Ford Shale, including the underlying lower Cenomanian Buda Limestone, the organic-rich lower unnamed shale and Middle Shale Member, the upper unnamed shale member, which has more interbedded limestones and corresponds to Oceanic Anoxic Event 2, the Langtry Member, and the overlying Austin Chalk.

members/sequences are discussed in detail by Donovan et al. (2012) and are summarized below.

Donovan and colleagues demonstrated the similarities between the east Texas subsurface and west Texas outcrop area by correlating units between the two with geochemical and petrophysical data (e.g., gamma ray logs). They base their four members around four mudstone-rich zones, which they interpret and marine condensed intervals. These highstands are bounded by five sequence boundaries. The lowermost is the contact between the Buda Limestone and Eagle Ford Shale, a regional unconformity that represents the transition between the Comanchean and Gulfian sequences (Sloss, 1963). A near-shore, shallow water sequence at the base of the Eagle Ford, with hummocky cross stratification and disarticulated oyster beds, slowly gives way to an anoxic, offshore mudstone facies. A sequence boundary, also delineating the boundary between the Lozier Canyon and Antonio Creek members, is placed after the peak TOC, corresponding to an increase in grainstone beds and %$CaCO_3$; the corresponding maximum flooding surface is placed at an inflection point in the natural gamma ray profile. The sequence boundary between the Antonio Creek and Scott Ranch Members is placed at a distinct lithologic change from dark gray, organic-rich mudstone to light gray calcareous shale interbedded with limestone. The maximum flooding surface is placed near the top of this interval at a slight increase in TOC, and is immediately followed by a sequence boundary. This boundary is marked by a color transition from light gray shale interbedded with grainstones to tan-colored, highly bioturbated marls and marked by a lag bed with pebble-sized rip-up clasts. This Langtry Member is characterized by a coarsening upward sequence with increasing wave-ripple grainstones toward the contact

with the Austin Chalk, with rip-up clasts again marking the boundary to wackestones interbedded with thin black mudstones of the basal Austin Chalk.

1.4 Locations and Methods

1.4.1 Study Sites

We examined a transect of three sites across the Comanche Platform for planktic and benthic foraminiferal assemblages, calcareous nannofossil assemblages, total organic carbon (TOC) and carbon isotopes from the Eagle Ford Shale. These data come from Lozier Canyon in Terrell Co., TX; Bouldin Creek, in Travis Co., TX, adjacent to a structural high called the San Marcos Arch; and from Swift Energy Company's Fasken A #1H Core, off the southeastern edge of the Comanche Platform on the Rio Grande Submarine Plateau, a deeper water site between two Early Cretaceous reef margins (Fig. 1). We compare these results to published foraminiferal data of Frush and Eicher (1975) from the western slope of the Comanche Platform at Ojinaga, Mexico, and the far west Comanche platform at Hot Springs in Big Bend National Park.

1.4.1.1 Lozier Canyon

Lozier Canyon, a "seasonal" (every few years in west Texas) river bed a few miles from the Mexican border and about nine miles west of the hamlet of Langtry, in Terrell County, TX, on private land leased to BP, contains a complete exposure of the Eagle Ford Shale on a natural, nearly vertical 55 m high face (Figure 2). Samples were collected at roughly half-meter intervals from freshly exposed rock. Detailed discussion of regional Eagle Ford geology and detailed sedimentological descriptions of the Lozier Canyon section from our fieldwork can be found in Donovan et al. (2012), but briefly: the Eagle Ford at Lozier Canyon is divided into four members. The Lozier Canyon

Member is comprised of light gray interbedded mudstones and grainstones with individual stacked beds of wave ripples and hummocks, overlain by laminated dark gray organic-rich mudstones alternating with thin, grainstone-prone limestones. The Antonio Creek Member is also a dark gray organic-rich mudstone alternating with grainstone-prone limestones, and is mainly differentiated by the occurrence of multiple bentonites beds throughout the member. The Scott Ranch Member consists of light-gray packstone-grainstone bedsets and bioturbated calcareous mudstones; the lithologic contact with the underlying Antonio Creek Member is abrupt, with a prominent grainstone and obvious color change. The Langtry Member is composed of highly bioturbated yellow marls overlain by yellow-ocre grainstones and mudstones, with wave ripples and small hummocks. Lozier Canyon is located on the southwestern part of the Comanche Platform.

Pessagno (1969) sampled Lozier Canyon at Highway 90 (which he described as a “classic exposure” of the Eagle Ford) as part of his regional biostratigraphic study. According to photographs included in his work, we sampled the same sections of the same exposure. He sampled at 10- to 20-foot (3-6 m) intervals at Lozier (for a total of eight samples), and so provides a coarse biostratigraphy. He described a paraconformity somewhere between 127 and 160 feet (~39-49 m). Samples below this paraconformity contain an assemblage of foraminifera that he found assignable to the *Rotalipora cushmani* Zone, and he assigned the samples above to the *Helvetoglobotruncana helvetica* Zone. An examination of Pessagno’s original picked slides at the Cushman Collection at the Smithsonian Natural History Museum didn’t reveal any *H. helvetica*; it is unclear whether he actually found this taxon in these samples or based the zonal

assignment on the absence of *Rotalipora* spp. or by occurrence of other early Turonian planktic species. Pessagno assigned the Austin Chalk exposed at Lozier to the now-defunct *Marginotruncana renzi* Zone.

1.4.1.2 Bouldin Creek

Bouldin Creek is a small stream located in Austin, with access near the intersection of S. 7th St. and W. Monrose St., whose banks contain vertically incomplete exposures of the Eagle Ford Group, locally mapped as the Pepper Shale, the Cloice Shale, the Bouldin Flags Formation, and the South Bosque Shale. Our samples come from a 10.7 m section that includes the upper Cloice Member, comprised of laminated calcareous mudstone; the Bouldin Flags Member, comprised of interbedded mudstones and grainstone with occasional wave ripples and common bentonites; the South Bosque Member, which is comprised of laminated calcareous mudrock; and the overlying Atco Member of the Austin Chalk. We took a few samples from a separate outcrop of the Buda Limestone and basal Pepper Shale a short distance downstream, but these turned out to be very poorly preserved and barren of foraminifera and nannofossils. The Austin area is perched in the center of the Comanche Platform on the eastern side of the San Marcos Arch, an area of very gradual tectonic uplift during the Late Cretaceous (Sohl et al., 1991; Donovan et al., 2012).

The Bouldin Creek outcrops represent a presumably identical stratigraphic package to that found in the nearby ACC #1 Core taken 11.2 miles to the north-northeast of Bouldin Creek and stored with the Bureau of Economic Geology in Austin. Calcareous nannofossils reported herein are from the ACC core, but not enough core material was available for foraminiferal, stable isotope, or TOC analyses, which were taken from

Bouldin Creek. We were able to retrieve excellent foraminiferal material from the outcrop (the best preserved of our three study sites), but the degraded nature of the exposure meant that many of the sedimentological features noted in the core are not visible in outcrop (especially the "Rubble/Condensed Zone" at the base of the Austin).

Pessagno (1969) also examined the Eagle Ford around Austin, TX, including our Bouldin Creek section, but his seven samples from this site only split the *R. cushmani* and *H. helvetica* zones, lumping all of the upper Eagle Ford and lower Austin into the latter. A more detailed paleoecological study by Lundquist (2000) examined the Eagle Ford, Austin, and Taylor Groups in central Texas, including the outcrop at Bouldin Creek and several subsurface cores. He documented an open ocean assemblage of planktics in the Pepper Shale (Figure 3) and a predominance of agglutinated benthics. The agglutinates are less common in the Cloice and Bouldin Flags (equivalent to the Antonio Member elsewhere), and biserial taxa become more prevalent in the assemblage. Above a Cenomanian/Turonian unconformity, the South Bosque Shale is dominated by biserial planktics and infaunal benthics, suggesting a more stressed environment. These changes were interpreted to have come about because of the displacement of a Boreal water mass in the Cenomanian (evidenced by the agglutinated benthics) by warm, dysoxic Tethyan waters. Lundquist interpreted an oceanic front separating these two water masses that

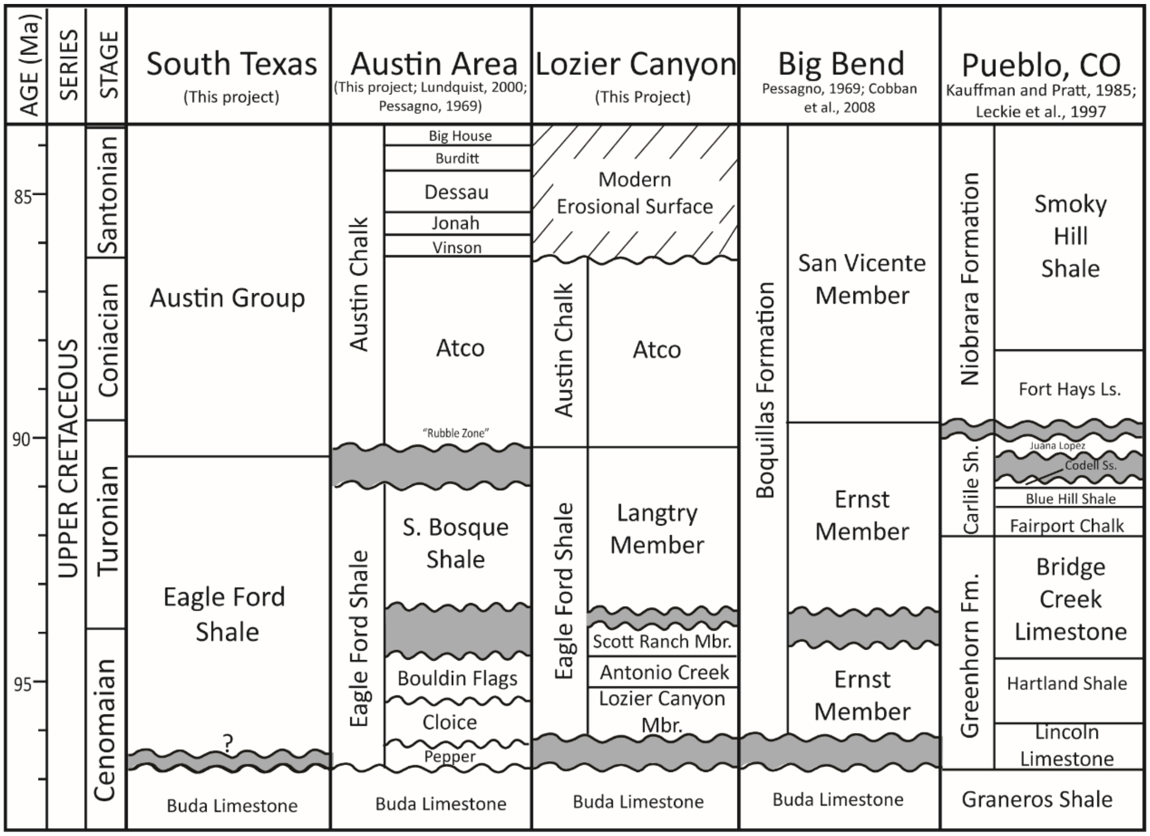

Figure 1.3. Chronostratigraphic correlation between south Texas and the Cenomanian-Turonian GSSP in Pueblo, Colorado. Correlation and stage boundaries based on our own data, as well as figures and descriptions from Pessagno, 1969; Kauffman and Pratt, 1985; Leckie et al., 1997; Lundquist, 2000; and Cobban et al., 2008. Ages based on Gradstein et al., 2012.

moved across the Austin area several times before Tethyan waters came to dominate during the Turonian. Lundquist also documents the occurrence of a "Rubble Zone" at the top of the Eagle Ford, containing abundant phosphate nodules, glauconite, and fish debris, presumed to represent an erosional surface below the Austin Chalk.

Jiang's (1989) nannofossil analysis of the Eagle Ford and Austin Chalk includes the Bouldin Creek site. Jiang suggested that the HO of *Helenea chiastia* and presence of *Lithraphidites acutum* and *Lithraphidites alatus* indicates the Cloice/Waller and Bouldin Creek members are upper Cenomanian, while the total range of *Eprolithus moratus* suggests that the South Bosque Member is Turonian. The LO of *Lithastrinus septenarius*, *Marthasterites spp.*, and *Liliasterites spp.* imply a late Turonian to early Coniacian age for the deposition of the basal Atco Member of the Austin Chalk.

1.4.1.3 Fasken Core

Swift Energy's Fasken A #1H Core is located in Webb County on the Rio Grande Submarine Plateau, off the eastern margin of the Comanche Platform. The cored interval available for study is 159.3 meters thick with a base at 2993.1 meters below surface, and includes the very top of the Buda Limestone (2.3 meters), the complete Eagle Ford Shale (119.0 meters), and the lower Austin Chalk (38.0 meters); samples were made available at roughly 2-meter intervals. Subsurface log picks of the Austin-Eagle Ford contact are inconsistent, however, and sometimes the Langtry Member of the Eagle Ford is lumped with the Austin; it is unclear if the base of the Austin was picked correctly in the Fasken. The Eagle Ford consists entirely of black, laminated shale with occasional pyrite nodules. Lithologic variability can be best seen from the gamma ray log, which shows a "marker

bed" at the top of the Middle Shale Member that is identical to that seen from outcrop gamma ray at Lozier Canyon.

1.4.2 Foraminiferal Methods

For foraminiferal population analysis, bulk rock samples were crushed to roughly centimeter chunks and soaked in a 3% solution of Miramine (a surfactant similar to Quaternary-O) and water for at least 24 hours, then washed over a 63-μm sieve and dried in an oven. Dried samples were split to obtain at least 300 individuals when possible (some samples did not yield 300 foraminifera), which were then picked and counted. Individuals that could not be identified to the genus level are categorized as "planktic spp." or "benthic spp." In poorly preserved intervals, these individuals made up a significant part of the assemblage. Because of the importance of planktic-benthic ratios to this study, and because unidentifiable foraminifera were nearly always planktic, we have included these individuals in the count totals. For nearly every "planktic spp." it was possible to determine whether the test was coiled or biserial, and so this information is included in our morpho-group proportions below (completely unidentifiable individuals are excluded). Significant sedimentary particles found in the foram wash were also counted. These include macrofossil debris (fish debris, inoceramid prisms, and echinoid spines), pyrite grains, sand grains, and glauconite grains, and are here displayed as a percentage relative to the total population of foraminifera.

For biostratigraphic purposes, we define the key Cretaceous planktic foraminiferal zones present in our study interval (after Caron, 1985; Gradstein, 2012; Huber and Petrizzo, 2014).

1.4.3 Calcareous Nannofossil Methods

Calcareous nannofossils were studied by Matthew Corbett of the University of Nebraska (see Lowery et al., 2014) using a Zeiss Photoscope III at a total magnification of 1250x using cross-polarized light, plane light, phase contrast, and through a one-quarter λ mica plate. Slides from outcrop and core samples were prepared using the double slurry and settling methods detailed by Watkins and Bergen (2003) and Geisen et al. (1999), respectively. Calcareous nannofossil biostratigraphy is addressed in detail by Corbett et al. (2014).

Several semi-quantitative methods for interpreting preservation are frequently used for Cretaceous material based on work by Roth and Krumbach (1986) and Williams and Bralower (1995). Roth and Krumbach (1986) and Erba (1992) note that *Watznaueria* negatively correlates to species richness in successions of poorly preserved material. Increasing abundances of *Watznaueria* indicate that increasing numbers of species are likely to have dissolved away. Thierstein (1981) and Roth and Krumbach (1986) suggest using 40% relative abundance of *Watznaueria* as a cut-off for samples that are likely altered from their original assemblage composition. A strong correlation between lower richness and higher relative abundance of *Watznaueria* is also used to imply diagenetic overprinting of an assemblage (Roth and Krumbach, 1986; Tantawy, 2008)

1.4.4 Geochemistry Methods

Stable isotopes of carbon are commonly measured from either inorganic carbonate crystals (i.e., “bulk carbonate”) or organic matter, the latter being far more isotopically depleted. Although both techniques faithfully capture trends in the global carbon cycle, bulk rock isotopes can sometimes be offset between shales and limestones,

which appear to be more susceptible to post-depositional alteration (e.g., Pratt and Threlkeld, 1984). For this reason, we only report samples from shales and exclude limestones in our $\delta^{13}C_{carbonate}$ analyses.

Bulk rock isotope samples were obtained by grinding roughly a gram of sample into a fine powder to ensure even dissolution. For $\delta^{13}C_{carbonate}$, this powder was reacted with phosphoric acid at 70°C to liberate CO_2 gas in a Kiel III automated carbonate preparation device inline with a ThermoElectron Delta-Plus mass spectrometer at the University of Massachusetts, Amherst. Values are reported relative to the Vienna Pee Dee Belemnite (VPDB) standard via regular calibration to an internal laboratory standard. Precision is better than 0.03‰ for $\delta^{13}C$.

Organic carbon isotope samples were decalcified using 1 N hydrochloric acid and rinsed with deionized water until a neutral pH was reached. Decalcified samples were dried, weighed into silver boats and then analyzed for total organic carbon (%TOC) using a Costech ECS 410 elemental analyzer coupled to a Thermo-Finnigan V Advantage Isotope Ratio Mass Spectrometer at the University of Massachusetts. $\delta^{13}C_{org}$ data were standardized to VPDB using internal standards. Crushed rocks samples (approximately 1 gram each) collected by Andrea Miceli Romero of the University of Oklahoma (see Lowery et al., 2014) were also sent to GeoMark Research, Inc. for TOC analysis.

1.5 Results

1.5.1 Geochemistry

1.5.1.1 Stable Isotopes

Both bulk rock and organic carbon isotope records show a strong positive excursion of 2-3‰ $\delta^{13}C$ VPDB at Lozier Canyon and in the Fasken Core (Figure 4).

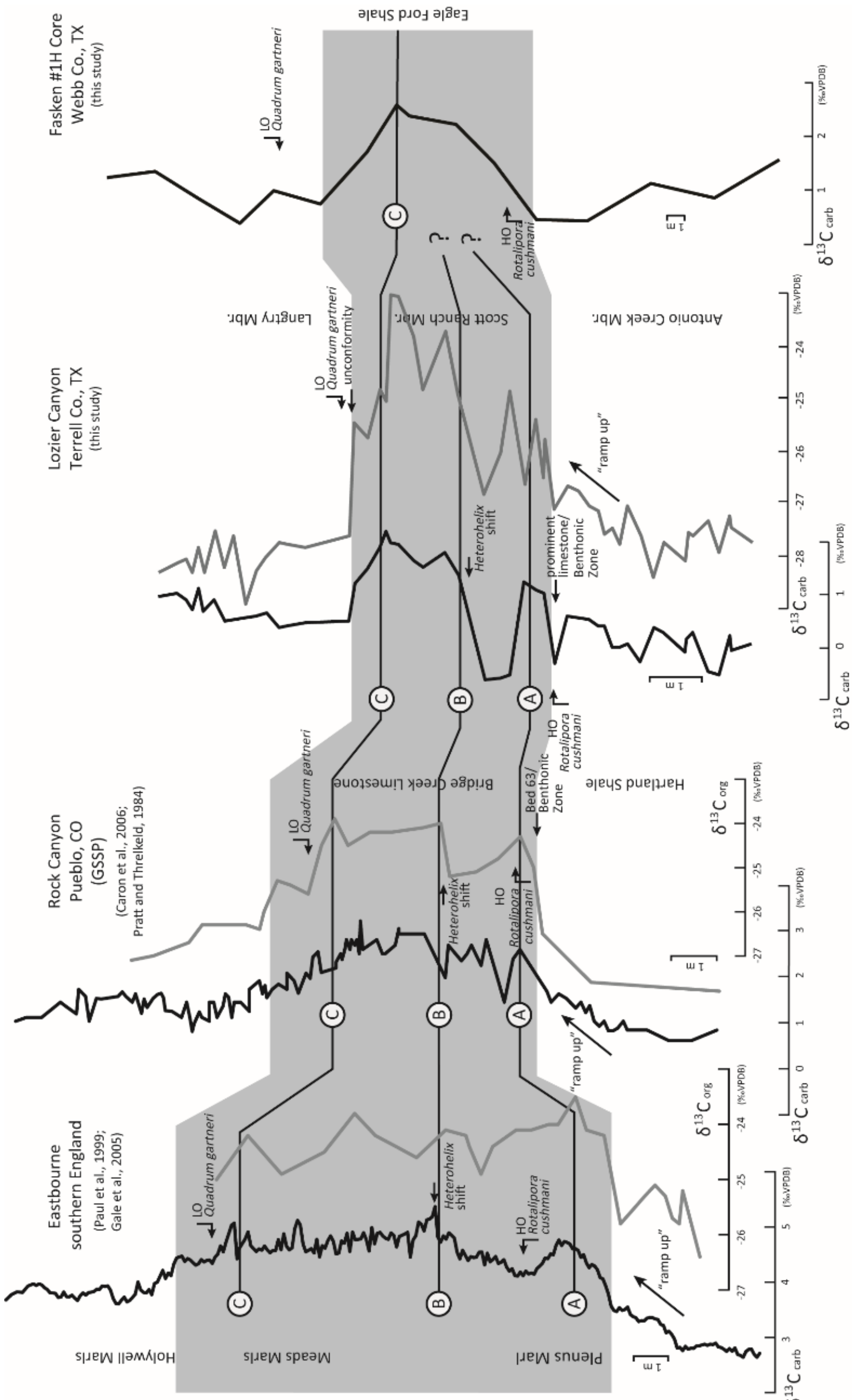

Eastbourne
southern England
(Paul et al., 1999;
Gale et al., 2005)
Rock Canyon
Pueblo, CO
(GSSP)
(Caron et al., 2006;
Pratt and Threlkeld, 1984)
Lozier Canyon
Terrell Co., TX
(this study)
Fasken #1H Core
Webb Co., TX
(this study)
Holywell Marls
Meads Marls
Plenus Marl
Bridge Creek Limestone
Hartland Shale
Langtry Mbr.
Scott Ranch Mbr.
Antonio Creek Mbr.
Eagle Ford Shale
LO
Quadrum gartneri
HO
Rotalipora
cushmani
Heterohelix
shift
"ramp up"
Bed 63/
Benthonic
Zone
unconformity
prominent
limestone/
Benthonic
Zone
A
B
C
1 m
δ13C carb
δ13C org
(‰VPDB)

Figure 1.5. Geochemical and foraminiferal assemblage data from the Lozier Canyon outcrop in Terrell Co., TX. Includes total gamma ray, organic carbon istopes, bulk carbonate carbon isotopes, Total Organic Carbon (TOC), %benthics, %infaunal benthics (light gray inset), benthic simple diversity (i.e., number of species; dashed line) %biserial planktics, %keeled planktics (light gray inset), %macrofossil debris (defined as inoceramid prisms, echinoid spines, and fish debris) and %pyrite grains. Sedimentary particle counts plotted as a percentage vs. total foraminifera. Major regionally defined sequence boundaries (SB), maximum flooding surface (MFS) and transgressive surface (TS) are notated on the plot. Gray bar delineates OAE2. See lithologic key in Figure 5b.

There is no carbon isotope record for the Bouldin Creek outcrop. At Lozier the excursion begins at the base of upper unnamed shale member (28.6 m; “marker bed” of Donovan et al., 2012) with an initial positive excursion, followed by a brief recovery to pre-excursion values around 32.0 m, and a longer positive excursion from 32.0 to 39.6 m, ending abruptly at the top of unnamed shale. This general structure in the data has been reported at many sites globally with an initial enrichment (“A”), a brief recovery (“B”), and a sustained plateau (“C”) as first described by Pratt and Threlkeld (1984) and subsequently found globally (e.g., Jarvis et al., 2006). In the Fasken, the excursion starts between 2938.1 and 2935 m, at the top of what is labeled in gamma ray logs as a “marker bed,” correlative to the “marker bed” at Lozier Canyon (Donovan et al., 2012). Unfortunately, due to poor sample resolution, we cannot resolve the structure of the curve. Orbital solutions for rhythmic bedding from the USGS Portland Core in Colorado by Sageman and colleagues (2006) put the duration of OAE2 at 847-885 kyr. Since the Fasken section is conformable, we can use this to estimate a sedimentation rate of 1.33 cm/kyr (±0.47 cm) at this location during the OAE interval.

1.5.1.2 TOC

The highest TOC at Lozier Canyon (Figure 5) can be found in the lower unnamed shale member, where values exceed 6 wt%. TOC is generally low through the Middle Shale Member and the initial part of OAE2 (~1 wt% hydrocarbon). The “C” part of the carbon isotope excursion in the upper unnamed shale corresponds to a second, smaller peak in TOC (>2 wt%), before dropping to almost zero in the Langtry Member (Lowery et al., 2014).

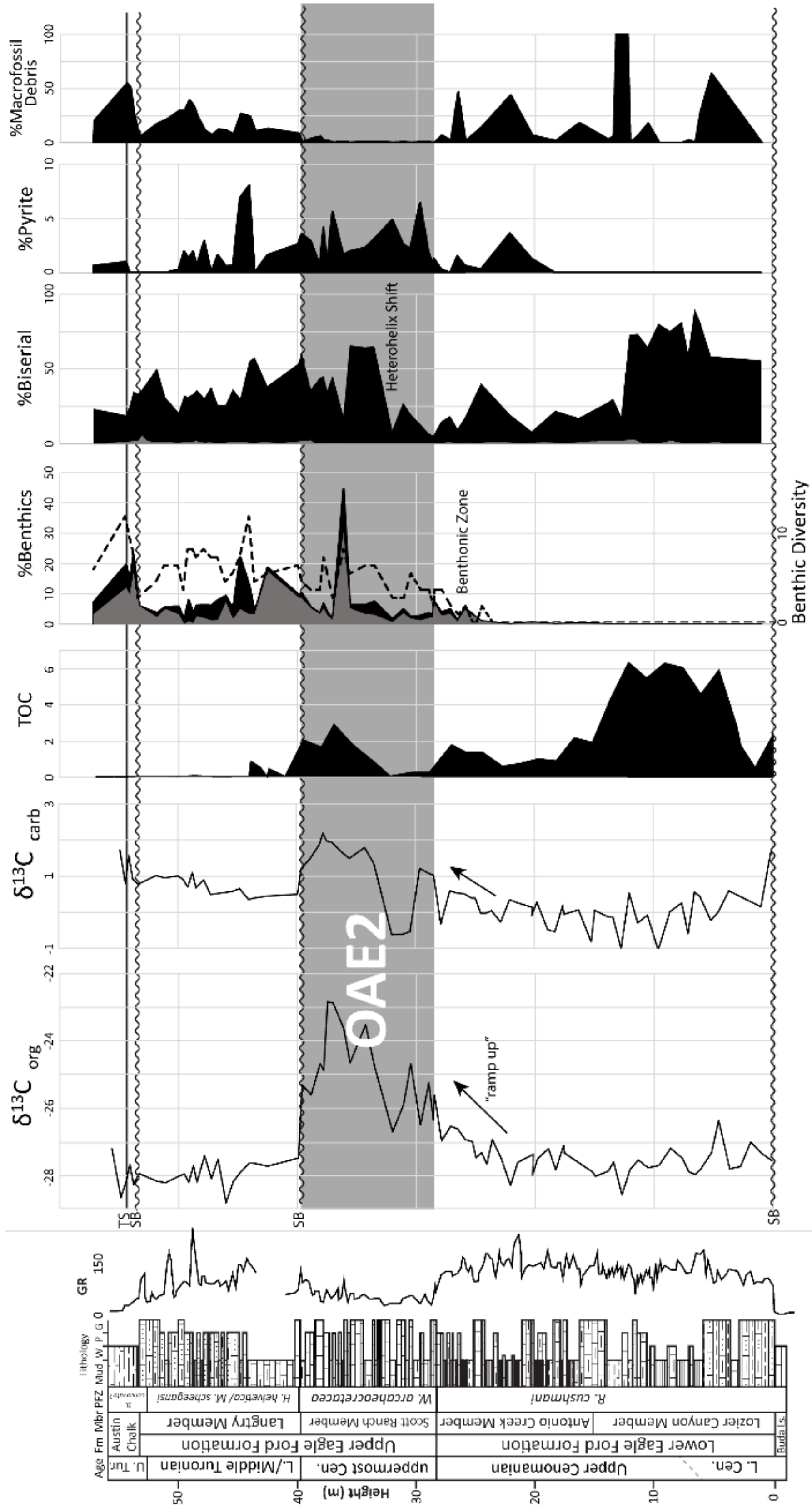
%Macrofossil Debris
%Pyrite
%Biserial
Heterohelix Shift
%Benthics
Benthonic Zone
Benthic Diversity
TOC
δ13C carb
δ13C org
OAE2
"ramp up"
TS
SB
GR
Lithology
Mud W P G
Age
Fm
Mbr
PFZ
Height (m)
L. Cen.
Upper Cenomanian
uppermost Cen.
L./Middle Turonian
U. Tur.
Lower Eagle Ford Formation
Upper Eagle Ford Formation
Austin Chalk
Buda Ls.
Lozier Canyon Member
Antonio Creek Member
Scott Ranch Member
Langtry Member
R. cushmani
W. archaeocretacea
H. helvetica/ M. schneegansi

Figure 1.5. Geochemical and foraminiferal assemblage data from the Lozier Canyon outcrop in Terrell Co., TX. Includes total gamma ray, organic carbon istopes, bulk carbonate carbon isotopes, Total Organic Carbon (TOC), %benthics, %infaunal benthics (light gray inset), benthic simple diversity (i.e., number of species; dashed line) %biserial planktics, %keeled planktics (light gray inset), %macrofossil debris (defined as inoceramid prisms, echinoid spines, and fish debris) and %pyrite grains. Sedimentary particle counts plotted as a percentage vs. total foraminifera. Major regionally defined sequence boundaries (SB), maximum flooding surface (MFS) and transgressive surface (TS) are notated on the plot. Gray bar delineates OAE2. See lithologic key in Figure 5b.

The Eagle Ford at Bouldin Creek contains two intervals enriched in TOC (Figure 6). The lower and larger (~7 wt%) is in the basal two meters of the outcrop in the Pepper and Cloice Shales. The second covers most of the South Bosque Shale above the lower unconformity and the "Rubble Bed" at the basal Austin, between 5.1 and 9.5 meters, with values averaging ~4 wt% (Lowery et al., 2014).

TOC in the Fasken core (Figure 7) steadily decreases from a peak of 6.4 wt% just above the Buda at 2970 meters below the surface, to a minimum of 1.82 wt% at 2901.5 meters, about 25 meters above the end of OAE2. TOC is variable in the Austin Chalk, ranging from 1.3-3.7 wt% (Lowery et al., 2014).

1.5.2 Foraminifera

1.5.2.1 Planktic Foraminifera

The lower five meters of the Eagle Ford at Lozier Canyon (Figure 5) are almost completely barren of foraminifera. Washed samples at the very bottom of the formation are almost entirely comprised of dolomite rhombs. Some cross-stratified sandy beds contain planktic foraminifera in thin section (not recovered in the wash and therefore not reflected in the counts), which were likely transported with the sand during storm events. The upper portion of the Lozier Canyon Member contains rare, poorly preserved planktic foraminifera, mainly of the genus *Heterohelix*, and abundant inoceramid prisms. This interval frequently did not yield 300 foraminiferal specimens, although this may be due to preservational factors. The upper 10 m of the Lozier Canyon Member yields more abundant foraminifera, but the assemblage is dominated by small specimens of *Heterohelix*. The Antonio Creek Member records a transition to an assemblage dominated by the trochospiral genus *Hedbergella* (~80%). Keeled taxa (i.e., *Rotalipora*

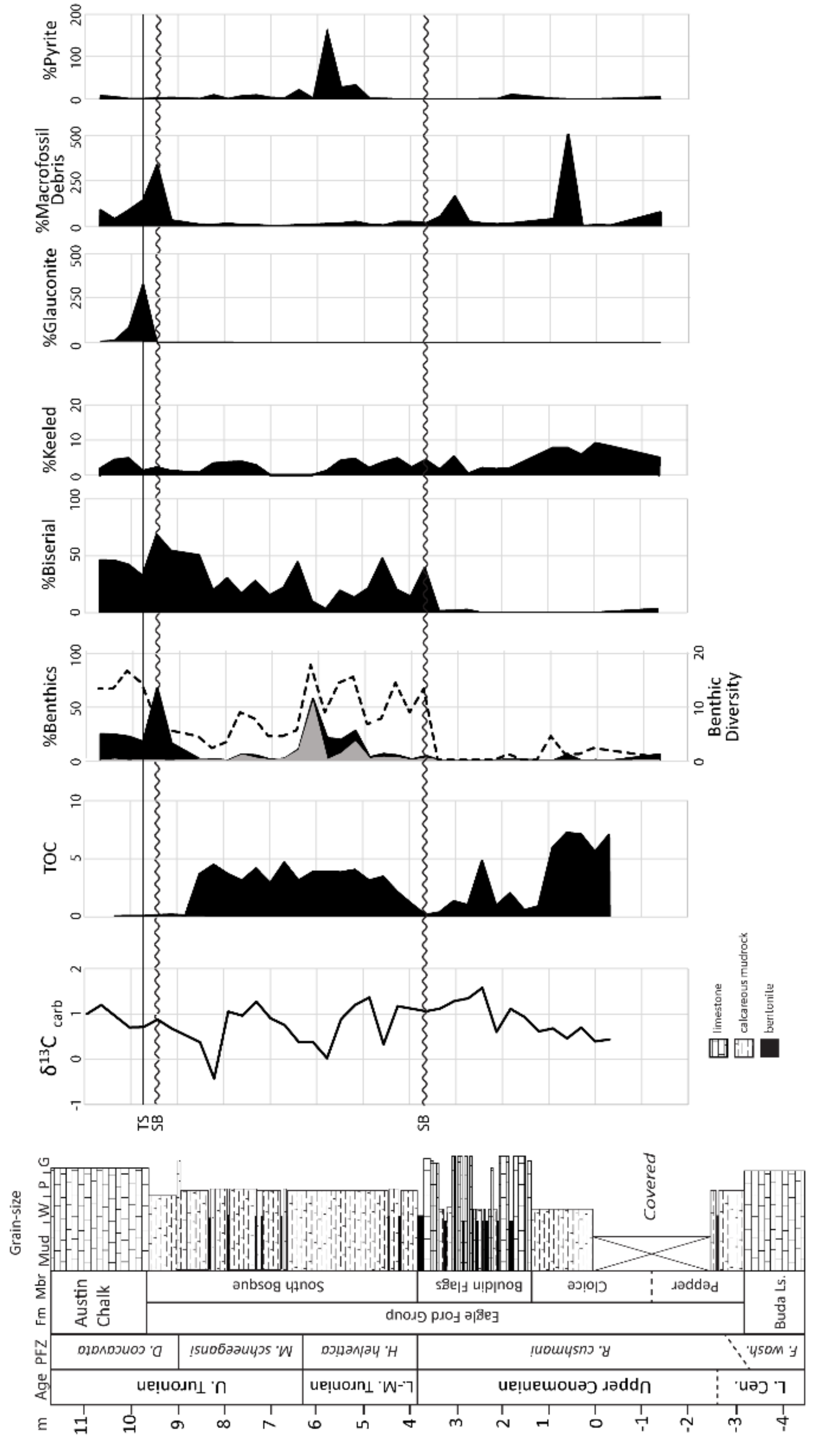

%Pyrite
%Macrofossil Debris
%Glauconite
%Keeled
%Biserial
%Benthics
Benthic Diversity
TOC
δ13C carb
TS
SB
limestone
calcareous mudrock
bentonite
Grain-size
Mud
W
P
G
Covered
m
Age
PFZ
Fm
Mbr
U. Turonian
L.-M. Turonian
Upper Cenomanian
L. Cen.
D. concavata
M. schneegansi
H. helvetica
R. cushmani
F. wash.
Austin Chalk
Eagle Ford Group
Buda Ls.
South Bosque
Bouldin Flags
Cloice
Pepper

Figure 1.6. Geochemical and foraminiferal assemblage data from the Bouldin Creek outcrop in Travis Co., TX. Includes bulk carbonate carbon isotopes, TOC, %benthics, %infaunal benthics (light gray inset), benthic simple diversity (dashed line) %biserial planktics, %keeled planktics, %glauconite, %macrofossil debris (defined as inoceramid prisms, echinoid spines, and fish debris), and %pyrite grains. Sedimentary particle counts are plotted as a percentage vs. total foraminifera. Major regionally defined sequence boundaries (SB), maximum flooding surface (MFS) and transgressive surface (TS) are noted on the plot. Note that planktic foram zones skip the latest Cenomanian *Whiteinella archaeocretacea* Zone and that there is major positive excursion in the carbon isotopes, both of which indicate an unconformity at the base of the Turonian.

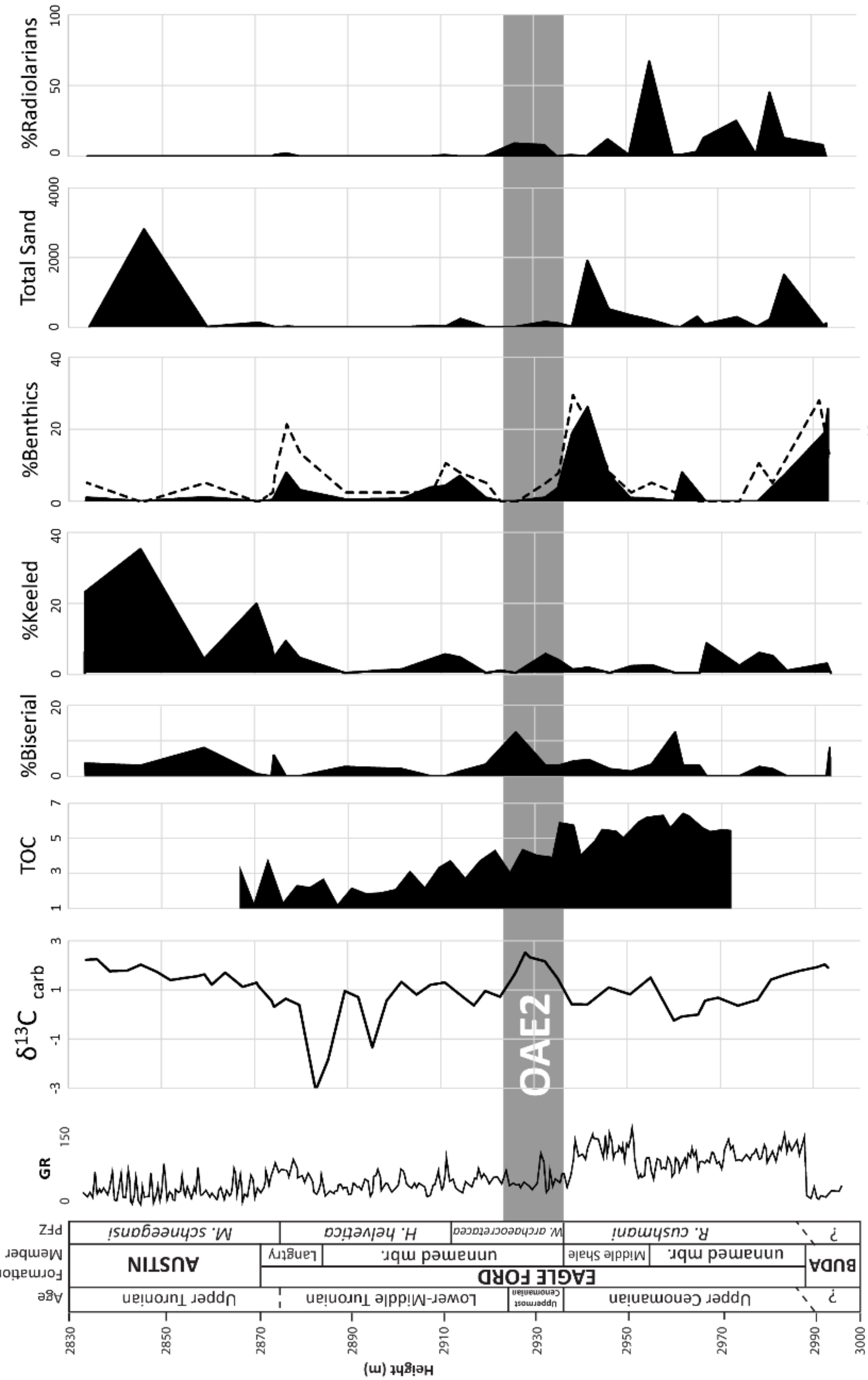

%Radiolarians
Total Sand
%Benthics
%Keeled
%Biserial
TOC
δ13C carb
GR
OAE2
Height (m)
Age
Formation
Member
PFZ
Upper Turonian
Lower-Middle Turonian
Uppermost Cenomanian
Upper Cenomanian
AUSTIN
EAGLE FORD
BUDA
Langtry
unnamed mbr.
Middle Shale
M. schneegansi
H. helvetica
W. archaeocretacea
R. cushmani

Figure 1.7. Geochemical and foraminiferal assemblage data from Swift Energy's Fasken A #1H core in Webb Co., TX. Includes total gamma ray, bulk carbonate carbon istopes, TOC, %biserial planktics, %keeled planktics %benthics, benthic simple diversity (dashed line) %infaunal benthics (not present), sand grains, and %radiolarians. Radiolarians are plotted as a percentage vs. total foraminifera. Gray bar delineates OAE2.

spp. and *Praeglobotruncana* spp.) are very rare but present throughout. The keeled genus *Rotalipora* and planispiral species *Globigerinelloides bentonensis* have their highest occurrence in the uppermost sample of the Antonio Creek Member (28.6 m). Keeled planktic foraminifera are completely absent from the Scott Ranch, while the planktic assemblages shift from trochospiral *Hedbergella*-dominance to biserial *Heterohelix*-dominance at 33.5 m. Interestingly, this interval also sees a nearly complete disappearance of inoceramid prisms (although rare inoceramids can be found in the outcrop). Keeled planktic foraminifera become present again in the base of the Langtry Member, while the percentage of *Heterohelix* in the assemblage decreases, but remains relatively high (>50%). Inoceramid prisms also return at this level. The percentage of the biserial planktic *Heterohelix* drops below 50% in the upper Langtry Member, and is replaced by a relatively diverse assemblage of *Hedbergella*, *Whiteinella* and keeled planktics including *Dicarinella* and *Marginotruncana*.

The lower two members of the Eagle Ford at Bouldin Creek (Figure 6) contain assemblages dominated by trochospiral planktics, notably *Hedbergella delrioensis, H. simplicissima,* and *H. planispira.* The keeled species *Praeglobotruncana delrioensis* is a minor but important component of the assemblage in the lower Eagle Ford. The most striking feature of the Bouldin Creek outcrop is the lowest occurrence (LO) of *H. helvetica* in the basal South Bosque, directly above the highest occurrence (HO) of *Rotalipora cushmani* at the top of the Bouldin Flags Member, suggesting an unconformity that has entirely erased the *Whiteinella archeocretacea* Zone. *Heterohelix,* which is dominant in the lower Eagle Ford at Lozier, is nearly absent here until the South Bosque Member. It shows highly variable abundance, but reaches an acme in the upper

South Bosque at 9.4 m, concurrent with a spike in macrofossil debris and epifaunal benthic foraminifera (see below) suggesting a sea level lowstand. This is immediately followed at 9.8 m by a decline in %biserial, %benthics, and %macrofossil debris, and a major peak in glauconite, which is extremely rare in the rest of the South Bosque. This interval corresponds to a "rubble zone" (that is not evident in outcrop but very evident under the microscope as a flood of glauconite and macrofossil debris) in what is labelled as the basal Austin Chalk in the nearby ACC #1 core.

Swift Energy's Fasken #1 core (Figure 7), located off the Comanche Platform on the Rio Grande submarine plateau, has intermittent preservation of foraminifera throughout the Eagle Ford. This is probably related to depth of burial (the Eagle Ford is ~2870-2990 meters below the surface). Preservation is generally the poorest in the middle Eagle Ford, but varies from sample to sample throughout. The best preserved samples have mostly pyritized foraminifera, which preserved detailed features (pores, aperture, etc.). Samples with no foraminifera (24 out of 69) are excluded from the population analysis because we suspect this is a result of poor preservation and not a true lack of foraminifera. Other workers have encountered similar preservation issues working in producing Eagle Ford wells; Denne et al. (2014) found foraminifera in thin section in intervals where the wash was barren.

Planktic foraminiferal populations in the Fasken are dominated by inflated trochospiral taxa, notably *Hedbergella delrioensis* and *Whiteinella spp.* Keeled genera (*Praeglobotruncana* and *Rotalipora* in the lower Eagle Ford and *Dicarinella* and *Marginotruncana* in the upper Eagle Ford and Austin Chalk) generally make up ~5% of the assemblage throughout the Eagle Ford, although they greatly increase in abundance

(20-30%) in the Austin. The biserial genus *Heterohelix* is rare (~5% with a few peaks at above 10%) throughout the section.

The Fasken is the only study site where we recognize radiolarians. Radiolarians are most common in heavily pyritized samples, so their individual peaks may be artifacts of preservation, but they are only present before OAE2, with a single sample containing a small peak at the end of the OAE2 isotope excursion.

1.5.2.2 Benthic Foraminifera

The lower Eagle Ford at Lozier Canyon (Figure 5) contains almost no benthic foraminifera (except for a single *Gavelinella* in the Lozier Canyon Member) until the upper part of the Antonio Creek Member (~26 m), where a sustained, though weak, benthic population made up almost entirely of the infaunal genus *Neobulimina* takes hold. This interval, which we suspect is correlative to the “Benthonic Zone” at Big Bend and in the WIS (Frush and Eicher, 1975), continues throughout the Scott Ranch Member and coincides with OAE2. At 43 m, the percentage of benthic individuals in the population reaches an acme of 36% before returning to background levels in the next sample. Brief pulses of benthic foraminferal abundances (“repopulation events,” e.g., Friedrich, 2010) have been reported elsewhere during the OAE2 interval, such as the Demerara Rise in the tropical Atlantic (ODP Leg 207; Friedrich et al, 2006). If other records are an indication, it is likely that there are other spikes in the benthic population that are not observed in our half-meter resolution; we do not find this acme event in our other Texas study sites. The benthic assemblage is dominated by the infaunal genus *Neobulimina*. The lower Langtry Member shows increased percent benthic values of 10-20%, still nearly entirely composed of *Neobulimina albertensis and N. canadensis.* The

upper Langtry shows an overall decrease in %benthic with values oscillating between 5-10%, but the benthic population diversifies to include more epifaunal taxa, notably *Planulina* and *Gavelinella*.

Benthic foraminifera are nearly absent from the lower members of the Eagle Ford at the Bouldin Creek outcrop (Figure 6), with the exception of a single sample in the basal Pepper, a single sample in the upper Cloice, and a single *Gavelinella* sp. in the Bouldin Flags. Because the OAE2 interval is completely missing at Bouldin Creek we cannot identify a "Benthonic Zone." However, both infaunal (*Neobulimina albertensis* and *N. canadensis*) and epifaunal benthics (*Gavelinella dakotensis*, *G. petita*, and *Planulina spp.*) become consistently present above the unconformity in the lower Turonian. There are two benthic foraminiferal acme events. The first, 58% of the total foraminiferal assemblage, at 6.1 m, is almost exclusively the infaunal taxon *Neobulimina*, although the sample immediately below (21% benthics) contains exclusively epifaunal species, dominated by *G. dakotensis*. The second benthic acme (9.4 m) is coincident with a peak in biserial planktics and macrofossil debris, and is immediately followed by a peak in glauconite. This event is stronger than the first (68% benthics), and contains exclusively epifaunal taxa dominated (173 out of 204 individual benthics) by *G. petita*.

The Fasken core (Figure 7) contains trends that are very different from the Eagle Ford on the Comanche Platform. Benthic foraminifera show several peaks, but the largest are in the lower Eagle Ford, below OAE2. With the exception of three specimens of *Bulimina fabilis* and a single *Bifarina* sp., the benthic population is composed exclusively of epifaunal taxa. The benthic assemblage is diverse throughout, but is generally dominated by *Lingulogavelinella* in the acme events (in some cases, the populations of

other benthic species stay constant, and a flood of *Lingulogavelinella* spp. cause the %benthics to increase substantially).

No agglutinated foraminifera were found in our study sites. This is in contrast to Lundquist (2000), who found abundant agglutinated benthics in the Pepper and Cloice shales near Austin. It is likely that weathering of the Bouldin Creek outcrop (where we only recovered one poorly-preserved sample from each the Pepper and the Cloice) destroyed the agglutinates, and that if we had access to core materials we could have duplicated Lundquist's (2000) results in these members.

1.5.3 Calcareous Nannofossils

The use of calcareous nannofloral assemblages for interpreting surface water fertility is well documented (Burns and Bralower, 1998; Gale et al., 2000; Erba, 2004; Eleson and Bralower, 2005; Watkins et al., 2005; Hardas and Mutterlose, 2007; Linnert et al. 2010, 2011)**.** Two genera in particular, *Biscutum* and *Zeugrhabdotus*, are believed to indicate mesotrophic conditions and high fertility based on their high abundance in areas of upwelling and elevated organic matter (Roth 1981, 1986, 1989; Roth and Bowdler, 1981; Roth and Krumbach, 1986; Watkins, 1986; Premoli Silva et al., 1989; Erba, 1992; Erba et al., 1992; Watkins et al., 2005; Hardas and Mutterlose, 2007). In lower fertility, oligotrophic surface water conditions, *Watznaueria* tends to dominate nannofossil populations (Roth and Krumbach, 1986; Erba et al., 1992; Williams and Bralower, 1995; Herrle, 2002, 2003; Watkins et al., 2005; Hardas and Mutterlose, 2007).

Calcareous nannofloral paleoecology from the southern and central Western Interior Sea is discussed in greater detail in Corbett and Watkins (2013), and a summary of their observations from across Texas is presented here. At Lozier Canyon (Figure 8a)

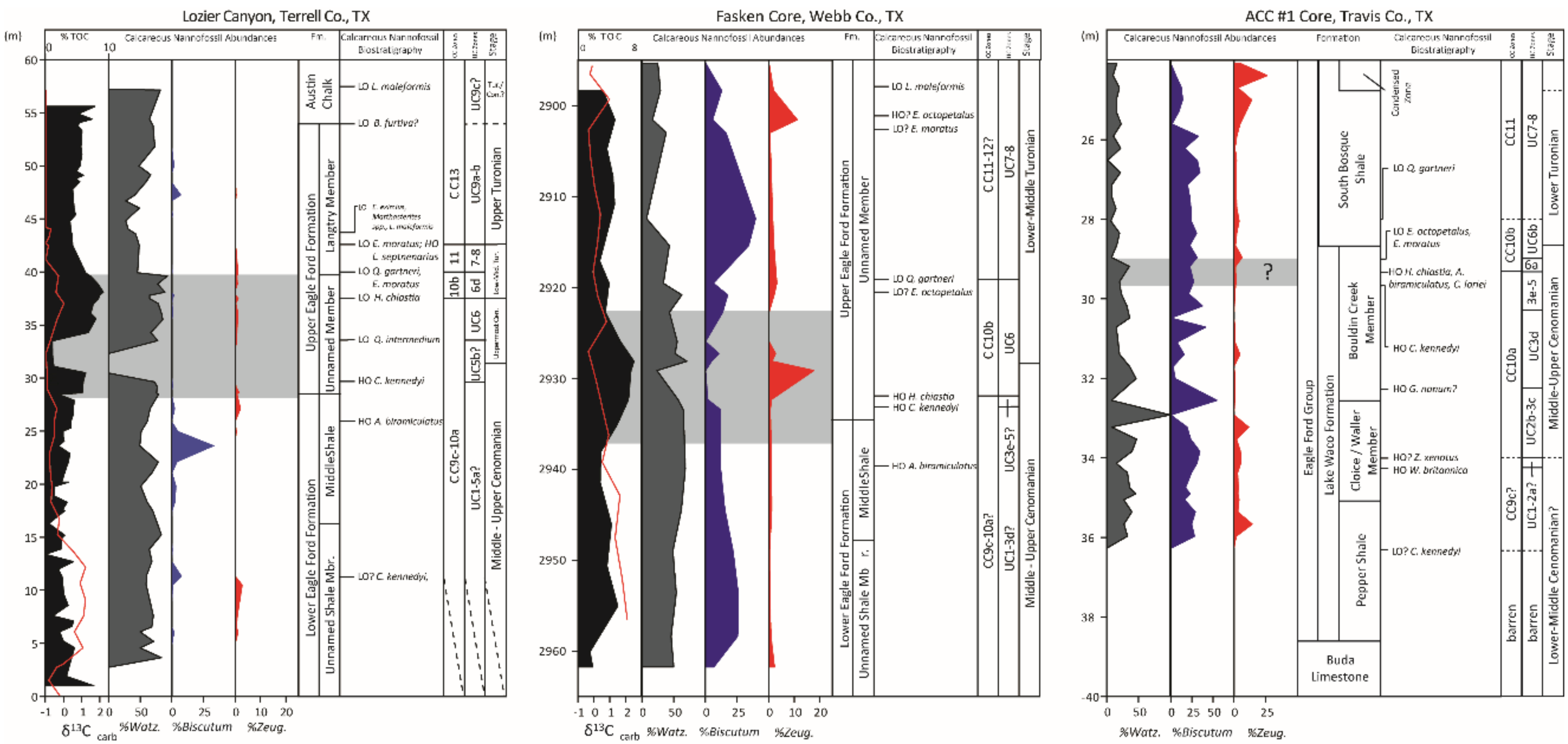

Figure 1.8. Nannoplankton assemblage data from the Lozier Canyon outcrops in Terrell County (**a.**), ACC #1 Core in Travis County, 11 miles SE of the Bouldin Creek outcrop (**b.**), and from the Fasken A #1H Core in Webb County (**c.**). Data include %*Watznaueria* spp., %*Biscutum* spp., and %*Zeugrhabdotus* spp., as well as the location of primary and secondary nannofossil datums. The relative abundance of *Watznaueria* spp. is very high at the Lozier locality suggesting that nannofossil assemblages have been altered by diagenesis. Bulk carbonate isotope data ($\delta^{13}C_{carb}$) highlighted in black fill; weight percent total organic carbon (wt% TOC) shown with red line. Gray bars show location of OAE2. Data from Corbett and Watkins (2013).

the relative abundance of *Watznaueria* ranges from ~50-75% through the upper Cenomanian lower Eagle Ford and the middle Turonian unnamed member of the upper Eagle Ford. This suggests the nannofossil recovery has been strongly affected by dissolution because *Biscutum* and *Zeugrhabdotus* make up less than 10% of the population through much of the section. As a result of this diagenetic overprinting, the data likely do not reflect the original death assemblage, and as a result TOC does not correspond to nannofossil paleoproductivity indicators. Preservation is better in the Fasken A #1-H and ACC #1 cores and can be compared with trends in planktic and benthic foraminifer abundance and TOC.

Watznaueria remains below 50% through most of the Eagle Ford in the ACC (Figure 8b) and Fasken (Figure 8c) cores, indicating the nannofossil abundances better reflect the original death assemblage. Populations preceding and following OAE2 are comprised of nearly 25-40% *Biscutum*. The abundance of *Biscutum* decreases to 10% or less through OAE2 in the Fasken core. Bio-chemostratigraphic interpretations reveal the interval spanning OAE2 to be missing from the ACC core and Bouldin Creek outcrops (Figures 4b and 6). No clear pattern in the abundance of *Zeugrhabdotus* is observed, though a small peak (~18%) is present in the uppermost Cenomanian of the Fasken core.

1.6 Discussion

1.6.1 Affinity with the Western Interior and Oceanographic Fronts

For the purposes of this study, we define an affinity to the Western Interior as rocks containing the following criteria: 1) peak TOC before the OAE2 interval; 2) foraminiferal faunal trends similar to those at Rock Canyon (e.g., “Benthonic Zone,” “*Heterohelix* shift,” HO of *Rotalipora* and *Globigerinelloides bentonensis* at or just after

the onset of OAE2); and 3) lithologic transition similar to the Hartland-Bridge Creek (i.e., dark gray organic rich shale overlain by light gray shale and limestones). All of our sites meet the TOC criteria, but only the platform sites meet the others.

The sites on the platform, including Frush and Eicher's 1975 Big Bend localities, show a lack of benthics before OAE2 and an obvious increase coincident with the onset of the anoxic event. Based on the well-documented structure of the OAE2 positive carbon isotope excursion, the last occurrence of *Rotalipora* at Lozier Canyon is earlier than at Rock Canyon. This south to north diachroneity was first noted in Big Bend by Frush and Eicher (1975) and has been interpreted to represent the south to north incursion of an oxygen minimum zone (OMZ) into the sea (Leckie et al., 1998). Trends in biserial planktic foraminifera follow different patterns at each site, and while Lozier records a "*Heterohelix* shift" as observed at Rock Canyon and elsewhere in the Western Interior (Leckie et al., 1998), it is difficult to label this trend at the other Texas sites. Lithologically, Lozier Canyon and Big Bend also bear a strong resemblance to the Hartland Shale and Bridge Creek Limestone, which includes a limestone bed at Lozier Canyon at the base of the Middle Shale Mbr. corresponding to the onset of OAE2, the extinction of *Rotalipora*, and the beginning of the "benthonic zone," just like Bed 63 at Rock Canyon and HL1 in Kansas (Cobban and Scott, 1972; Hattin, 1975; Eicher and Diner, 1985; Elder and Kirkland, 1985).

The Fasken contains very few biserial planktics throughout, which is indicative of its deeper water, more open-marine location; Cenomanian-Turonian *Heterohelix* is generally associated with marginal environments and epeiric seas (Leckie, 1987; Leckie et al., 1998). Likewise, it has far more keeled planktic foraminifera, which tend to live

deeper in the water column and are therefore also indicative of an open ocean setting (Ando et al., 2010).

Because sites on the Comanche Platform, especially the western platform, are very similar to the Western Interior, while the Fasken Core, to the southeast of the platform and in deeper water, bears no similarity to the Western Interior except for TOC trends, we conclude that the transition between the Western Interior Sea and the open ocean occurs at the edge of the Comanche Platform. But what controls organic carbon production, why is it the only similarity between the Fasken Core and the other sites, and why is it different from the global trend?

1.6.2 TOC Trends, Oxygenation, and Productivity

The ratio of planktic to benthic foraminifera (P/B ratio, or %planktic to total foraminifera) is commonly used as a qualitative proxy for sea level and proximity to shore (e.g., Murray, 1976; Gibson, 1989; Hayward, 1990; Van der Zwaan et al., 1990; Leckie and Olson, 2003). However, in environments prone to dysoxia the P/B ratio is also a useful proxy for bottom water oxygenation (Van Hinsbergen et al., 2005). Proportions of major morpho-groups of planktic foraminifera are also useful proxies for bottom water or water column oxygenation, including biserial (*Heterohelix,* a generalist surface-dwelling genus that dominated stressed environments where other taxa do poorly), trochospiral (large, inflated thermocline to surface dwelling genera that include *Hedbergella*, *Whiteinella*, and *Archaeoglobigerina*), and keeled taxa (*Rotalipora*, *Praeglobotruncana, Dicarinella,* and *Marginotruncana*; genera that generally lived at deeper thermocline depths and/or normal marine environments), and the relative proportion of infaunal, typically low-oxygen tolerant benthic taxa (*Neobulimina*,

especially, and other buliminids and rectilinear taxa) vs. epifaunal benthic taxa (*Gavelinella, Planulina, Lingulogavelinella,* and related trochospirally-coiled genera). Numerous studies have documented the usefulness of these foraminiferal groups for paleoceanographic interpretations across the Western Interior (e.g., Eicher and Diner, 1985; Leckie, 1985; Leckie et al., 1991; Fisher et al., 1994; Leckie et al., 1998; Caron et al., 2006).

Calcareous nannoplankton assemblages indicate late Cenomanian surface water fertility through the high TOC intervals was comparable between the Fasken core and the Cloice Member (equivalent to the Middle Shale, Figure 3) of the Eagle Ford in the ACC core. Higher abundances of *Biscutum* during intervals of high TOC suggest elevated productivity in the photic zone led to an increased flux of organic matter into bottom waters and anoxia. Decreases in TOC and nannoplankton productivity indicators track each other. Slatt et al. (2012) show that the lower Eagle Ford is dominated by Type II kerogen, which indicates a marine source, further suggesting that the high TOC in the lower Eagle Ford is due to enhanced production.

The benthic foraminifera of the lower Eagle Ford agree with this interpretation, as do the planktics, although their signal is more complicated. The assemblages at Lozier Canyon (Figure 5) are initially dominated by biserial opportunist planktic foraminifera until trochospiral surface dwellers increase in abundance; deeper-dwelling keeled planktics remain rare, suggesting normal salinity but relatively shallow water (see below). In fact, biserials track TOC fairly closely at Lozier, while inoceramid abundance is roughly inversely related to biserial abundance. At Rock Canyon, Caron et al. (2006) recorded higher abundances of inoceramids when TOC is elevated but not at peak; a

similar relationship is observed Lozier Canyon, with higher abundances of inoceramids at the transitions to rising and falling TOC levels. Bouldin Creek (Figure 6) has a fairly diverse, healthy planktic assemblage with a relatively diverse assemblage of keeled taxa and almost no biserials, even in the lower Eagle Ford where TOC is highest. Proximity to the shallow San Marcos Arch may have resulted in better mixing and a more oxic water column at Bouldin Creek. At Lozier Canyon, benthic foraminifera are generally anti-correlated to TOC (Figure 9a). During the highest TOC intervals, benthic foraminifera are nearly absent. As TOC decreases, benthic foraminifera increase, initially just the low oxygen tolerant infaunal taxa (e.g., *Neobulimina albertensis*). The persistence of low-oxygen taxa when TOC is at or near zero, even as benthic foraminifera are more abundant and fairly diverse, suggests the persistence low-oxygen conditions even as anoxia abated. At Bouldin Creek, this only partially holds true (Figure 9b). While benthics are absent in the highest TOC intervals, moderate TOC in the early Turonian coincides with high benthic values. In this case, clearly dysoxia did not prevent foraminifera from colonizing the area, perhaps reflecting decadal- to semi-annual variability not resolved in our data.

Recently published data from a Shell core drilled to the east of Lozier Canyon in the Maverick Basin support the interpretation of anoxia. Eldrett et al. (2014) show an enrichment of redox-sensitive trace elements, including Mo, U, V, Cu, and Ni, in the Lower Eagle, coincident with an interval of enriched TOC prior to OAE2, and declining to near zero during the anoxic event, suggesting anoxia in the Lower Eagle Ford and oxic conditions during OAE2.

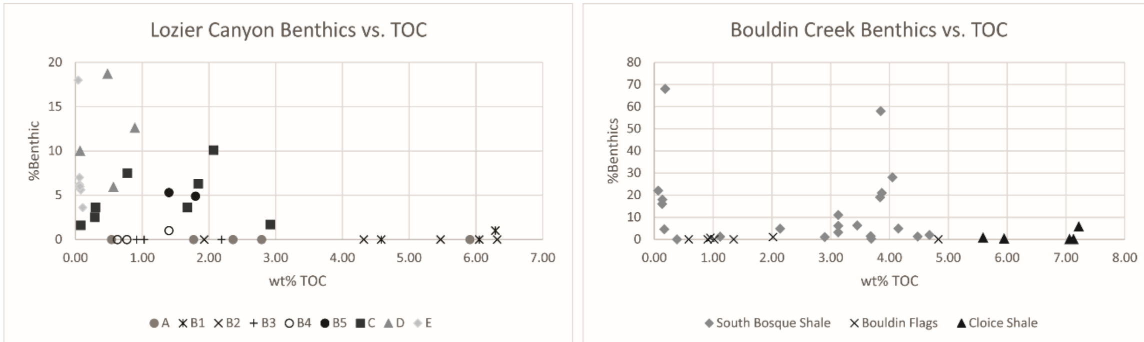

Figure 1.9. Benthic foraminifera abundance vs. TOC cross plots for Lozier Canyon (A) and Bouldin Creek (B). Lozier Canyon is broken up by organic-facies (see Donovan et al., 2012 for detailed discussion): Facies A is lower Lozier Canyon Member, and which is totally barren of foraminifera (in this case, TOC-driven oxygen levels are not the limiting factor for foraminifer abundance); Facies B1 and B2 are the high TOC interval of the upper Lozier Canyon Member; Facies B3, B4, and B5 correspond to the Antonio Creek Member and are transitional from moderately high TOC (B3) to low TOC (B5); Facies C corresponds to the Scott Ranch Member (which corresponds to OAE2); Facies D and E correspond to the lower and upper Langtry Member. Bouldin Creek data is divided by members.

The relationship between benthic foraminifera and carbon isotopes should also be noted. At Lozier, as elsewhere (Figure 4), the positive carbon isotope excursion begins prior to the prominent limestone bed at the base of the Scott Ranch Member (equivalent to Bed 63 at Rock Canyon). At both Rock Canyon and Lozier Canyon, this precursor enrichment coincides with a slight increase in benthic foraminifera prior to the widespread "benthonic zone" at the onset of OAE2 (Elderbak et al., *in press*). The benthonic zone is weakly developed at the Lozier section, but still present.

Benthic foraminifera in the Fasken occur as isolated peaks, rather than a broad high mirroring TOC values. These trends are not artifacts of preservation; the peaks show clear trends of changing abundance in the samples before and after the acme, and the core contains abundant and occasionally well-preserved planktic foraminifera in samples with and without benthics. However, it seems highly unlikely that an epifaunal assemblage reminiscent of relatively shallow, oxic bottom waters would be in situ on an upper slope with high TOC laminated black shale. We believe these peaks in benthic abundance are due to downslope transport from a much shallower, better oxygenated location. Although there is not a concomitant influx of *Heterohelix* with the epifaunal benthics, the presence of quartz grains in some samples, which roughly correspond to benthic peaks, support the interpretation of displaced benthic foraminifera.

It seems likely that surface water productivity is driving organic matter preservation, which is controlling bottom water oxygenation, which in turn is driving benthic foraminiferal abundance and diversity. Long-term change in surface water productivity, we believe, is driven by changes in sea level. We hypothesize the bathymetry-restricted flow into the WIS from the Gulf of Mexico facilitated bathymetry-

induced upwelling of nutrients on and around the Comanche Platform. Wind-driven surface flow over the Stewart City Reef Trend would have brought more nutrients onto the platform, until eventually sea level rose high enough that surface flow would have less and less interaction with bathymetric features, and so upwelling (and productivity/OM content/anoxia) decreased gradually as sea level rose through the late Cenomanian. Alternatively, nutrients may have been supplied by runoff from the Ouachita Highlands to the northeast at this time (Sohl, 1991). We reject this hypothesis because it doesn't explain why TOC decreased as sea level increased, and moreover, we would expect to see an increase in weathering-derived nutrient flux, rather than the observed decrease, with the onset of OAE2 (Jenkyns, 2010).

The area of the Eagle Ford play (Figure 1) is roughly parallel to shelf structure of the southern and eastern Comanche Platform, as might be expected if surface-flow over the buried older reef trends is driving upwelling. We suggest that the margin of the Comanche Platform was a localized upwelling cell that facilitated the production and burial of organic matter responsible for the Eagle Ford play today.

TOC enrichment in the Western Interior, on the other hand, is likely driven by enhanced preservation caused by restriction and stratification (e.g., Arthur and Sageman, 2005). While TOC trends in Texas and the Western Interior may appear to be unrelated events that coincidentally move in parallel, we suggest that the observed changes are related by a common driver: sea level rise. In Texas, Late Cenomanian sea level slowly rose, reducing the effect of surface currents and bathymetry-induced upwelling. Likewise, in the Western Interior, Late Cenomanian sea level rise brought increased communication with the open ocean and decreased stratification, eventually culminating

in a dramatic increase in normal marine taxa and benthic foraminifera (Benthonic Zone), temporarily ventilating the water column (Leckie, 1985; Elderbak et al., in press).

1.6.3 Sea Level Variability/Sequence Stratigraphy

Sea level trends through the Cretaceous are well-known, and have been studied in Texas for over a century (Hill, 1887a,b). Sloss (1963) defined the 1st-3rd order sequences of the region, including the 3rd-order Eagle Fordian sequence. More recent work has further refined local sequence interpretations, as Donovan et al. (2012) described four 4th-order cycles in the Eagle Ford at Lozier Canyon. Planktic and benthic foraminiferal population trends, as well as sedimentary particles (dolomite rhombs, glauconite grains, macrofossil debris, etc.) record sea level changes across the Eagle Ford and serve to augment Donovan and colleagues' conclusions.

Above the disconformity at the top of the lower Cenomanian Buda Limestone, the Lozier Canyon Member records relatively low sea level. This is suggested by the occurrence of stacked hummocks and wave ripples (Donovan et al., 2012), as well as authigenic dolomite rhombs in the base of the member. The formation of these evaporite minerals indicates relatively shallow water depths and hypersalinity in west Texas during basal Eagle Ford time. High evaporation is to be expected in the subtropics during the hottest interval of the Cretaceous, but to explain even local hypersalinity that was strong enough to form evaporites, the Comanche Platform must have been fairly shallow and restricted. The Aptian and Albian reef buildups of the Stewart City Reef Trend probably served as a barrier to communication with surrounding normal marine waters of the Tethys and the brackish waters of the WIS. As sea level rose during the late Cenomanian,

these conditions abated, and gave way to the high productivity conditions described above.

There is no microfossil evidence for the sequence boundary between the Lozier Canyon Member and the Antonio Creek Member. The slight increase in the percentage of benthic foraminifera beginning above the base of the Antonio Creek Member is presumably caused by improving conditions caused by rising sea level as evidenced from sedimentological features (Donovan et al., 2012). Similarly, there is no evidence for a sequence boundary between the Antonio Creek and Scott Ranch Members. Indeed, this level, equivalent to Bed 63 at Rock Canyon in Colorado and Bed HL-1 in Kansas, is conformable and is generally agreed to represent a isochronous flooding surface deposited as sea level rose rapidly and pelagic carbonate sedimentation began (e.g., Hattin, 1975; Meyers and Sageman, 2004; Elder et al., 1994; Tibert et al., 2003; Meyers and Sageman, 2004; Arthur and Sageman, 2005).

The end of the OAE2 carbon-isotope excursion is truncated by a sequence boundary at Lozier Canyon. At Bouldin Creek, on the shallow San Marcos Arch, several nannofossil bioevents are condensed within a meter or less and the entire *W. archaeocretacea* Zone and OAE2 carbon isotope excursion are missing. The *W. archaeocretacea* Zone is also severely truncated at Hot Springs on the western margin of the platform (Frush and Eicher, 1975). This sequence boundary marks the beginning of the Langtry Member (equivalent to the South Bosque in the Austin area), where foraminiferal assemblages show a 4^{th}-order T-R cycle with a decrease in benthic foraminifera toward a maximum flooding surface roughly halfway through the member

(indicated by a nadir in %benthics and %*Heterohelix*) and then increasing toward a second sequence boundary at the top of the Eagle Ford.

The Langtry Member/South Bosque Member records shallower water depths toward the end of the Eagle Ford Cycle as evidenced by the increase in %benthic foraminifera, benthic macrofossils (inoceramids and echinoids), and return to hummocky bedforms. The end of the Eagle Ford Cycle is evident in a large late middle Turonian sea level fall that is equivalent to the Codell Sandstone Member of the Carlile Shale in southern Colorado, Kansas, and New Mexico, and represented as a major unconformity further north in the WIS (Hattin, 1975; Laferriere, 1987; Kauffman and Caldwell 1993; Haq et al. 1987; Hancock and Walaszczyk, 2004). This sea level fall includes an erosional surface at Bouldin Creek and perhaps Lozier Canyon as well, although the data here are equivocal and it could be a lowstand without any erosion. The unconformity is characterized by acmes in %benthic and %biserial planktics, and gaps between nannofossil zones CC11 and CC13. This sequence boundary is immediately overlain by a thin (<1 m) transgressive lag deposit at both locations characterized by a sharp decrease in %benthics and %biserials, and the sudden appearance of glauconite at Bouldin Creek. In the Austin area, this event has been well documented as a "Rubble Zone" at the base of the Austin Chalk, filled with fish debris, glauconite, and phosphate nodules (e.g., Stephenson, 1929; Jiang, 1989; Lundquist, 2000). Some samples in this interval also contain reworked early Turonian taxa (e.g., *Eprolithus octopetalus*). The "Rubble Zone" has traditionally been mapped as part of the basal Atco Member of the Austin Chalk, with the unconformity as the Eagle Ford-Austin boundary. This interval is equivalent to the transgressive upper Turonian Juana Lopez Calcarenite Member of the Carlile Shale, a

similar fossiliferous transgressive lag found in some locations in the WIS (particularly the southern WIS) between the Codell and the Fort Hays Member of the Niobrara Formation.

1.7 Conclusions

1. The Cenomanian-Turonian strata of the Comanche Platform is similar to the southern Western Interior Sea (WIS), repeating paleoecological, geochemical, and lithologic patterns well known from the center of the sea. The Eagle Ford Shale represents a 3rd-order transgressive-regressive sequence that is equivalent to the Greenhorn Cycle in the U.S. Western Interior Basin.
2. The Lozier Canyon and Bouldin Creek outcrop sections of the Eagle Ford on the Comanche Platform bear strong resemblance to sections of the Greenhorn and Carlile formations in the southern WIS based on planktic and benthic foraminiferal trends, including the "Benthonic Zone" at the onset of OAE2 and the "*Heterohelix* shift" during OAE2, dominance of the infaunal benthic foraminifer *Neobulimina albertensis*, and nannofossil assemblages. The Swift Fasken core, located on the South Texas submarine platform, records a deeper, more oceanic setting based on greater abundances of keeled planktic foraminifera, low abundances of *Heterohelix*, and abundances of radiolarians, particularly in the lower Eagle Ford.
3. Organic matter content in the lower Eagle Ford was driven by elevated primary productivity. A local, bathymetrically-induced upwelling cell developed off the southeastern flank of the Comanche Platform, along the South Texas submarine plateau, between the Albian Stuart City (Edwards) and Aptian Sligo shelf margin trends.

4. Total Organic Carbon (TOC) values, nannofossil assemblages, and radiolarian abundances all suggest that peak productivity occurred before the onset of Oceanic Anoxic Event 2 (OAE2), as recorded in the lower Eagle Ford. Productivity waned with rising sea level during the latest Cenomanian as the upwelling cell weakened and/or nutrients became increasingly sequestered in coastal wetlands and estuaries. OAE2 is associated with improved circulation between the Comanche Platform and the Western Interior Sea, and perhaps incursion of an oxygen minimum zone from the Gulf of Mexico.
5. Bottom water oxygenation is correlated to TOC, and benthic foraminifera are very rare or absent where TOC is elevated. The OAE2 interval was associated with improved benthic oxygenation, but the presence of pyrite and dominance of infaunal *Neobulimina* at the Lozier section suggest the persistence of dysoxia at the seafloor and euxinic conditions within the sediments. The post-OAE2 interval at Lozier is marked by improved benthic oxygenation as indicated by greater abundances and diversity of benthic foraminifera and macrofossils.
6. The thickness variability of the Eagle Ford on and adjacent to the Comanche Platform is driven entirely by paleo-water depth and submarine erosion. Shallow sites near the rimming reef buildups or the San Marcos Arch are thinned, due both to lower accommodation and truncation due to relatively shallower water and submarine erosion. Deeper sites off the margins of the platform appear to be conformable and are therefore expanded. It is likely that the western slope sites are also expanded due to siliciclastic input from the adjacent tectonic uplift.

CHAPTER II

REDOX CHANGES ASSOCIATED WITH OAE3 IN COLORADO AND KANSAS

2.1 Abstract

Coniacian-Santonian Oceanic Anoxic Event 3 (OAE3) is the last and least studied of the Mesozoic anoxic events. It is mainly known from the central and South Atlantic, Caribbean region, and the Western Interior US, where it is associated with an abrupt increase in total organic carbon (TOC) and corresponding trace metal indicators for anoxia. However, the nature of redox conditions before this major shift is largely unknown. Were anoxic conditions confined to the sediments, and how was life on the seafloor and in the water column affected by anoxia? Here we present micropaleontological evidence of changing redox conditions before OAE3 and of sustained water column anoxia during OAE3 and deposition of the Smoky Hill Shale Member of the Niobrara Formation in Colorado and Kansas. Benthic foraminifera, which are sensitive to dissolved oxygen and do not typically inhabit anoxic bottom waters, decline prior to the onset of the event in the middle Coniacian, which is marked by a sudden disappearance of benthic foraminifera, followed by a brief recovery and slow decline as anoxic conditions were again reestablished. Steady-state anoxia persisted for nearly 3 myr in the central sea, showing some signs of recovery toward the top of the Niobrara. Our findings suggest that deteriorating conditions eventually reached a tipping point, at which point oxygen concentrations collapsed.

2.2 Introduction

The Mesozoic Era was punctuated with multiple intervals of enhanced organic carbon production and preservation, resulting in the widespread deposition of black shales due to the development of dysoxic to anoxic conditions in the deep sea, on continental margins, and in epicontinental seas (e.g., Schlanger and Jenkyns, 1976). These intervals, termed Oceanic Anoxic Events (OAEs), are globally characterized by a positive excursion in carbon isotopes caused by the burial of vast amounts of isotopically light organic carbon (e.g., Scholle and Arthur, 1980).

The Coniacian-Santonian interval includes the last widespread deposition of black shales in the Mesozoic, termed OAE3 by Arthur and Schlanger (1979). Organic-rich blacks shales from this interval are well documented from the central and South Atlantic, Caribbean, and surrounding epicontinental seas, with well-known localities summarized in Wagreich (2009), including Demerara Rise (ODP Site 1259), the deep Ivoirian Basin (ODP Site 959), the continental shelf off Cote D'Ivoire, Walvis Ridge (DSDP Site 530), Angola Basin (DSDP Site 364), the Maracaibo Basin of Venezuela, and the US Western Interior.

Some of these black shales, like Demerara Rise, are continuous from the Cenomanian-Turonian OAE2 (e.g., Erbacher et al., 2004), while others are shorter-lived and often diachronous (Wagreich, 2012). OAE3 is characterized by a longer (up to 5 myr), more modest (~0.5‰ VPDB) carbon isotope excursion than OAE2 (Wagreich, 2012), although the magnitude of the excursion may be muted by the widespread deposition of chalks that also characterizes this interval (Locklair et al., 2011). The

organic and inorganic carbon burial of OAE3 precedes the general cooling of the Santonian-Campanian (Huber et al., 2002; Friedrich et al., 2012).

Cretaceous strata in the Western Interior Sea (WIS) of North America record both OAE3 and the older, better-understood and more widely distributed OAE2. These two events are expressed very differently from each other in the WIS, and generally record trends that are opposite to that of the contemporaneous world ocean. The OAE2 interval in the WIS records the transition from low oxygen conditions prior to the event to well-oxygenated conditions as the event began (e.g., Eicher and Worstell, 1970; Leckie et al., 1998), while elsewhere the opposite trend is observed. OAE3 in the WIS is represented by anoxia and organic carbon burial in what is now a significant hydrocarbon play (the Niobrara Fm.) during a time when many marine basins of the world record increasing oxygen (e.g., Locklair et al., 2011).

These differences make the WIS an important and potentially illuminating region for the overall evolution of Late Cretaceous oceanography and climate. Trace metal geochemistry from the upper Turonian-lower Campanian Niobrara Formation recovered in the Encana Aristocrat-Angus core in the Denver Basin suggests a rapid onset of euxinic (i.e., anoxic and sulfidic) conditions coincident with an increase in total organic carbon (TOC) and a modest carbon isotope excursion that records the regional onset of OAE3 (Figure 1; Locklair et al., 2011; Joo and Sageman, 2014). Unfortunately, trace metal proxies can only detect fully anoxic conditions and cannot provide information about where in the water column or sediments anoxia occurred. It is not clear from existing data whether the decline in dissolved oxygen was really as abrupt as suggested by trace metals, or what effect these conditions had on organisms living in the WIS.

Foraminifera, marine protists with a readily preservable shell, or test, are often used to ascertain changes in redox conditions (e.g., Bernhard, 1986), and the presence or absence of taxa that occupy various ecological niches can yield information about where in the water column or sediments these changes occurred. Here we present planktic and benthic foraminifer paleoecological data spanning the onset and duration of OAE3 in the central part of the sea from two cores near the Colorado Front Range and a classic series of outcrops in western Kansas to determine: 1) if there is any evidence for changes in dissolved oxygen prior to the onset of OAE3; 2) whether anoxia was limited to bottom waters or whether it intruded into the upper water column; and 3) the biotic response to these changes.

2.3 Locations

The Western Interior Basin records five third-order sea level cycles during the Cretaceous (Kauffman, 1984). A late Turonian-Coniacian transgression deposited hemi-pelagic chalks and marls across the Western Interior basin from the Tethyan margin of Texas through Boreal Canada (Kauffman and Caldwell, 1993). Carbonate-rich sediments in the central and eastern part of the sea (Colorado-Kansas) comprise the Niobrara Formation. The Fort Hays Limestone Member represents the maximum transgression of the Niobrara Sea, while the three chalky units of the overlying Smoky Hill Member represent three fourth-order transgressive pulses (Hattin and Cobban, 1977).

In central Colorado and western Kansas, the Fort Hays is comprised of thick beds of limestone and much thinner beds or seams of interbedded shale. The Smoky Hill varies on roughly decimeter scale between organic-rich marls and organic-poor limestones. Scott and Cobban (1964) assigned these beds to seven informal units: lower

shale and limestone, lower shale, lower limestone, middle shale, middle chalk, upper chalky shale, and upper chalk. The boundaries of these informal units are generally considered to be synchronous across the Colorado-Kansas area (Hattin, 1982).

2.3.1 Portland Core

In June of 1992, the USGS #1 Portland Core was drilled in the Cañon City Embayment near the town of Florence, CO, as part of the Western Interior Drilling Project (Fig. 1; Dean and Arthur, 1998). The upper portion of the core recovered a 78.6-m section of the lower Niobrara Fm., including the Fort Hays Limestone and the lower shale and limestone, lower shale, lower limestone, and middle shale units of the Smoky Hill (Dean and Arthur, 1998).

2.3.2 Aristocrat Angus Core

Encana Energy's Aristrocrat Angus #1 Core, located in a productive hydrocarbon zone in Weld Co., CO, in the Denver Basin (Fig 1), recovered a complete section of the Niobrara Fm., which was donated to Northwestern University for scientific study. Trace metal data summarized in Figure 1 demonstrate the broad changes of redox conditions through the OAE3 interval, which begins at the base of the lower shale unit of the Smoky Hill (Figure 1). In particular, these data show an abrupt increase in Mo at the base of the lower shale, indicating euxinia (e.g., Tribovillard et al., 2006), coincident with a sudden increase in TOC. This is preceded by a decrease in Mn, which is generally enriched in oxic environments but can be complicated by other factors (e.g., Tribovillard et al., 2006), suggesting – but not proving – a decrease in oxygen below this level (Locklair et al., 2011). Bulk organic carbon stable isotopes for the Angus Core show a small, short excursion beginning above the base of the lower shale (Joo and Sageman, 2014).

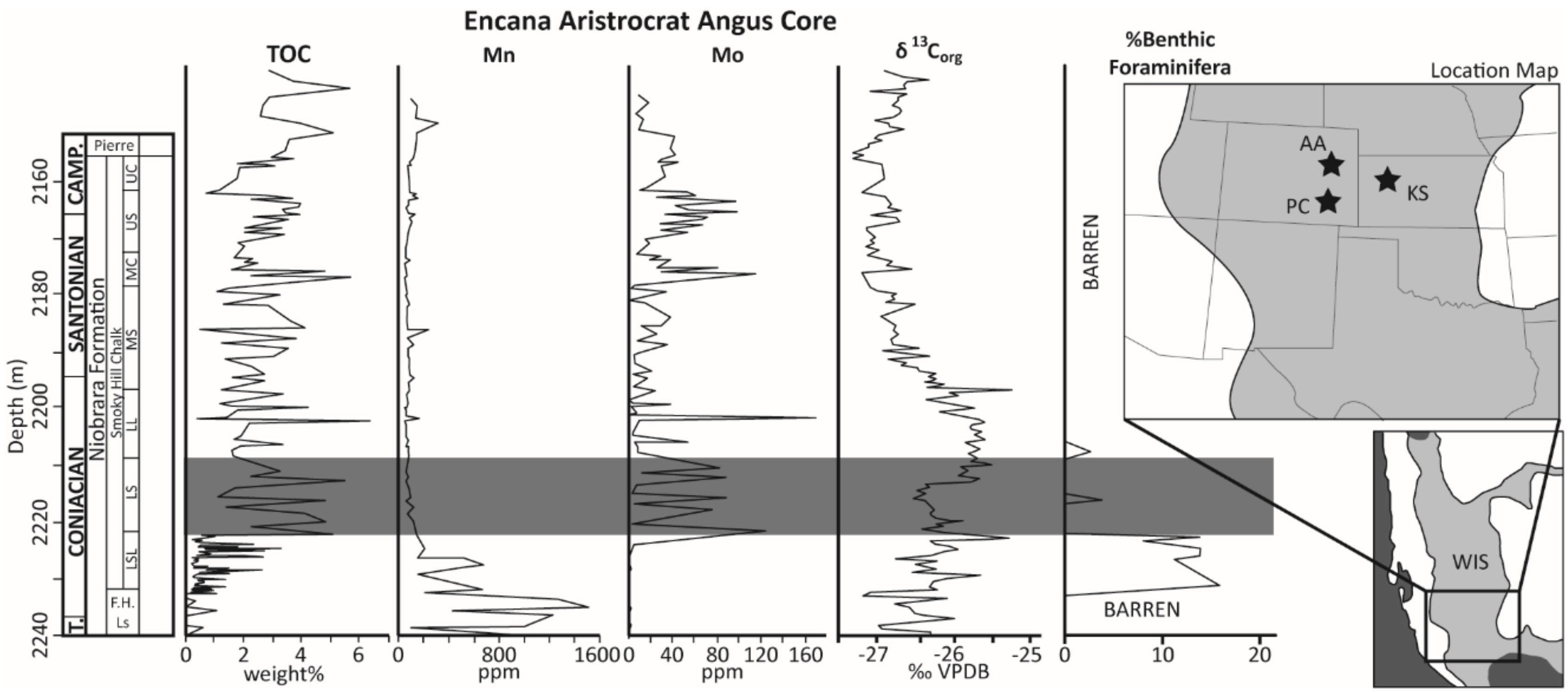

Figure 2.1. Location map and geochemical and benthic foraminiferal data for the Aristorcrat Angus Core. See text for discussion. TOC, Mn, and Mo are redrawn from Locklair et al., 2011; $\delta^{13}C$ redrawn from Joo and Sageman, 2014. AC= Aristocrat Angus Core; PC = Portland Core; KS = Kansas outcrops. WIS map and inset both redrawn from Blakey, showing early Coniacian HST. Gray bar denotes lower shale unit. Ammonite biozones abbreviations: *P.h.*, *Prionocyclus hyatti*; *P.g.*, *P. germari*; *S.m.*, *Scaphites mariasensis*; *S.p.*, *S. preventricosis*; *S.v.*, *S. ventricosus*; *C.v.*, *Clioscaphites vermiformis*; *D.e.*, *Desmoscaphites erdmanni*; *D.b.*, *D. bassleri*; *S.l.*III, *Scaphites leei* III; *S.h.*I, *Scaphites hippocrepis* I.; *S.h.*II, *S. hippocrepis* II; *S.h.*III, *S. hippocrepis* III.

2.3.3 Kansas Outcrops

The Niobrara Fm. in western Kansas is exposed in a series of low-relief outcrops, from which Hattin (1982) constructed a composite section comprised of 25 outcrops along the Smoky Hill River, south of Interstate 70 (Fig. 1). These outcrops are significantly more carbonate-rich than correlative sections in eastern Colorado, with chalk being the dominant lithology and the less carbonate-rich layers consisting of chalky marl. Carbonate content increases to the east, with maximum carbonate content near the eroded feather edge of the Niobrara Fm. in central Kansas (Hattin, 1982).

The only paleoecological contributions on the Colorado-Kansas Niobrara Fm. are by Frerichs and Dring (1981) and Martinson et al. (1998). These authors suggest that either bottom water anoxia or sea level variability, respectively, were the dominant control on benthic foraminiferal abundance.

2.4 Methods

Foraminifera were sampled at approximately 1-m resolution in both cores and all nine outcrop localities. Samples from the Fort Hays include only limestones and not shale interbeds. Samples were soaked, sieved, dried, and picked following standard techniques discussed in Lowery et al. (2014). Samples were picked from the >63 micron size fraction to obtain a population of at least 300 individuals, which were divided into major paleoecological groups (i.e., total benthic, biserial planktic, and keeled planktic). Keeled planktic foraminifera are consistently of very low abundance throughout the section (<1% in nearly every sample), and are reported as simple diversity (i.e., number of species present) in order to provide some record of their response to ecosystem changes.

2.5 Results

2.5.1 Angus Core

Unfortunately, poor preservation of foraminifera in the Angus Core meant that useful population data were only recovered from the lower shale and limestone unit of the Smoky Hill. Organic-rich intervals of the Smoky Hill often do not contain any visible carbonate grains, while the chalky units are composed of crystalline calcite. The Fort Hays Limestone is also completely recrystallized, with euhedral calcite crystals visible under the microscope. Equivalent units across the Western Interior Basin contain rich assemblages of foraminifera, and the main difference in the Angus Core is depth of burial. These strata come from 2200 m below the surface in a producing hydrocarbon zone, so it is most likely that the lack of foraminifera is due to diagenesis.

The one exception is the lower shale and limestone, which contains a diverse assemblage of foraminifera (Figure 1). Benthic foraminifera comprise up to 15% of the total foraminiferal assemblage, which is greater than the abundance of benthics in the lower chalky shale at other sites. If the foraminiferal population was affected by post-depositional dissolution, it is likely that it would result in a higher percentage of benthics, which are generally larger and more robust and thus more likely to resist dissolution than the small, porous planktics.

2.5.2 Portland Core

Preservation in the USGS Portland #1 Core is much better, likely due to its much shallower depth of burial. The Fort Hays Limestone has generally elevated %benthic values (~10-15%), with the highest values at the base of the member (Figure 2). The lower limestone and shale unit of the Smoky Hill Chalk shows a marked decrease to ~5% benthics. The lowermost sample in the lower shale is completely barren of foraminifera.

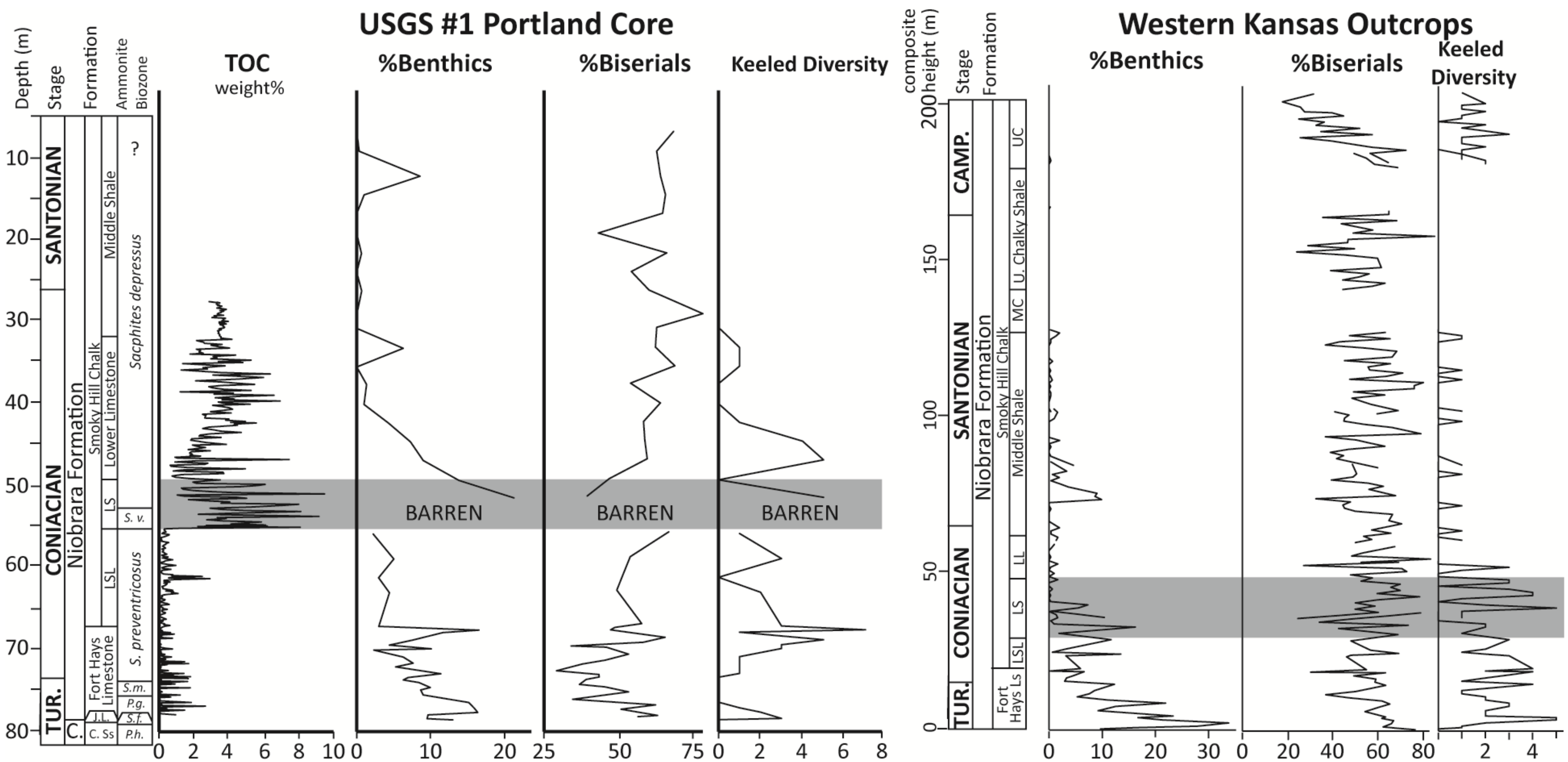

Figure 2.2. TOC and foraminiferal abundance data for USGS Portland #1 Core and foraminiferal abundance data for Kansas outcrop composite section. See text for discussion. Portland Core TOC from Locklair et al., 2011. Gray bar denotes lower shale unit. Ammonite biozones abbreviations: *P.h., Prionocyclus hyatti*; *P.g., P. germari*; *S.m., Scaphites mariasensis*; *S.p., S. preventricosis*; *S.v., S. ventricosus.*

Above this level, %benthics peak to their highest abundance in the core (21%), and then gradually decline through the rest of the lower shale and into the lower limestone unit, eventually reaching zero around 40 m. Above this level, two widely separated samples contain a few benthics, while several others contain single individuals.

Keeled planktic foraminiferal diversity follows roughly similar trends. The lower Fort Hays has few keeled species. Values quickly increase toward the top of the member, before declining again in the lower chalk and shale unit. Immediately after the barren interval the values peak but then fall to zero before recovering in the next sample and staying elevated, and then declining over the next 5 m or so. This decline follows the same pattern as the relative benthic abundance trend but lags by about 5 m. Biserial planktic foraminifera show meter-scale oscillations, but generally hover around 50% of the total planktic assemblage for the entire core.

2.5.3 Kansas Outcrops

Foraminiferal trends in Kansas are very similar to those observed in the Portland Core, and extend our dataset through the upper part of the formation (Figure 2). This 200-m interval is a composite section of nine outcrops along a roughly 50-mile length of the Smoky Hill River. Trends in overlapping sections tend to be similar. Like the Portland Core, benthic foraminifer abundance peaks in the lower Fort Hays Limestone, and declines in the overlying lower shale and limestone unit. Unlike the Portland Core, there are no barren samples in the lower shale, at least within our 1-m resolution, and %benthic values jump right into the brief recovery seen in the Portland Core. At this level there is a section break, and the top few samples of Locality 1 show extremely low %benthics, while the bottom few samples of Locality 17, which are stratigraphically equivalent,

show relatively elevated samples. The uppermost part of the Kansas outcrops are the most weathered, and often display lower values than stratigraphically equivalent samples in other outcrops. If this is taken into account, %benthic values decrease in the same way that they do in the Portland Core. Above the lower shale, benthics are rare or absent, briefly recover for several samples around 70 m to around 10% and then decline again to 1-2% of total foraminifera before trailing off to zero in the lower part of the middle chalk unit. With the exception of two individuals, they are not present in the rest of the section.

Keeled planktic foraminifer diversity also follows a similar pattern as in the Portland Core, with few to no keeled species in the lowermost Fort Hays, a rapid increase to a peak in the upper Fort Hays, a general decrease through the lower shale and limestone and then a recovery and brief plateau above the middle part of the lower shale. Keeled diversity remains elevated above the stratigraphic level that benthic foraminifera begin to decrease, although here there is considerable meter-scale variability. In the middle shale, keeled diversity decreases before reaching zero in the upper part of the Smoky Hill. Unlike benthics, however, keeled planktics return in the upper chalk. Biserial planktic foraminifer abundance in Kansas is generally around 60% of the total planktic assemblage, and oscillate about 10% on roughly meter-scale.

2.6 Discussion

Foraminiferal paleoecology in the Fort Hays Limestone Member suggests a likely response to relative sea level change; higher %benthics and low keeled diversity in the lower Fort Hays give way to lower %benthics and higher keeled diversity toward the top of the member, which records the highstand of the Niobrara Cycle (Kauffman, 1984). In the lowermost Smoky Hill Shale Member, the lower shale and limestone unit, %benthic

values continue to decrease, even though relative sea level may have been falling at that time and an opposite trend in %benthics might be expected. Benthic foraminiferal abundances of ~5% (Portland Core and Kansas) and 10-15% (Angus Core; possibly artificially high due to preferential preservation of benthics) are far too low for a shallow sea that was ~100-150 m deep during maximum transgression (Arthur and Sageman, 2005), and likely shallower, though perhaps not normal marine; in the modern ocean %benthic values of 10% or less are indicative of upper to middle bathyal depths (500-1000 m; e.g., Culver, 1988; Leckie and Olson, 2002), at least in oxic conditions. In addition to possible dissolved oxygen influences on benthic foraminiferal abundances, food supply is also a major control on benthic assemblages (e.g., Jorissen, 2007). However, organic carbon was preserved in the sediments, suggesting that food was not a limiting factor on benthic life. Changing salinity could also affect benthic assemblages, especially if riverine runoff induced a stable stratification of the water column, which in turn could have reduced seafloor oxygenation. However, reduced salinity would also directly affect planktic assemblages, and we would expect to see a large increase in the proportion of biserial planktics, opportunistic taxa that thrive when other species are stressed. The fact that biserials stay relatively constant, and their small-scale fluctuations don't track benthic abundances, suggests that salinity stratification was not the primary reason for low benthic foraminiferal abundances.

This leaves changes in dissolved oxygen as the most likely primary environmental stress on benthic foraminifera in the Smoky Hill Shale. The extremely depressed and declining %benthic values in the lower shale and limestone at all three sites suggest a decline in benthic oxygen concentrations before the onset of anoxia as indicated by trace

metal markers and elevated TOC values. The lowest sample in the lower shale is barren in the Portland Core, and represents a nadir in benthic abundance in Kansas. Immediately above this level %benthics peaks and then begins a slow decline. Keeled planktic foraminiferal diversity follows a similar pattern, but the decline begins later than the decline in benthics. This suggests that growth of an oxygen minimum zone starting on the seafloor (at 100-150 m, roughly the upper depth limit of oxygen minimum zones in the open ocean) and expanding upward in the middle part of the water column, where keeled planktics lived.

Following a brief recovery in the upper part of the lower shale and into the lower limestone, benthic and keeled planktic foraminifera decrease, with occasional brief, one-off repopulation events – oxygenation events, perhaps caused by strong storms in the sea (e.g., Friedrich, 2010). This steady state persists through the top of the Smoky Hill Chalk in the Kansas outcrops, equivalent to ~3 myr, during which time TOC remains elevated and almost no benthic foraminifera live in the relatively deep central axis of the Niobrara Sea.

The pattern seen in the Smoky Hill Shale – slow decline, sudden crash and then, eventually, a new steady that persists for millions of years – suggests a hysteresis-like relationship with low oxygen concentrations or their underlying cause. Slowly declining oxygen in the central sea reached a threshold that suddenly shifted the system into a new normal; some internal feedback caused a brief recovery before settling into a steady state that became entrenched for some 3 million years. The onset of OAE3 – and perhaps, by extension, other OAEs – was not as abrupt as it appears from the lithologic and

geochemical record; slow changes and threshold values may play a larger role in the development of anoxia, at least in restricted basins, than previously thought.

A fluctuating strandline along the western edge of the sea during Coniacian-Santonian time (e.g., Molenaar et al., 2002) suggests that relative sea level changes may be responsible for fluctuating carbonate content of the Smoky Hill Member, but this was not the principle driver of anoxia at the seafloor, which was largely independent of carbonate content. Increased riverine runoff (as evidenced by palynomorph assemblages; Da Gama et al., 2014) and nutrient input during the regression of the Niobrara Sea likely drove marine productivity and excess organic matter flux to the seafloor creating oxygen stress to the benthos and anoxic to euxinic conditions, which were exacerbated by increasing restriction of the sea as long-term sea level fell.. This is particularly true in the central and eastern parts of the sea, which were bathed in warm, oxygen-poor Tethyan water (Arthur and Sageman, 2005). Sites on the western margin of the Niobrara Sea saw little change in benthic populations (e.g., Kent, 1968; De Gama et al., 2014), as cool, well-oxygenated Boreal waters and shallower water depths kept the western margin more habitable for benthic life. The mechanisms of hypoxia development in shallow seas have major implications for restricted environments such as the US western interior sea, as well as continental shelves, a topic as relevant to future change as it is to the past.

2.7 Conclusions

1. A long (~3 myr) period of organic-rich shale deposition and bottom-water anoxia, as evidenced by a lack of benthic foraminifera and concurrent changes in redox sensitive trace metals, characterizes much of the Smoky Hill Shale Member of the Niobrara Fm. This interval corresponds to Oceanic Anoxic Event 3.

2. Prior to the “onset” of OAE3, defined by an abrupt increase in TOC, abnormally low abundance of benthic foraminifera suggests a gradual decrease in dissolved oxygen.
3. A rapid shift to anoxia in the lower Smoky Hill Shale was preceded by a slow decline in benthic dissolved oxygen suggesting that a threshold condition drove the depositional system of this restricted basin into a new steady state. High organic matter production/preservation and bottom water anoxia or euxinia persisted virtually unchanged for at least 3 million years during the post-Ft. Hays regression.
4. Anoxia and TOC enrichment in the middle part of the sea was made possible by increased riverine nutrient flux, the presence of warm, low-oxygen Tethyan waters in the central and eastern parts of the sea, and the overall restricted nature of the WIS during the regressive phase of the Niobrara cycle.

CHAPTER III

PALEOCEANOGRAPHIC CONTROLS ON THE DEVELOPMENT OF ANOXIA IN THE NIOBRARA SEA

3.1 Abstract

The Cretaceous Western Interior Sea (WIS) of North America contains excellent records of the Cenomanian-Turonian Oceanic Anoxic Event (OAE) 2 and the Coniacian-Campanian OAE3. However, the expression of these events differs greatly between in terms of lithology, dissolved oxygen concentrations, organic matter preservation, resulting in vastly different environments for marine life. OAE2 is associated with transgression and generally improving oxygenation and salinity, and low organic matter concentration in the WIS, while OAE3 is associated with regression, high organic matter preservation, and declining oxygenation. Foraminifera, which are sensitive to changes in dissolved oxygen and are commonly used to track water mass changes, are uniquely suited to study changes in paleoceanographic conditions in the WIS. This paper synthesizes new and previously published planktic and benthic foraminiferal data, clay mineralogy, and geochemistry across the southern portion of the Western Interior Sea, from Wyoming to Texas and Kansas to western Colorado through the Turonian-Campanian Niobrara sea level cycle, in order to understand changes in paleoceanographic conditions before and during OAE3 in order to understand why it differs from OAE2, and to determine whether a common mechanism controls organic carbon burial during both events.

Foraminiferal data reveal several important trends across the epicontinental sea: 1) during the transgression of the Niobrara Sea in the middle and late Turonian (Juana

Lopez Calcarenite, Montezuma Valley Shale and its equivalent Sage Breaks Shale) benthic foraminiferal abundance generally increases, and as transgression continues keeled foraminifera begin to invade the central and eastern portions of the study area. 2) As the transgression slows in the early Coniacian and reverses into regression, so too do the previously increasing markers for oxygenation reverse, slowly declining until a point in the middle Coniacian *Scaphites ventricosis* ammonite zone, equivalent to the base of the lower shale unit of the Smoky Hill, where they rapidly shift, briefly recover, and then drop again to zero, suggesting benthic and deep water column anoxia. 3) On the western margin of the sea, the transgression is also associated with increasing abundance and diversity of benthic foraminifera. During regression, a slow decline is not observed, but a barren interval develops across several sites in NW Colorado, followed by a brief recovery characterized by very low diversity, and then a rapid decline to a long interval with no benthic foraminifera, similar to the Front Range. 4) Clay mineralogy at Mesa Verde shows a correspondence between periods of foraminiferal abundance and increased discrete illite and chlorite, two clay minerals associated with mechanical weathering in cold, dry conditions, and thus likely from a northern source. Periods of low to zero foraminifera correspond to high kaolinite, which is associated the chemical weathering of feldspars in warm, moist conditions, and therefore likely local to the southern part of the seaway. Taken together, these data suggest that falling sea level restricted the flow of open ocean waters into the WIS, slowing circulation, which was driven by the interplay between Boreal and Tethyan water masses. When sea level was high and circulation between Boreal and Tethyan water masses was active, they mixed to form a third, denser water mass that sank and flowed out of the sea, ventilating the

benthos on its way. Relative sea level, therefore, is the ultimate primary control on the redox state of the WIS. Thus global events are preserved through the filter of local sea level history in an active tectonic foreland basin: OAE2, despite representing a global interval of widespread anoxia, is associated with sea level rise, and so was generally ventilated in the WIS; OAE3, despite representing a global interval of increasing oxygenation, is associated with sea level fall, and so was generally anoxic in the WIS.

3.2 Introduction

The Western Interior Sea (WIS) of North America spans a large interval of the Cretaceous, and records five second-order sea level cycles (Kauffman, 1984). Each of these cycles is exposed in countless outcrops along the entire expanse of the WIS, from Mexico to Canada and from Utah to Kansas, and as such the WIS records a long and dynamic history of paleoceanographic investigations (e.g., Gilbert, 1895; Eicher and Worstell, 1970; McNeil and Caldwell, 1981; Kauffman, 1984; Pratt, 1985; Kauffman and Caldwell, 1993; Pratt et al., 1993; Slingerland et al., 1996; Dean and Arthur, 1998a; Leckie et al., 1998; Longman et al., 1998; Schröder-Adams et al., 1998; West et al., 1998; Meyers et al., 2001; Molenaar et al., 2002; Snow et al., 2005; Nielsen et al., 2008; Locklair et al., 2011; Sageman et al., 2014; Corbett et al., 2014; Elderbak et al., 2014; Schröder-Adams, 2014). The oceanographic history of the southern portion of the sea is perhaps best known from the Cenomanian-Turonian Greenhorn Cycle, the highstand of which represents the maximum transgression of the WIS and the highest sea levels of the Mesozoic (Vail et al., 1977; Hancock and Kauffman, 1979; Haq et al., 1987; Hardenbol et al., 1998; Haq, 2014)

The WIS was less than normal marine during much of its history, as evidenced by a dearth of normal marine macrofauna (e.g., echinoids, corals, bryozoans; Kauffman, 1975, 1984; Leckie et al., 1998). When sea level was low, a shallow carbonate platform in Texas acted as a sill, separating the WIS from the Gulf of Mexico (Lowery et al., 2014). During transgressions, rising sea level eventually overcame this sill and allowed normal marine water from the south to enter the sea, bringing with it salinity-sensitive macro- and microfossils (Cobban and Reeside, 1952; Eicher and Worstell, 1970; Kaufmann, 1977; McNeil and Caldwell, 1981; Eicher and Diner, 1985; Bralower, 1988; Caldwell et al., 1993; Watkins et al., 1993; Leckie et al., 1998). These normal-marine organisms first colonized the deep central axis of the sea, which was located along what is now the Front Range of the Rocky Mountains, from northeast New Mexico to southeast Wyoming (Eicher, 1969; Sageman and Arthur, 1994). During the Cenomanian-Turonian Greenhorn and Turonian-Campanian Niobrara sea level cycles of the Western Interior, marine incursion during sea level transgression/highstand also coincides with the deposition of carbonate-rich lithologies across the sea: hemi-pelagic carbonates through the central and eastern portions of the sea, with correlative concretion horizons and marls along the western side, which was proximal to the Sevier Highlands and received high terrigenous flux (e.g., Kauffman, 1984).

The Greenhorn Cycle coincided with Oceanic Anoxic Event 2, a period of enhanced organic matter production that caused widespread marine anoxia (no dissolved oxygen) widespread organic carbon preservation and black shale deposition across the world ocean, and represented a major perturbation of the carbon cycle (Schlanger and Jenkyns, 1976). During this time, the WIS was out of phase with the global trend of

OAE2, with high organic matter and dark-gray shale prior to the event and abrupt oxygenation at the onset followed by declining oxygenation through the latter part of the event. The abrupt improvement in benthic conditions at the onset of OAE2 coincided with the normal marine incursion described above (e.g., Pratt and Threkeld, 1984; Meyers et al., 2005). Although substantial anoxia didn't characterize the seaway during OAE2, the WIS did feel the effects of OAE2 as the warm southern waters brought in a low oxygen water mass from regions where anoxia did develop, which resulted in hypoxic (i.e., a qualitative physiological state of low-oxygen stress) conditions that curtailed diversity (e.g., Leckie, 1985; Eicher and Diner, 1985; Leckie et al., 1998; Caron et al., 2006; Elderbak et al., 2014).

Following regression in the middle Turonian, which signaled the end of the Greenhorn Cycle, a rapid late Turonian transgression began the final truly marine sea level cycle of the WIS, the Turonian-Campanian Niobrara cycle. The Niobrara coincides with the youngest Oceanic Anoxic Event (OAE) of the Cretaceous, the enigmatic Coniacian-Campanian OAE3 (Arthur and Schlanger, 1979). The WIS contains one of the best-known records of OAE3 (e.g., Scholle and Arthur, 1980; Dean and Arthur, 1998b; Locklair et al., 2011; Lowery et al., in prep), known mainly from the Niobrara Formation, a carbonate-rich sequence of limestones and shales deposited along the deep central axis of the sea. Unfortunately, the oceanographic trends which are so well-known from the Greenhorn Cycle break down for the Niobrara.

The Niobrara Sea was smaller than its predecessor (e.g., Molenaar et al., 2002), and yet it was much more carbonate rich, even well into the late Coniacian-early Campanian regression. The Coniacian-Santonian was a global period of enhanced

carbonate production (e.g., Locklair et al., 2011) but the mechanism for this carbonate production in the WIS is not known. Carbonate lithologies, which are chiefly composed of coccoliths, are generally associated with carbonate-rich southern waters that brought the nannoplankton into the sea (e.g., Caldwell et al., 1993; Longman et al., 1998). OAE3 is locally associated with enhanced organic carbon production and anoxia (e.g., Locklair et al., 2011; Lowery et al., in prep), unlike OAE2, which is not associated with much local organic carbon burial and only got second-hand anoxia from the incursion of a low-oxygen water mass. OAE3 is also associated with a sea level fall, unlike the late transgression that is coincident with OAE2 (e.g., Kauffman, 1984).

So what was going on in the Niobrara Sea? The earliest hypothesis, by Gilbert (1895), postulated that wet/dry climate cycles driven by orbitally-forced insolation changes caused dilution of carbonate production and resulted in the observed limestone/shale lithologies of the Niobrara. More recent work has expanded upon this hypothesis, with several oceanographic models suggesting, alternatively, siliclastic dilution or increased or decreased productivity due to circulation changes or stratification, all driven by changes in freshwater flux into the sea (e.g., Fisher, 1991; Hay et al., 1993; Slingerland 1996). Foraminifera are powerful tools for studying water mass, salinity, and redox changes, but have not yet been rigorously applied to this problem. We synthesize new and published foraminiferal and geochemical datasets from 10 sites across the southern Western Interior Sea, from Wyoming to Texas and western Colorado to Kansas (Figure 1) to understand the oceanographic history of the Niobrara Sea, and address the following questions: 1) What caused the increased production/preservation of organic matter and development of anoxia? 2) Why is the western side of the sea different from

the central and eastern sides? 3) Why was the Niobrara Cycle more carbonate rich, despite being more restricted?

3.3 Background

3.3.1 Tectonics

The Western Interior Sea, which ran from the Canadian Arctic to Mexico, was a tectonically created basin in which sea level and sediment accumulation was ultimately controlled by the high rates of tectonic activity in the Late Cretaceous (e.g., Gurnis, 1993). The subduction of the Farallon Plate beneath the western boundary of the North American Plate induced mantle-flow driven dynamic subsidence that pushed the region below sea level, regulated accommodation, and, along with eustasy, ultimately controlled stratigraphy and sea level cycles within the WIS (Pang and Nummendal, 1995; Liu and Nummendal, 2004; Liu et al., 2005, 2008, 2011, 2014). Superimposed on this mega-regional structural control, and driven by the same overall forces, terrane accretion on the western margin of North America drove the Sevier Orogeny, characterized by a narrow fold and thrust belt along the western shore of the WIS (e.g., Armstrong, 1968; Schwartz and DeCelles, 1988). Load thrusting along the Sevier Mountains drove flexural subsidence which, superimposed on epeirogenic subsidence, formed a foreland basin along the western margin of the WIS (Pang and Nummendal, 1995; Liu et al., 2014). The thickest sediments in the WIS are found in this foreland basin, due to proximity to the sediment source (i.e., the Sevier Highlands) and very high accommodation (e.g., Weimer, 1978; Ryer and Lovekin, 1986; White et al., 2002). Individual thrusting events are linked to sea level transgressions across the sea (Kauffman, 1984; Villien and Kligfield, 1986; Elder et al., 1994; Pang and Nummendal, 1995; Liu et al., 2014).

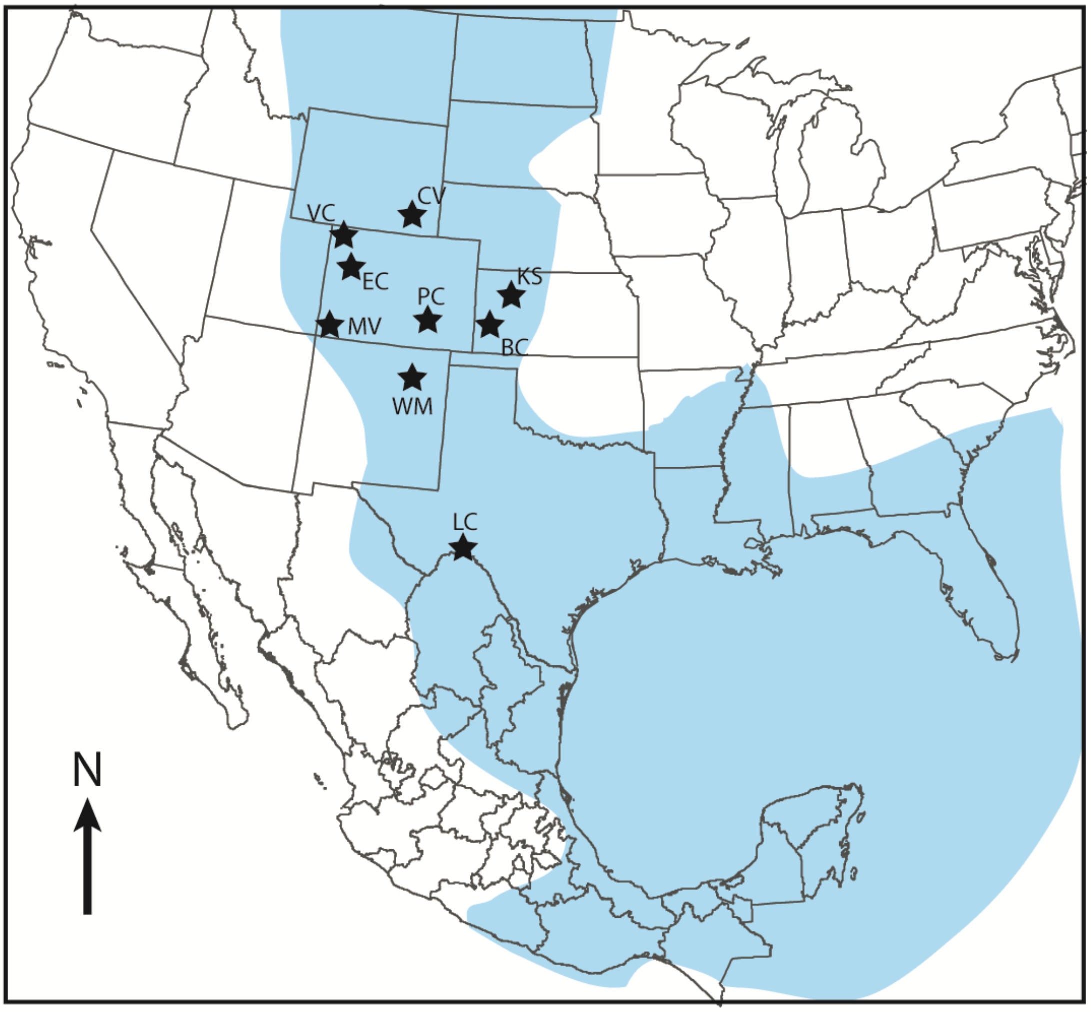

Figure 3.1. Location Map showing the early Coniacian maximum transgression of the Niobrara Sea. From North to South, sites are: CV, Centennial Valley; VC, Vermillion Creek; EC, Elk Creek; KS, Kansas outcrops; PC, USGS #1 Portland Core (~15 miles west of Pueblo reference section); BC, Amoco Rebecca Bounds #1 Core; MV, Mesa Verde; WM, Wagon Mound; LC, Lozier Canyon. Modified from Merewether et al., 2011.

The tectonically-driven bathymetry of the WIS can be generalized as a deep western foreland basin with high terrigenous flux in Arizona, Utah, and western Colorado and Wyoming, a deep central axis along the modern Colorado Front Range, and a stable eastern “hinge zone” of slowly declining subsidence rates attached to the stable central craton of North America (Figure 2; Kauffman, 1984).

3.3.2 Sea Level and Lithology

Hancock and Kauffman (1979) and innumerable subsequent authors have shown that Western Interior third-order sea level cycles are generally synchronous with global eustatic cycles throughout the Cretaceous (Figure 2). If Cretaceous eustasy was largely driven by elevated seafloor spreading rates (e.g., Larson, 1991a,b), then changes in these rates would also have caused changes in the rate of subduction of the Farallon Plate beneath North America, which would then have caused changes in the rates of dynamic subsidence and tectonically-induced sea level changes in the WIS; indeed, times of eustatic rise are generally correlated with active plutonism/volcanism in the WIS (Kauffman, 1984). It is therefore difficult to say for sure whether eustasy or local tectonism was the primary control on sea level in the WIS, or whether it is even possible meaningfully differentiate the two.

The primary tectonoeustatic sea level fluctuations in the WIS are roughly 10 myr in duration, and therefore equivalent to 3rd-order sea level cycles (Figure 2; e.g., Vail et al., 1977). These sea level cycles were the primary control on sedimentation in the Western Interior, expressed as a regionally-correlative fining-upward sequence of clastics and increasingly calcareous facies during transgressive and highstand systems tracks, and the same facies sequence in reverse during regression (Kaufmann, 1984). Transgressions

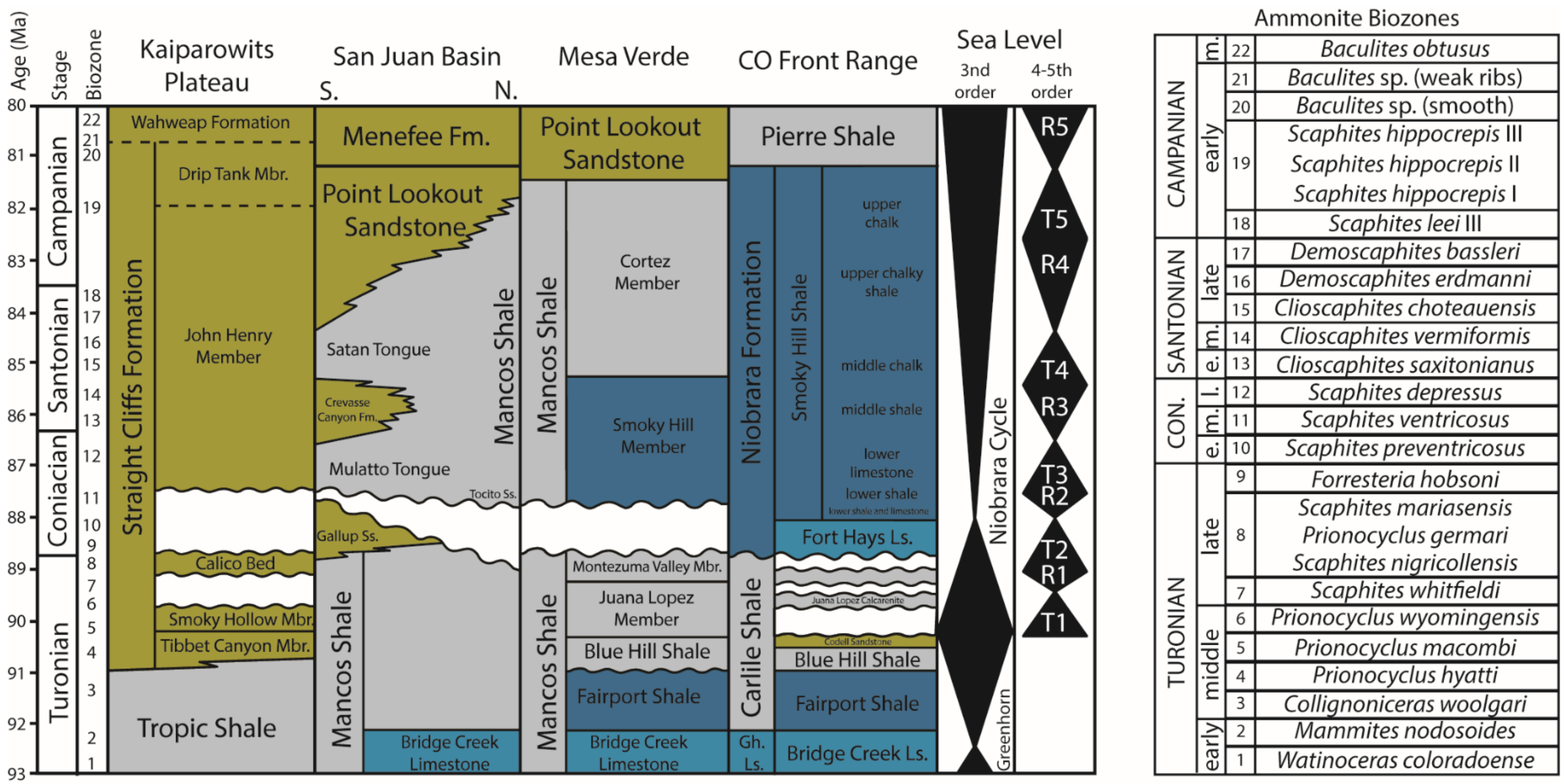

Figure 3.2. West-to-east summary of stratigraphy, sea level change, and biostratigraphy of the Greenhorn and Niobrara Cycles. Yellow represents sandy facies, dark blue represents calcareous shales, light blue represents hemi-pelagic limestone, and white represents marine shales. Gray areas represent unconformities. Note multiple unconformities during Niobrara transgression, as well as the fact that western areas that were marine shale during the Greenhorn are shoreface or terrestrial sands during the Niobrara, suggesting the seaway was much smaller. Stratigraphy and correlations after Leckie et al., 1997; sea level cycles after Kauffman, 1984; Ammonite biozones after Leckie et al., 1997 and Merewether et al., 2011.et al., 2011.

are more commonly cut with unconformities than regressions, which are generally more complete (Kauffman, 1969, 1977, 1984). Transgressive and highstand facies in the central axis and eastern portion of the basin are characterized by hemipelagic carbonates, with gradually decreasing carbonate content toward the foreland basin to the west, which was characterized by a thick accumulation of medium- to fine-grained clastic sediments (McGookey et al., 1972; Kauffman, 1984).

3.3.3 Climate and Circulation

Regional, climate-induced sedimentary signals are super-imposed on the global tectonoeustatic sea level cycles as 4^{th}-5^{th} order cycles on Milankovitch time scales (e.g., Meyers et al., 2001; Locklair and Sageman, 2008). Cyclic changes in sedimentation on 1-10 m scales are very common in the WIS, and are commonly expressed as couplets of, for example, limestone and shale (Kauffman, 1984). Lithologic cycles in the Western Interior were first recognized by G.K. Gilbert in 1895, who proposed climate-controlled changes in terrigenous flux as a dilution mechanism to explain limestone-marl cycles in the Niobrara Formation. More broadly, changes in precipitation, evaporation, and climate induced water mass changes and mixing have had a broad effect on the lithology and biota of the Western Interior.

The precise mechanism(s) translating variations in precipitation and/or water mass to changes in terrigenous and/or pelagic sedimentation are still debated. The oldest and simplest hypothesis is that of Gilbert (1895), who proposed wet-dry cycles, where the wet period increased terrigenous flux, which diluted the pelagic carbonate sedimentation and resulted in the deposition of marl and mudrock, and dry periods and decreased terrigenous flux resulted in the deposition of limestones; in both cases, terrigenous flux is

what changes while pelagic carbonate sedimentation remains the same. Other mechanisms are more complex and involve changes in circulation and carbonate productivity in the sea.

Macro and microfossil biogeography from the WIS and adjacent open ocean sites suggest two water masses entered the sea during maximum transgression: a warm, normal marine Tethyan water mass from the south and a cool, brackish Boreal water mass from the north, which formed a counterclockwise gyre, with warm Tethyan waters to the east and cool Boreal waters to the west (Kent, 1968; Eicher and Worstell, 1970; Frush and Eicher, 1975; Kauffman, 1984; Pratt, 1985; Eicher and Diner, 1985; Hay et al., 1993; Slingerland et al., 1996; Leckie et al., 1998; Elderbak et al., 2014; DaGama et al., 2014). These two water masses may have mixed to form a third, denser watermass through a process called caballing that would have sunk and flowed out of the seaway as a bottom current (Fisher, 1991; Hay et al., 1993). This hypothesis is problematic during periods of anoxia, however, as downwelling of surface water would ventilate the seafloor (Slingerland et al., 1996). Slingerland et al. (1996) proposed a modification of this caballing model where surface runoff from both margins of the sea, deflected to the right by the Coriolis force, created the engine to drive the counterclockwise gyre (Kump and Slingerland, 1999; Flogel et al., 2005). Increased freshwater flux would have strengthened the gyre, starving the basin center of terrigenous sediments and allowing for the deposition of pelagic carbonates, a reverse of Gilbert's original dilution model. Nutrients were likely input into the system by terrigenous influx and upwelling, driven by bathymetric highs (Leckie, 1998; Corbett and Watkins, 2013; Elderbak et al., 2014; Lowery et al., 2014).

Various authors have tested the veracity of the dilution model in the Niobrara Formation, and have reached different conclusions. Laferriere (1992) found that oxygen isotope values of well-preserved inoceramid clams in the Fort Hays Limestone did not vary between limestones and shales, suggesting that if runoff did vary during these times it did not affect salinity in the basin (an unlikely scenario). $\delta^{18}O$ values do show a slight east-west gradient, with more negative values in the central part of the seaway indicating slightly lower salinity or warmer temperatures. While this may imply higher runoff in the west, a similar gradient in Mn abundance in the same samples indicated to Laferriere a water mass gradient, with Mn-enriched inoceramids on the eastern side of the seaway associated with the northward movement of a Tethyan water mass. Dean and Arthur (1998b) undertook a comprehensive geochemical study of the Niobrara from several cores and outcrops across the central part of sea, focusing on major and minor elements, total organic carbon (TOC), and %carbonate. They found that lithologic variability in the Niobrara is controlled by a combination of surface water (primarily carbonate) productivity, dilution by siliciclastic flux, and changes in bottom water oxygenation and the preservation of organic matter, and that all three of these factors were ultimately controlled freshwater flux from the western margin and transgressive-regressive cycles driven by local tectonics or global eustasy (Dean and Arthur, 1998b). Most recently, Locklair and Sageman (2008) used advanced spectral techniques to develop a robust astrochronology of the entire Niobrara Formation using high-resolution wireline resistivity data from a core in the central part of the seaway. Their comparison of sedimentation rates between chalk and marl facies, with higher rates of deposition in the marls, suggests a dilution mechanism driven by increased terrigenous accumulation in the

marls. Interestingly, they also found a 1.7-myr cyclicity between decimeter-scale lithologic changes, which differs significantly from the expected 2.3-myr “grand cycle” of eccentricity and suggest, like Dean and Arthur before them, that this may represent tectonoeustatic cycles driven by changes in sea level or accommodation (Locklair and Sageman, 2008).

3.3.4 Niobrara Cycle

Following the middle Turonian regression of the Greenhorn Sea, a late Turonian-Coniacian transgression deposited hemipelagic chalks and marls across the Western Interior Basin from the Tethyan margin of Texas through Boreal Canada (McNeil and Caldwell, 1981; Kauffman and Caldwell, 1993; Schröeder-Adams et al., 1998). Carbonate-rich sediments in the central and eastern part of the sea comprise the Niobrara Formation (Figure 2), which gives its name to the third-order Niobrara Cycle (Hattin, 1975; Kauffman, 1977, 1984; Laferriere and Hattin, 1989).

The Niobrara Cycle is geochronologically asymmetrical from Colorado to Kansas due to a large unconformity at the base of the Niobrara Formation that increases both stratigraphically and temporally to the east (Figure 3). In many areas east of the Front Range the early transgressive phase of the cycle is preserved only as a transgressive lag deposit (Juana Lopez calcarenite member of the Carlile Shale) or as reworked Codell Sandstone (which represents the lowstand of the previous cycle) in the basal Fort Hays (Hattin, 1975; Hattin and Cobban, 1977; Kauffman, 1977). In western Colorado and southern Wyoming, the Montezuma Valley Member of the Mancos Shale (Leckie et al., 1997) and Sage Breaks Shale (Fisher et al., 1985), respectively, occur between the Juana Lopez and Fort Hays Limestone, but these units are relatively thinner than the highstand

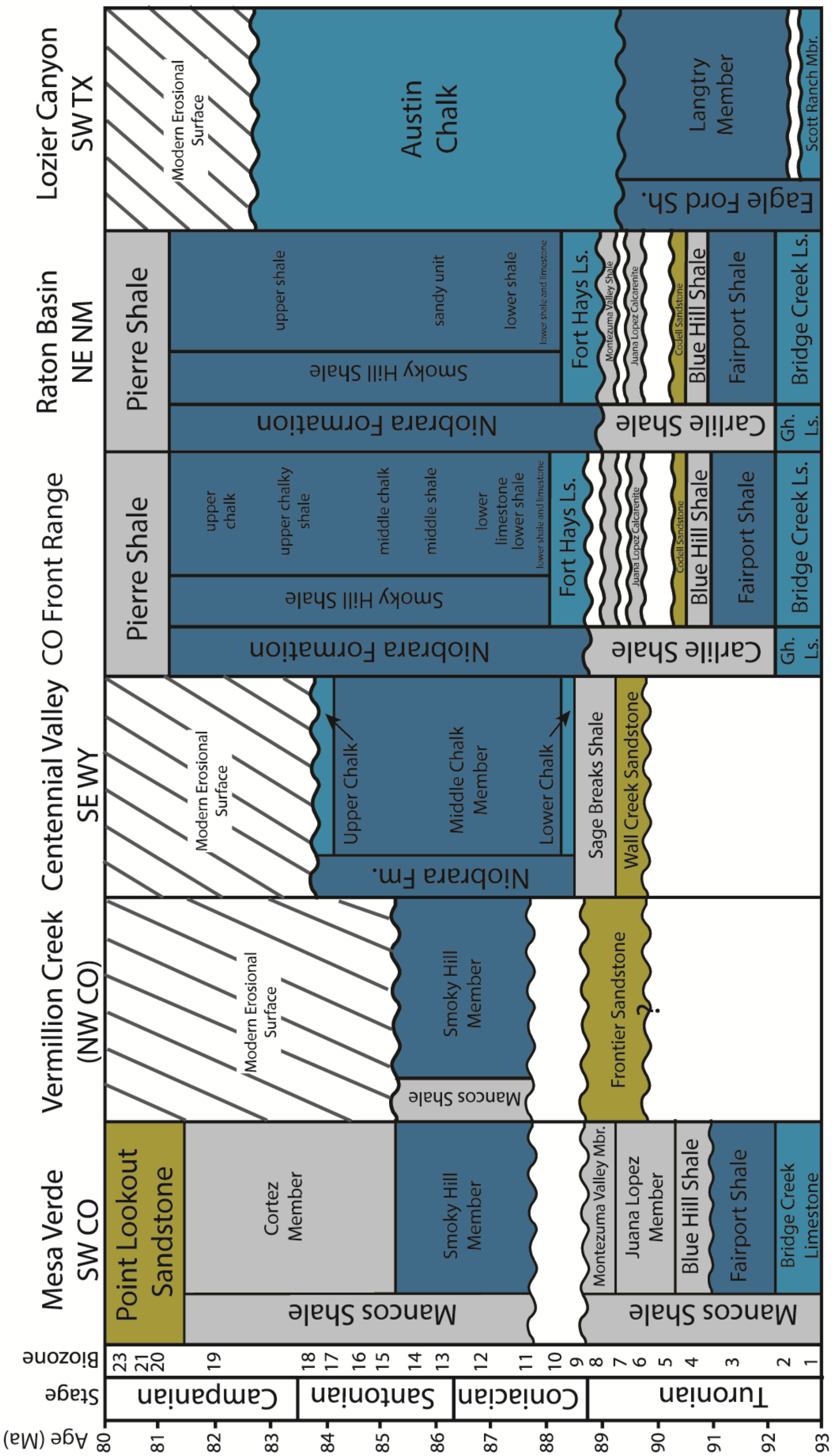

Age (Ma)
Stage
Biozone
Campanian
Santonian
Coniacian
Turonian
Mesa Verde SW CO
Point Lookout Sandstone
Cortez Member
Mancos Shale
Smoky Hill Member
Montezuma Valley Mbr.
Juana Lopez Member
Blue Hill Shale
Fairport Shale
Bridge Creek Limestone
Vermillion Creek (NW CO)
Modern Erosional Surface
Mancos Shale
Smoky Hill Member
Frontier Sandstone
Centennial Valley SE WY
Modern Erosional Surface
Upper Chalk
Middle Chalk Member
Lower Chalk
Niobrara Fm.
Sage Breaks Shale
Wall Creek Sandstone
CO Front Range
Pierre Shale
upper chalk
upper chalky shale
middle chalk
middle shale
lower limestone
lower shale
lower shale and limestone
Smoky Hill Shale
Niobrara Formation
Fort Hays Ls.
Juana Lopez Calcarenite
Codell Sandstone
Blue Hill Shale
Fairport Shale
Bridge Creek Ls.
Carlile Shale
Gh. Ls.
Raton Basin NE NM
Pierre Shale
upper shale
sandy unit
lower shale
lower shale and limestone
Smoky Hill Shale
Niobrara Formation
Fort Hays Ls.
Montezuma Valley Shale
Juana Lopez Calcarenite
Codell Sandstone
Blue Hill Shale
Fairport Shale
Bridge Creek Ls.
Carlile Shale
Gh. Ls.
Lozier Canyon SW TX
Modern Erosional Surface
Austin Chalk
Langtry Member
Eagle Ford Sh.
Scott Ranch Mbr.

Figure 3.3 Stratigraphic correlations between main study sites. Elk Creek is very similar to Vermillion Creek CO; Colorado Front Range shows representative section for Portland Core, Berthoud State Core, Rebecca Bounds Core, and Kansas outcrops. The main difference between these sites is variable thickness of the Juana Lopez and Codell preserved (one or both are missing at some sites) and carbonate content, which is higher to the east. See Figure 2 caption for explanation of lithologies and ammonite biozones.

and regressive equivalents of the Smoky Hill Member of the Niobrara Formation. The Fort Hays Limestone Member represents the maximum transgression of the Niobrara Sea, while the three chalky units of the overlying Smoky Hill Member represent three fourth-order "transgressive pulses" (Hattin and Cobban, 1977; Kauffman et al., 1977; Molenaar, 1983).

The Niobrara exhibits a variable lithology across its broad lateral extent, but generally has the highest carbonate content to the east and south, particularly in Kansas, with decreasing carbonate with increasing proximity to the western margin of the sea in western Colorado and Utah, where the Niobrara correlates to the carbonate-rich Smoky Hill and Cortez members of the massive Mancos Shale (Figure 3). In central Colorado and Kansas it is divided into two formal units: the Fort Hays Limestone Member and the Smoky Hill Chalk Member (Scott and Cobban, 1964; Hattin, 1982). In central Colorado, the Fort Hays is comprised of thick beds of limestone with very thin interbedded seams of black shale; to the south and west, marly interbeds may be of significant thickness. The Smoky Hill varies on roughly decimeter scale between organic-rich marls and organic-poor limestones. Scott and Cobban (1964) assigned these beds to seven informal units: lower chalk and shale, lower marl, lower chalk, middle marl, middle chalk, upper chalky shale, and upper chalk (Fig. 2).

Fort Hays equivalent sediments are missing from the Mancos Shale of Western Colorado, and no marine sediments of Niobrara age are found much further west, indicating the sea was smaller and more restricted than the Greenhorn Sea, which extended far into Utah (e.g., Leckie et al., 1997; Molenaar et al., 2002).

chalk and shale, lower marl, lower chalk, middle marl, middle chalk, upper chalky shale, and upper chalk (Fig. 2).

Fort Hays equivalent sediments are missing from the Mancos Shale of Western Colorado, and no marine sediments of Niobrara age are found much further west, indicating the sea was smaller and more restricted than the Greenhorn Sea, which extended far into Utah (e.g., Molenaar et al., 2002).

3.3.5 Oceanic Anoxic Event 3

The Coniacian-Santonian interval records the last major, widespread deposition of black shales of the Mesozoic. Organic-rich blacks shales of this age are well documented from the South Atlantic, Caribbean Sea, and surrounding epicontinental seas, with well-known localities including Demerara Rise (ODP Site 1259; e.g., Erbacher et al., 2004), the deep Ivoirian Basin (ODP Site 959; e.g., Mascle et al., 1996; Wagner et al., 2002), the continental shelf off Cote D'Ivoire (e.g., Pletsch et al., 2001), Walvis Ridge (DSDP Site 530; e.g., Dean et al., 1984), Angola Basin (DSDP Site 364; e.g., Dean et al., 1984); Maracaibo Basin, Venezuala (e.g., De Romero et al., 2003; Rey et al., 2004), Magdalena Valley, Colombia (e.g., Rangel et al., 2000), and the Western Interior US (e.g., Dean and Arthur, 1998b; Locklair et al., 2011). During this same period, the eastern Tethys is characterized by the deposition of Cretaceous Oceanic Red Beds (CORBs), the result of generally oxic conditions associated with paleoceanographic changes brought about by the opening of the South Atlantic (Wang et al., 2005, 2011; Trabucho-Alexandre et al., 2011).

The widespread deposition of Coniacian-Santonian black shales in parts of the South Atlantic, Central American Sea, and Western Interior US lead Arthur and

Schlanger (1979) to term this interval Oceanic Anoxic Event 3. Unlike older OAEs, there is no definable "event" with OAE3, just a general interval of enhanced black shale burial. Although some of these black shales span the entire interval (and some, like Demerara Rise, are continuous from the Cenomanian-Turonian OAE2; e.g. Erbacher et al., 2004) others span only a portion of the event, and are often diachronous (Wagreich, 2012). Additionally, the positive carbon isotope excursion associated with OAE3 is more muted than that of previous OAEs, ~0.5‰ VPDB for OAE3 vs. ~2.0‰ for OAE2 (e.g., Joo and Sageman, 2014). Although this would seem to indicate slower rates of organic carbon deposition (burying ^{12}C enriched organic matter and enriching the oceans in ^{13}C) than earlier OAEs, Locklair et al. (2011) suggested the true magnitude of the carbon isotope excursion is obscured by the burial of carbonate associated with the thick chalk sequences also deposited at this time, as the enhanced burial of carbonate, enriched in ^{13}C compared to organic carbon, would cause a negative excursion.

Lack of a strong isotope excursion, OAE3's expression as a long interval rather than an easily definable "event," and its limited geographic extent have resulted in debate as to whether it should be termed an Oceanic Anoxic Event (Wagreich 2009, 2012). However, the protracted temporal expanse of black shales associated with the Coniacian-Santonian anoxic event (~5 myr; Wagreich 2009), and the general correlation of this carbon burial with global cooling in the Santonian-Campanian (e.g., Huber et al., 2002; Frerichs et al., 2012), suggests that this is a significant interval in the climate evolution of the Late Cretaceous, and as such deserves an increased research focus whether it truly qualifies as an OAE or not.

3.4 Location and Methods

This study synthesizes new and previously published data from across the southern half of the Western Interior Sea, from Wyoming to Texas (Figure 1). Biostratigraphic correlations are based on well-established molluscan zones (Figure 2) built and refined over decades of research in the WIS (Scott and Cobban, 1964; Kauffman et al., 1993; Walaszczyk and Cobban, 2000; Merewether et al., 2011). For simplicity's sake, disparate sections will be compared to a general Niobrara reference section (Figure 4), based on Scott and Cobban's stratigraphic description of the outcrops along the Arkansas River near Pueblo, CO. Although not the type section of the Niobrara (this was described by Meek and Hayden, 1861, along the Niobrara River in what is now NE Nebraska), the Pueblo section has the benefit of lying along the deep central axis of the sea, a well-studied, relatively central location ideal for correlation. Individual study locations are grouped by geographic region and discussed below.

3.4.1 Central and Eastern Sea

3.4.1.1 Portland Core

The USGS #1 Portland Core was drilled near the town of Florence, CO, located at the foot of the Colorado Front Range in what is known as the Cañon City Embayment, as part of the Western Interior Drilling Project (Dean and Arthur, 1998a). The upper portion of the core recovered a 78.6-m section of the lower Niobrara Fm., including the Fort Hays Limestone and the lower shale and limestone, lower shale, lower limestone, and middle shale units of the Smoky Hill (Dean and Arthur, 1998a). TOC and %$CaCO_3$ measurements from the Portland Core were collected by Dean and Arthur (1998a). Macrofossil biostratigraphy is correlated from the nearby Pueblo, CO outcrops of the

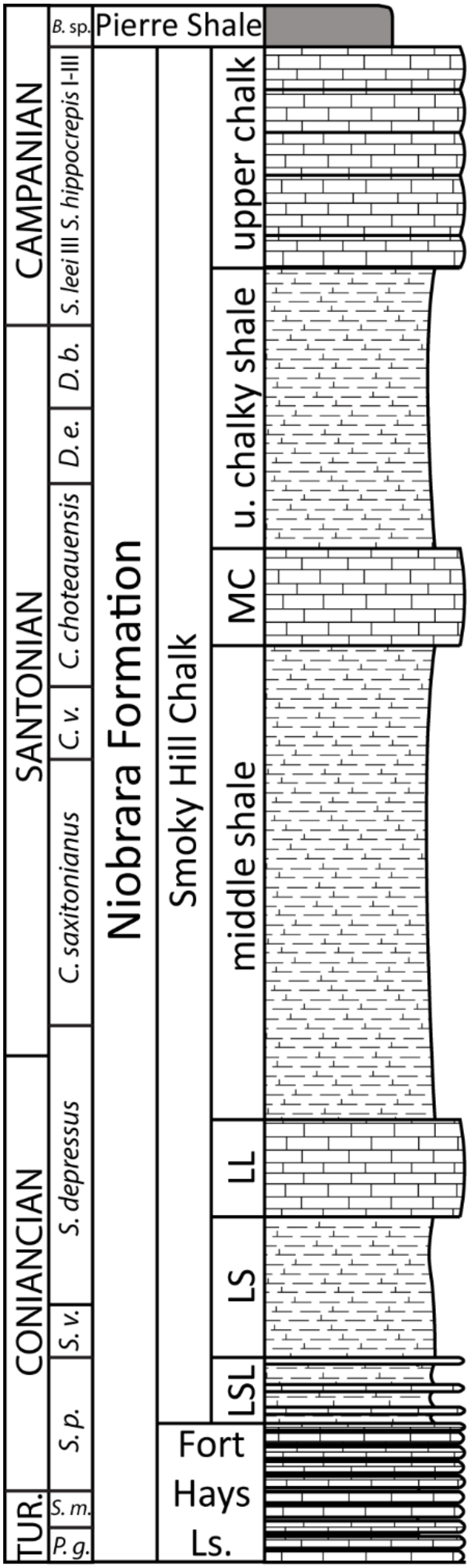

Figure 3.4. Stratigraphic column for idealized Front Range Composite Section, based of description of Pueblo outcrops by Scott and Cobban, 1964. See Figure 2 for description of ammonite zones. LSL, lower shale and limestone unit; LS, lower shale unit; LL, lower limestone unit; MC, middle chalk unit.

Niobrara based on work by Scott and Cobban (1964). Foraminifera were collected from the Niobrara section in the USGS core repository in Denver in the fall of 2012. Abundance data from the limestone beds of the Fort Hays and from both shale and limestone beds of the Smoky Hill are presented by Lowery et al. (in prep.); the present study includes additional samples from the shale interbeds of the Fort Hays Limestone to show variability between limestone/shale couplets. Hill (Dean and Arthur, 1998a). TOC and %$CaCO_3$ measurements from the Portland Core were collected by Dean and Arthur (1998a). Macrofossil biostratigraphy is correlated from the nearby Pueblo, CO outcrops of the Niobrara based on work by Scott and Cobban (1964). Foraminifera were collected from the Niobrara section in the USGS core repository in Denver in the fall of 2012. Abundance data from the limestone beds of the Fort Hays and from both shale and limestone beds of the Smoky Hill were presented by Lowery et al. (in prep.); the present study includes additional samples from the shale interbeds of the Fort Hays Limestone to show variability between limestone/shale couplets.

3.4.1.2 Bounds Core

Amoco Production Company's Rebecca K. Bounds #1 Core was drilled in Greely Co., Kansas and is stored in the USGS Core Research Center in Denver, CO (Dean and Arthur, 1998a). Like the Portland Core, it only recovered the lower portion of the Niobrara Formation, including a complete, 24.3-m section of the Fort Hays Limestone and a 20.4-m thick section of the Smoky Hill Chalk, including the limestone and shale and lower shale units. TOC, %CaCO3, and major and trace element abundance data for the Bounds Core were collected by Dean and Arthur (1998b). Foraminiferal abundance data for the Niobrara was collected at high resolution by Sterzinar (2005).

3.4.1.3 Kansas Outcrops

Because neither the Bounds Core nor Portland Core recovered the entire Niobrara Formation (and other cores were unsuitable for foraminiferal analysis; Lowery et al., in prep.), a composite outcrop section from western Kansas, along the Smoky Hill River, is included to understand foraminiferal trends through the upper Smoky Hill Chalk. Nine representative and mostly overlapping outcrops were chosen from a 25-outcrop section originally described and correlated by Hattin (1982) south of Interstate 70 in Trego, Gove, and Logan counties. The Niobrara in Kansas is significantly more carbonate-rich than eastern Colorado, with chalk and chalky marl being the dominant lithologies. In general, carbonate content increases in an eastward direction across the entire Niobrara Sea, with maximum carbonate values found in the eroded feather-edge of the Niobrara in central Kansas; the eastern shoreline is not preserved.

3.4.2 Western Sea

3.4.2.1 Mesa Verde, CO

The slopes below Point Lookout at Mesa Verde National Park represent the primary reference section of the Mancos Shale (Leckie et al., 1997). The middle portion of this thick package of marine sediments corresponds to the Niobrara Cycle, with Juana Lopez Calcarenite Member and the type section of the Montezuma Valley Member unconformably underlying the Smoky Hill Member of the Mancos. This unconformity spans the uppermost Turonian *Prionocyclus quadratus* zone to the middle Coniacian *Scaphites ventricosus* zone. The Montezuma Valley Member contains 7 septarian concretion horizons that are correlative to the 7 limestone beds described in the upper Turonian Ft. Hays Member of the Niobrara Formation in the Raton Basin of northeastern

New Mexico (Scott et al., 1986; Sikora et al., 2004; Kennedy et al., 2012; Section 3.4.1, below). The overlying Smoky Hill Member is equivalent to the middle Coniacian lower shale to middle Santonian middle shale units of the Smoky Hill of the Front Range, and the overlying Cortez Member, which has a gradation contact with the Smoky Hill, is equivalent to the middle Santonian middle chalk unit to the basal Campanian upper shale unit of the Front Range.

Detailed macrofossil biostratigraphy for the Mesa Verde section was documented by Leckie et al. (1997). Foraminiferal abundance data for the Niobrara-equivalent portion of the Mancos (Montezuma Valley, Smoky Hill and Cortez Members) was presented in an unpublished Masters Thesis by Erica Sterzinar (2005). Clay mineral abundance data for the same interval was similarly presented in an unpublished Masters Thesis by Connie Hayden Scott (1992).

3.4.2.2 Vermillion Creek, CO

The Niobrara-equivalent portion of the Mancos Shale is also exposed in NW Colorado along the valley of Vermillion Creek in Moffat Co., from which samples were collected and counted for foraminifera by Kent (1968). The Mancos in this part of Colorado is correlated to the Colorado Front Range by macrofossil biostratigraphy (Reeside, 1955). Although originally termed the Niobrara Member of the Mancos Shale, we follow the nomenclature of Leckie et al. (1997) and term this interval the Smoky Hill Member, which more properly reflects its stratigraphic equivalence. The Smoky Hill Member, which is comprised of calcareous shale,overlies the Frontier Sandstone, and is Coniacian-Santonian in age, likely equivalent to the lower chalky shale through middle shale units of the Niobrara in Colorado (*Scaphites ventricosus-Clioscaphites vermiformis*

ammonite zones). The base of the Smoky Hill Member at Mesa Verde is also in the *S. ventricosus* zone, suggesting they are roughly the same age. Kent sampled the lower 457 m of the Niobrara-equivalent Mancos Shale and reported planktic:benthic (P:B) ratio and the occurrence of certain benthic foraminifera he considered diagnostic (Kent, 1968).

3.4.2.3 Elk Creek, CO

Kent also sampled 304 m of the Smoky Hill Member of the Mancos Shale in west-central Colorado, along Elk Creek, about 2 miles north of New Castle, in Garfield Co. Although the thickness is similar to the Vermillion Creek section, sedimentation rates at Elk Creek must have been lower (or a significant amount of time is missing, a hypothesis for which there is no other evidence), as the middle Santonian inoceramid clam *Platyceramus platinus*, found with its ever-present crust of *Ostrea congesta*, was identified 200 m above the base of the Frontier Sandstone (Kent, 1968). Unfortunately, this is the only age-diagnostic fossil reported for this section, but it suggests that most, if not all, of Smoky Hill-equivalent time is preserved here. Based on well-developed biostratigraphy at the other western sections (i.e., Mesa Verde and Vermillion Creek; Leckie et al., 1997; Kent, 1968), it is presumed that the Fort Hays is also missing, and that the interval directly above the Frontier Sandstone is equivalent to the lower shale and limestone unit of the Front Range. Like Vermillion Creek, Kent's reported data include P:B ratio and the ranges of benthic taxa he considered significant.

3.4.3 Northern Sea

3.4.3.1 Centennial Valley, WY

The Niobrara Formation of southeastern Wyoming loses the characteristic carbonate variability of its Front Range counterpart a few hundred miles south. Rocks of

the Fort Hays Limestone are entirely missing, with chalks and shales equivalent to the Smoky Hill unconformably overlying the (mostly) Montezuma Valley-equivalent Sage Breaks Shale. Macrofossil biostratigraphy from nearby Rock River show an upper Turonian-lower Coniacian unconformity spanning the upper *Prionocyclus germari* zone in the top of the Sage Breaks Shale to the upper *Scaphites ventricosus* zone in the basal Niobrara (Merewether et al., 2011). *P. germari*, and its inoceramid-equivalent, *Mytiloides scupini*, are found in the lower Fort Hays Limestone at Pueblo, suggesting that the Sage Breaks Shale, like the Montezuma Valley, is equivalent to carbonate facies further to the south and east. This fits the general south-north diachronaity of the onset of limestone deposition in the Niobrara Cycle, with the base of limestone/chalk facies in Texas predating the base of limestone/chalk facies in New Mexico, which in turn predates equivalent lithologies in southern Colorado, and so on through Colorado and Wyoming (Walaszczyk and Cobban, 2000).

Above the Turonian-Coniacian unconformity, the Niobrara is divided into a lower chalky member, an upper shale member, and an upper chalky member. Original stratigraphy grouped the Sage Breaks Shale into the Niobrara as a lower shale member (e.g., Rubey, 1930; Thomas, 1936). Frerichs (1979) suggested the elevation of the Sage Breaks to formation-rank, which is followed here. This renders the name "Upper Shale Member" of the Niobrara confusing, and this member will be referred to from here on out as the "Middle Shale Member." Frerichs (1979) sampled the entire 110 m thickness of the Sage Breaks in Centennial Valley, from the lower contact with the Wall Creek Sandstone to the upper contact with the Niobrara. Frerichs et al. (1975) sampled the entire thickness of the Niobrara at an adjacent locality in Centennial Valley, which

includes 7 m of Lower Chalk Member and 63 m of the Middle Shale Member near State Secondary Highway 207. The upper 3.6 m of the Middle Shale and the entire 2.4 m thickness of the Upper Chalk were not exposed at this outcrop, and were sampled by Frerichs along Mill Creek, about 9 miles north of the Centennial Valley locality. It is not clear from the literature if these sections were correlated by anything other than stratigraphic thickness. Both studies – Frerichs et al. (1975) and Frerichs (1979) – were primarily concerned the planktic foraminifera of both formations, but recorded P:B ratios and foraminiferal numbers, which allow comparison to the other study sites.

3.4.4 Southern Sea

3.4.4.1 Wagon Mound, NM

The Raton Basin of northeast New Mexico contains approximately 6 m of Fort Hays Limestone overlain by 244-274 m of Smoky Hill (Scott et al., 1986). Despite being roughly the same longitude as the Portland Core/Pueblo outcrops, the Niobrara in NE New Mexico is significantly less carbonate-rich, perhaps due to a more proximal western shoreline than found in Colorado. The Fort Hays Limestone consists of 7 limestone beds (each <50-cm thick) with thick shale interbeds, and the Smoky Hill loses its obvious limestone-shale units, with the exception of the lower limestone and shale. The middle Smoky Hill is characterized by a “Sandy Interval” equivalent to the uppermost Coniacian-lower Santonian middle shale unit of the Front Range, while the overlying portion equivalent to the middle limestone and upper chalky shale units are characterized by plain shale (Scott et al., 1986).

The Fort Hays at Wagon Mound is underlain by the Montezuma Valley Member of the Carlile Shale, which is underlain by a thick (>5 m) partial section of the Juana

Lopez Calcarenite Member of the Carlile, a transgressive lag deposit that consists primarily of sand-sized inoceramid prisms. The Juana Lopez here is made up of an upper calcarenite and a lower shale unit interbedded with thickening-upwards hummocky beds of calcareous sand (in this case, inoceramid prisms). This lower shaly unit was attributed to the Blue Hill Shale Member of the Mancos by Sikora et al. (2004), but this is lithologically very similar to the shaly middle unit of the Juana Lopez in its type area of north-central New Mexico and in southwestern Colorado (Dane et al., 1966; Leckie et al., 1997). On the Front Range and further east the Juana Lopez is completely erased by multiple unconformities or intermittently represented as very thin horizons (e.g., <0.5 m at Rock Canyon). The outcrop at Wagon Mound, ~ 1 mile north of the town, adjacent to the southbound lane of I-25, is about 30- m thick in total, and includes 4.5 m of Juana Lopez, 5 m of Montezuma Valley, and 12 m of Niobrara, topping out in the lower limestone and shale unit of the Smoky Hill, overlain by Quaternary basalt and a contact-metamorphosed zone of Smoky Hill that was not sampled.

3.4.4.2 Lozier Canyon, TX

The Austin Chalk of Texas is partially equivalent to the Western Interior Niobrara Formation (e.g., Lundquist, 2000; Gale et al., 2007; Cobban et al., 2008). Basal limestone facies in the Austin Chalk in west Texas has been dated to the upper Turonian *Scaphites nigricollensis* ammonite zone (Cobban et al., 2008), while the basal Austin Chalk from a core in east Texas has been dated to the middle Turonian *Marginotrunacana schneegansi* planktic foraminiferal zone (Lowery et al., 2014). These are the youngest limestones associated with the transgressive phase Niobrara Cycle, and are chronostratigraphically-equivalent to terrigenous facies in the central WIS. A 28-m thick section of the lower

Austin Chalk was sampled along US Highway 90 ~6 miles west of the town of Langtry, near the well-studied Lozier Canyon locality of the Cenomanian-Turonian Eagle Ford Shale. Samples were collected from every limestone bed, starting just above the lower contact with the Eagle Ford Shale. Thin black shale interbeds, like those found in the Fort Hays Member of the Niobrara in western Kansas and eastern Colorado, were also sampled but the shale was too weathered to yield any fossil material. Data are also included from the upper, Carlile Shale-equivalent interval of the Eagle Ford Shale at Lozier Canyon (Lowery et al., 2014).

3.5 Discussion/Interpretation

3.5.1 Central and Eastern Sea

Foraminiferal trends from all sites on the Colorado Front Range and western Kansas follow a similar pattern (Figures 5-7), described in detail by Lowery et al. (in prep.). Broadly, %benthics are highest in the Fort Hays Limestone Member, with highest values at the base and decreasing toward the top of the member. The overlying lower chalk and shale unit of the Smoky Hill Member records a decline benthic values compared to the Fort Hays, with a slight decline from the base to the top of the unit. The overlying lower shale then displays a brief sharp decline (with a short barren interval in the Portland Core) before %benthic values briefly recover and then slowly decline through to the base of the lower limestone. Another brief, smaller recovery follows before values fall to zero in the lower middle shale and no benthic foraminifera are recorded through the remainder of the Smoky Hill.

Keeled planktic foraminifera follow a similar overall trend. Keeled planktic diversity increases through the Fort Hays (the opposite of the pattern seen in %benthics),

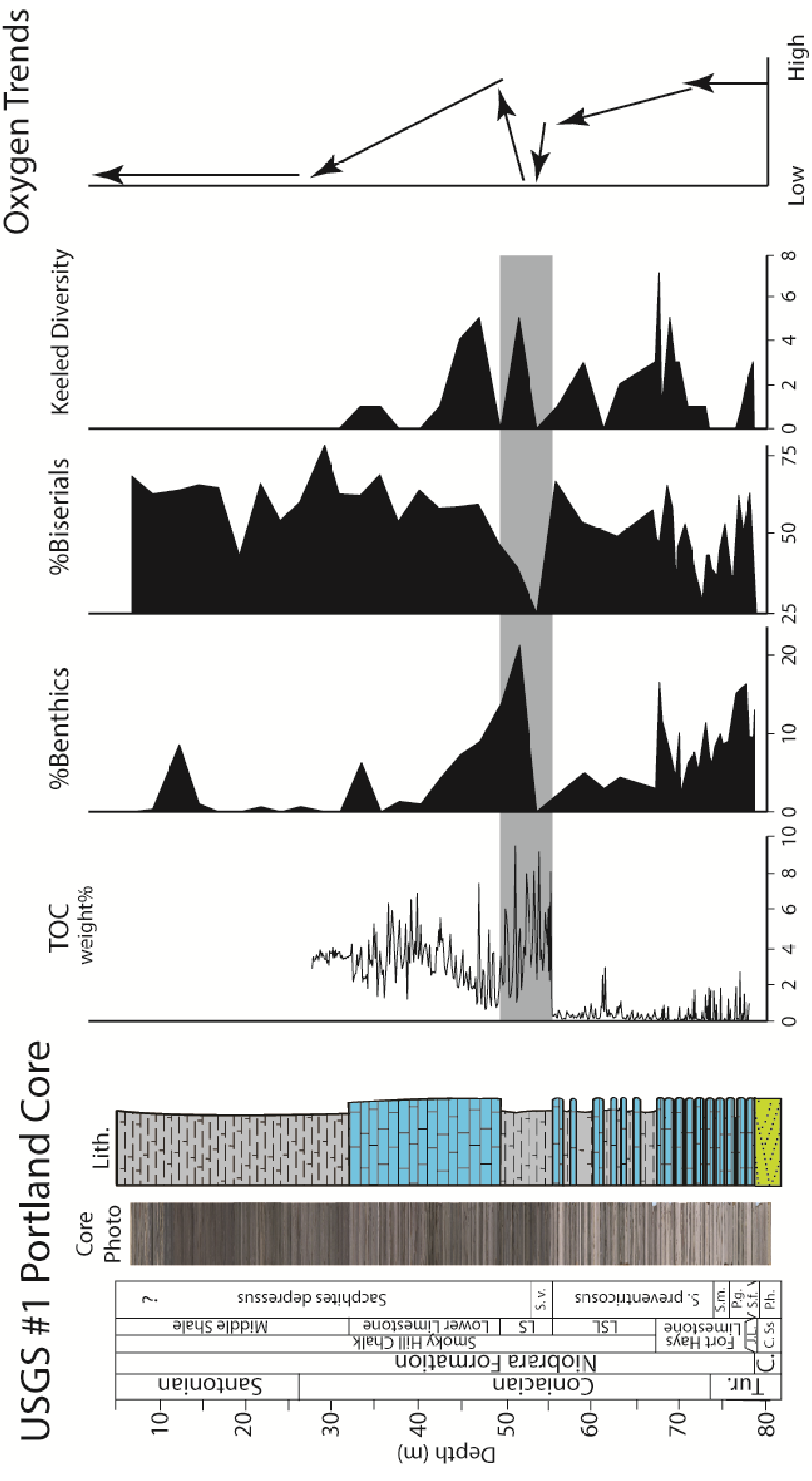
USGS #1 Portland Core
Depth (m)
Santonian
Coniacian
Tur.
Niobrara Formation
Smoky Hill Chalk
Fort Hays Limestone
Middle Shale
Lower Limestone
LS
LSL
Sacphites depressus
S. v.
S. preventricosus
S.m.
P.g.
S.f.
P.h.
C. Ss
Core Photo
Lith.
TOC weight%
%Benthics
%Biserials
Keeled Diversity
Oxygen Trends
Low
High

Figure 3.5. Summary of %Benthic foraminifera (vs. total foraminifera), %Biserial planktic foraminifera (vs. total planktics), and the simple diversity of keeled planktic foraminifera from the USGS #1 Portland Core. Right column show general oxygen trends implied by foraminiferal paleoecology. TOC after Dean and Arthur, 1998b. See Figure 2 for explanation of ammonite biozones.

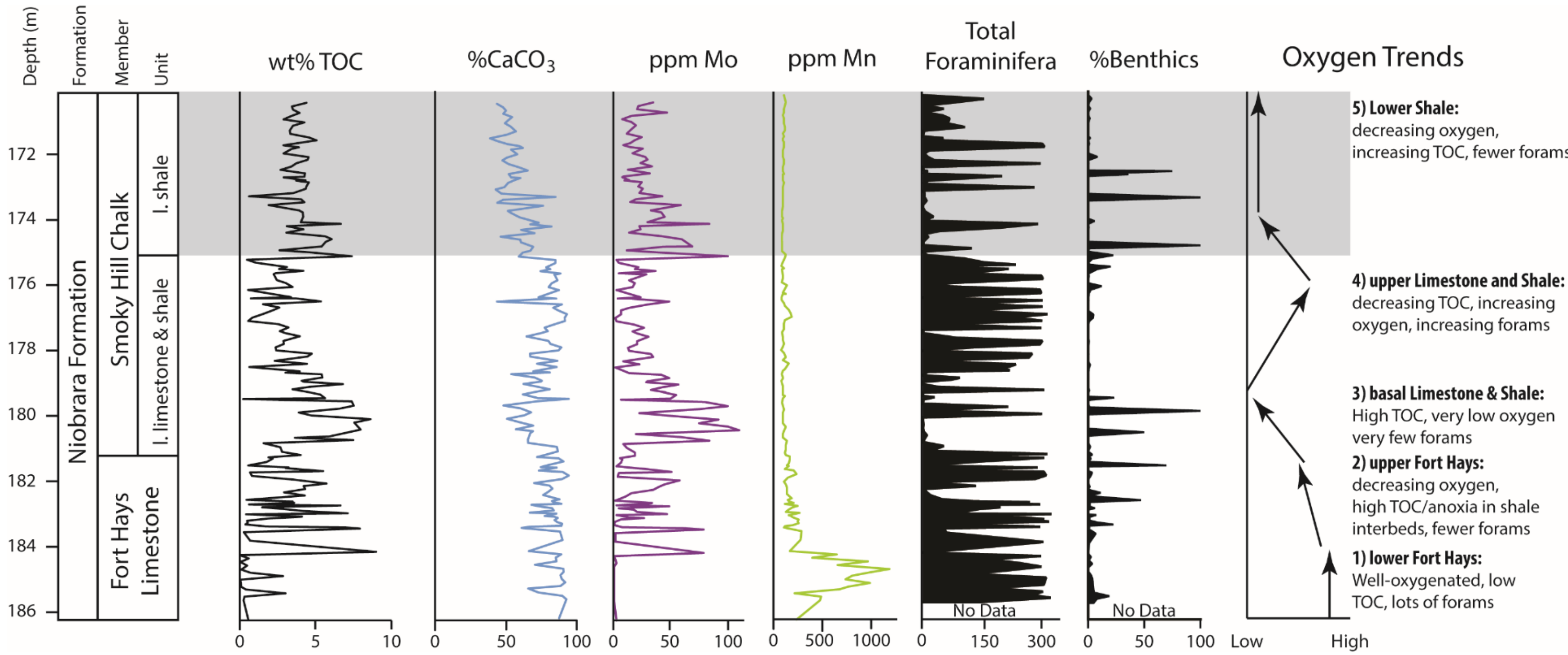

Figure 3.6. Summary of foraminiferal assemblages (Sterzinar, 2005) and geochemical trends for the Amoco Rebecca Bounds #1 Core. Foraminiferal Number represents total foraminifera found in each sample; note correlation between low foraminiferal number and high TOC/Mo. %Benthic foraminifera is vs. total Foraminifera. Geochemical data from Dean and Arthur (1998b). Note peak in Mn in lower Fort Hays, suggesting oxic conditions (a hypothesis supported by high foraminiferal number). Upper Fort Hays shows increasing Mo in shale interbeds (note correlation between high Mo, low %carbonate, and high TOC). Limestone and shale unit shows transition, with high Mo/TOC and lower foraminiferal number in lower part of the unit, with slight recovery at the top, before transition to lower shale unit. The lower shale is characterized by euxinia (high Mo) and is mostly barren of foraminifera.

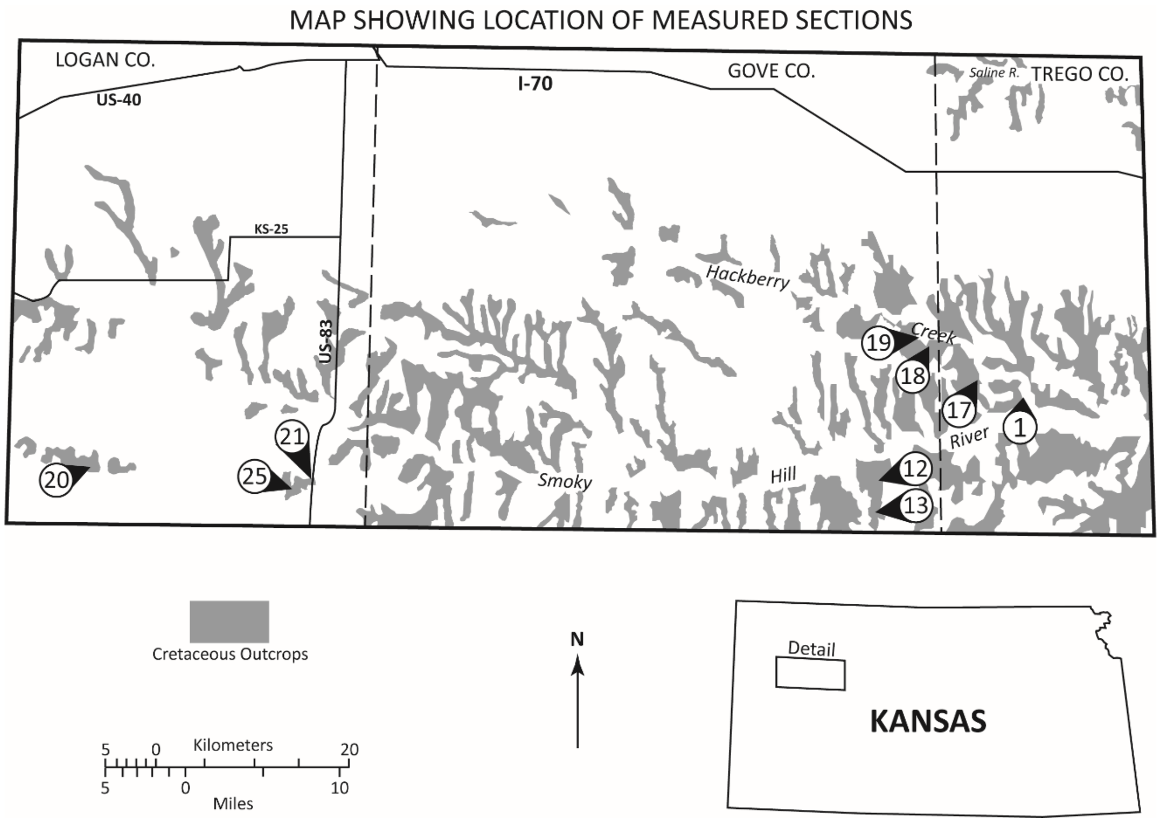

Figure 3.7a. Location map showing position of outcrops used to construct composite section. Redrawn from Hattin, 1982.

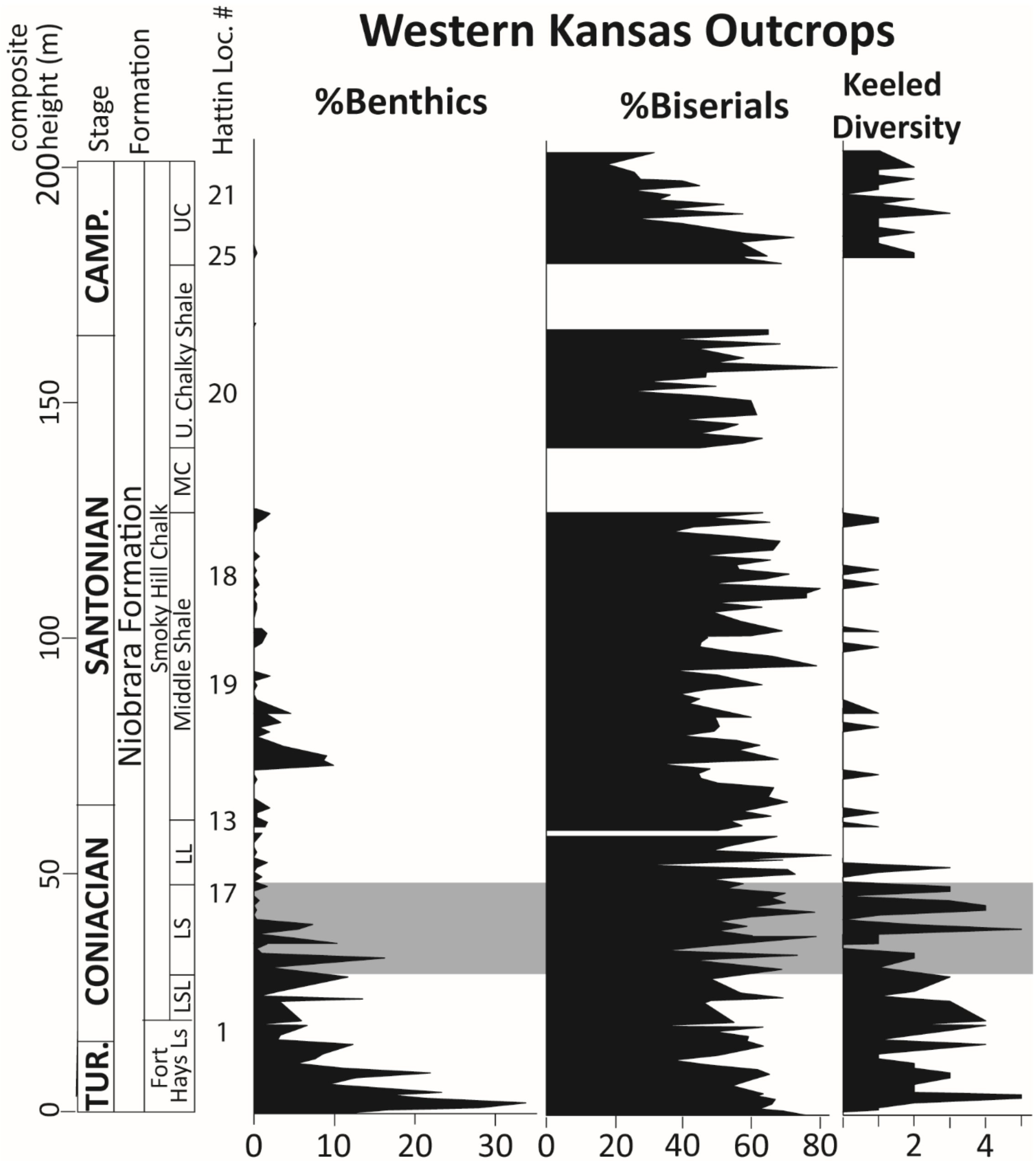

Figure 3.7b. Summary of %Benthic foraminifera (vs. total foraminifera), %Biserial planktic foraminifera (vs. total planktics) and the simple diversity of keeled planktic foraminifera from the Kansas outcrop composite section. LSL, lower shale and limestone unit; LS, lower shale unit; LL, lower limestone unit; MC, middle chalk unit; UC, upper chalk unit. Gray bar shows interval of lower shale unit..

then decreases slightly in the lower limestone and shale of the Smoky Hill. In the lower shale, keeled planktics briefly disappear before recovering at the same level as the benthics and the eventually trailing off. However, the keeled decline lags behind the benthic decline, and keeled species don't completely disappear until the upper part of the middle shale. In the upper chalk in Kansas, keeled diversity makes a recovery, with several species returning and increasing diversity toward the top of the section.

A slight exception to this trend can be found in the high-resolution data from the Bounds Core (Figure 6). There, many samples in the Ft. Hays Member to lower shale unit of the Smoky Hill Member are barren or have few specimens of benthic foraminifera (<10% in samples with >100 foraminifera recovered). Perhaps the important variable here is foraminifera number (literally, the number of individuals found in a sample), which shows clear variability throughout the study interval. Samples were split and counted to ~300, where possible, which gives the data an artificial ceiling, but broadly, foram number is highest in the lower Fort Hays, declines in the upper Fort Hays (with more samples with <300 individuals), declines more in the lower portion of the lower limestone and shale, increases in the middle lower limestone and shale, decreases at the top of the unit and decreases further in the lower shale. This trend broadly mirrors the %benthic and keeled diversity trends seen in other Front Range sites. There are 2.5 or 3 broad cycles in TOC, %CaCO3, Mo, and total foraminifera in this interval of the Niobrara suggesting climatic forcing, perhaps the 400-kyr long eccentricity cycle.

The Front Range is also where the most robust geochemical data is found. TOC values for the Portland Core, Bounds Core, and several cores in the Denver Basin (e.g., Berthoud State Core – Dean and Arthur, 1998b; Aristocrat Angus Core – Locklair et al.,

2011) show a rapid increase at the base of the lower shale. This level also contains increasing trace metal markers for anoxia, particularly molybdenum, while markers for oxygenation (manganese) are only enriched in the lower Fort Hays (Dean and Arthur, 1998b; Locklair et al., 2011).

In order to compare to clay mineralogy from Mesa Verde (see below), major and trace element abundance data from the Bounds Core and the Berthoud State Core, in the Denver Basin at roughly equivalent to the Pueblo section, were plotted (Figure 8). The key benefit of the Berthoud State Core data, dissected in detail by Dean and Arthur (1998b), is that it allows a comparison of sedimentological trends from the central part of the seaway to be directly compared to clay mineral data from the Mesa Verde, while also comparing those trends to well-established TOC, %$CaCO_3$, and trace metal data from the same samples. In particular, the ratio of K to Fe and Mg (K/Fe+Mg) likely records the ratio of discrete illite (high K) to smectite (high Fe and Mg). The ratio of Na to K (Na/K), meanwhile is either related to the abundance of Na-rich mixed-layer clays from a volcanic source or may record changes in sediment source or precipitation, with low Na/K ratios reflecting an increased flux of discrete illite (high K), indicative of drier climates, and high Na/K ratios reflecting an increased flux of kaolinite (high Na), indicating increased weathering of feldspars under moist conditions. These data show declining discrete illite through the Smoky Hill Member, suggesting a shift from dry to warm and moist conditions, or a change in sediment source area. Na/K data show a slight increase in Na (presumably kaolinite) associated with carbonate-rich intervals of the Ft. Hays and Smoky Hill, suggesting increased precipitation/runoff at this time, or a slight shift in sediment source area.

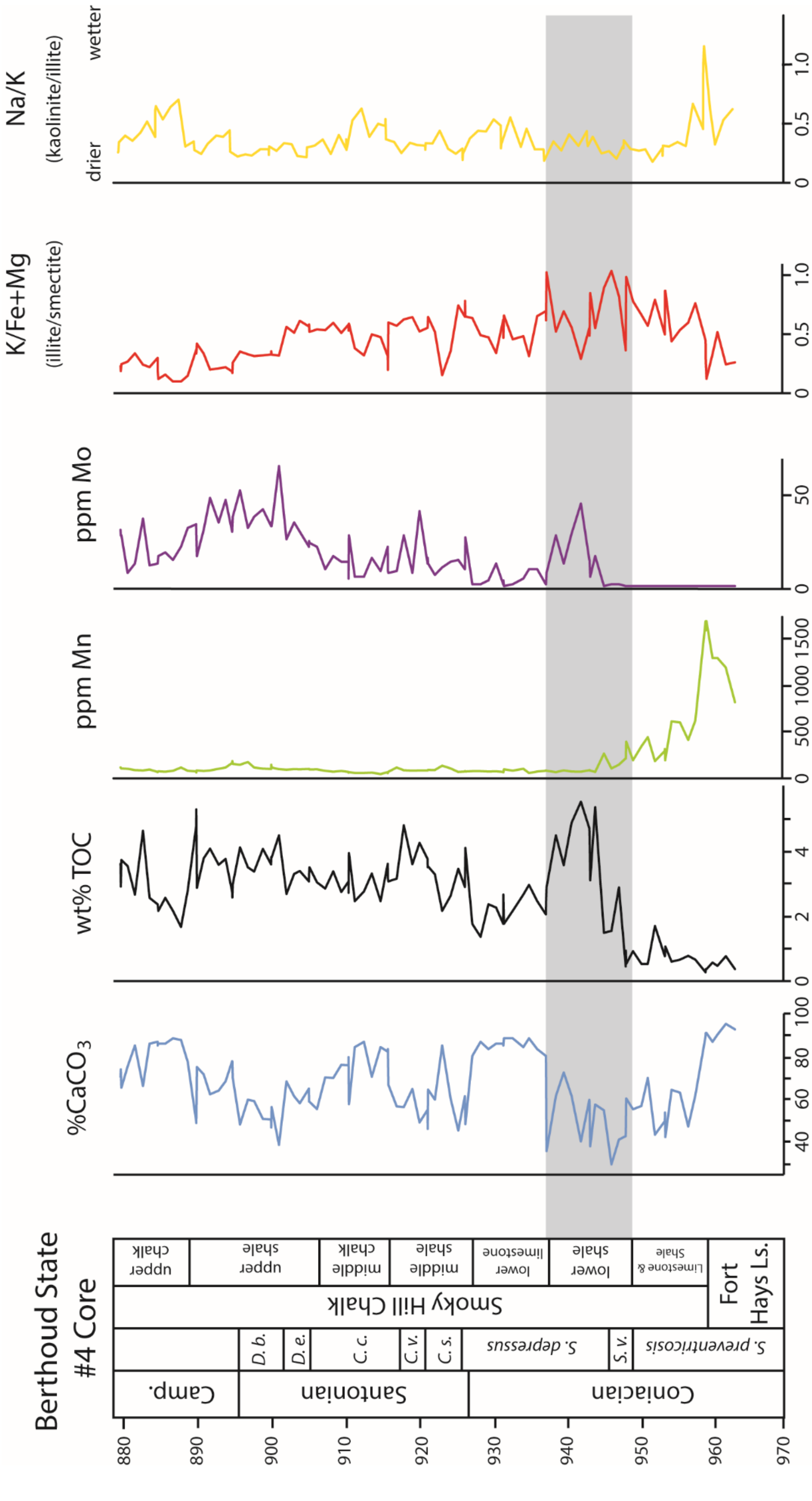

Berthoud State #4 Core
%CaCO$_3$
wt% TOC
ppm Mn
ppm Mo
K/Fe+Mg
(illite/smectite)
Na/K
(kaolinite/illite)
drier
wetter
Camp.
Santonian
Coniacian
D. b.
D. e.
C. c.
C. v.
C. s.
S. depressus
S. v.
S. preventricosis
Smoky Hill Chalk
Fort Hays Ls.
upper chalk
upper shale
middle chalk
middle shale
lower limestone
lower shale
Limestone & Shale

Figure 8. Major and trace element data from the Coquina Oil Berthoud State #4 Core, replotted from Dean and Arthur (1998b). %Carbonate; weight% total organic carbon (TOC); ppm Mn, which is enriched in oxic environments; ppm Mo, which is enriched in euxinic environments; ratio of K to Fe plus Mg, where K likely responds to discrete illite and Fe plus Mg likely correspond to volcanogenic smectite; and ratio of Na to K, where Na is likely associated with chemically-weather kaolinite, and K is likely associated with mechanically-weathered discrete illite. Ammonite biostratigraphy projected from Pueblo outcrops as reported in Scott and Cobban (1964) based on the widely-acknowledged assumption that unit boundaries within the Smoky Hill Chalk are isochronous across the Front Range.

3.5.2 Western Sea

In southwestern Colorado, the Mesa Verde section contains an expanded Juana Lopez and Montezuma Valley interval that is not well-preserved in eastern Colorado, although the latter is at least partially equivalent to the lower Ft. Hays. These units represent much of the transgression of the Niobrara cycle. In northwestern CO, the transgressive Niobrara sequence is missing at the Vermillion Creek and Elk Creek sections, including the Ft. Hays Member, and the Smoky Hill Member of the Mancos directly overlies the Frontier Sandstone (Figure 3).

In the Montezuma Valley Member of the Mancos Shale at Mesa Verde, foraminifera are fairly abundant and increasing in number (Figure 8). %Benthics are lower than in the underlying Juana Lopez Calcarenite, perhaps reflecting increasing water depths, but calcareous benthics make up the largest portion of the benthic population of the section. Clay minerals are dominated by kaolinite, which suggests either a proximal environment or generally warm and wet conditions favoring the chemical weathering of feldspars (Dean and Arthur, 1998b). Discrete illite and chlorite are generally associated with mechanical weathering, and thus drier/cooler conditions (Dean and Arthur, 1998b). Mixed layer illite/smectite is generally low during the Niobrara Cycle at Mesa Verde and does not show any discernable trend, which suggests that the contribution of altered volcanic ash to the clay assemblage was minimal and relatively constant throughout the interval.

The unconformity separating the Montezuma Valley Member of the Mancos Shale from the overlying Smoky Hill Member is obvious in both foraminiferal and clay mineral trends (Figure 9). The portion of the Smoky Hill Member that corresponds to the

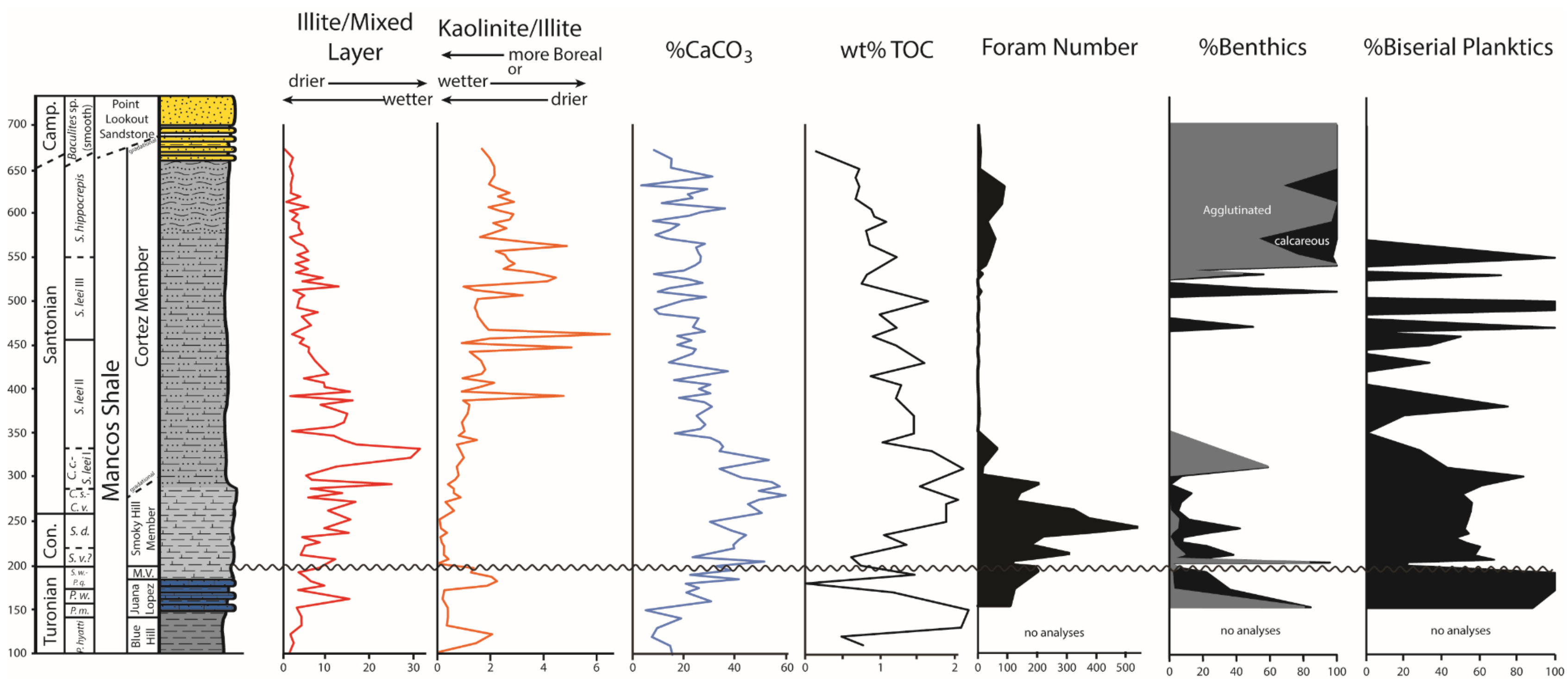

Figure 9. Summary of foraminiferal assemblages, %carbonate, and wt% TOC (Sterzinar, 2005) and clay mineralogy (Hayden Scott, 1992) at Mesa Verde. Foram Number is number of individuals in the sample; %Benthics is vs. total foraminifera; %Biserial Planktics is vs. total planktic foraminifera. See Figure 2 for explanation of ammonite biozones and see text for discussion of clay mineralogy proxies for climate and circulation.

middle and upper Coniacian *S. ventricosus* and *S. depressus* zones (lower shale – lower limestone unit equivalent) records the highest foraminiferal abundance, decreasing benthics, relatively high biserial planktics, and major shifts in clay mineralogy. Specifically, kaolinite declines to a general nadir, and discerete illite dominates, relatively high but declining chlorite.

At Elk Creek and Vermillion Creek, the Smoky Hill Member contains significantly higher %benthic values than are seen at Mesa Verde (40-60% vs. 20-40% at Mesa Verde; Figures 10-11; Kent, 1968). At both localities a nadir in benthics occurs in the middle of this interval. At Vermillion Creek, where the section is tied to molluscan biostratigraphy (Reeside, 1955), the barren interval corresponds to the top of the upper Coniacian *S. depressus* zone, equivalent to the lower shale unit on the Front Range. The top of the Vermillion Creek section is in the middle Santonian *C. vermiformis* zone, and although %benthics varies and includes relatively high peaks, benthic diversity severely decreases, with only a few species ranging to the top of the section. At Elk Creek, this same trend of decreasing diversity is observed, but above ~300 m benthics abruptly disappear for the rest of the section. This likely corresponds to the barren upper Santonian interval in the Cortez Member at Mesa Verde.

In the Cortez Member at Mesa Verde, foraminiferal abundance declines to zero in the upper Santonian, and the ratio of kaolinite to illite gradually increases. Toward the top of the Cortez Member, in the basal Campanian *S. hippocrepis* zone (upper-upper chalky shale to upper chalk unit equivalent) these trends abate, as foraminifera return, albeit at much lower abundance than seen lower in the section. This new assemblage is completely dominated by benthic foraminifera, particularly agglutinated benthics.

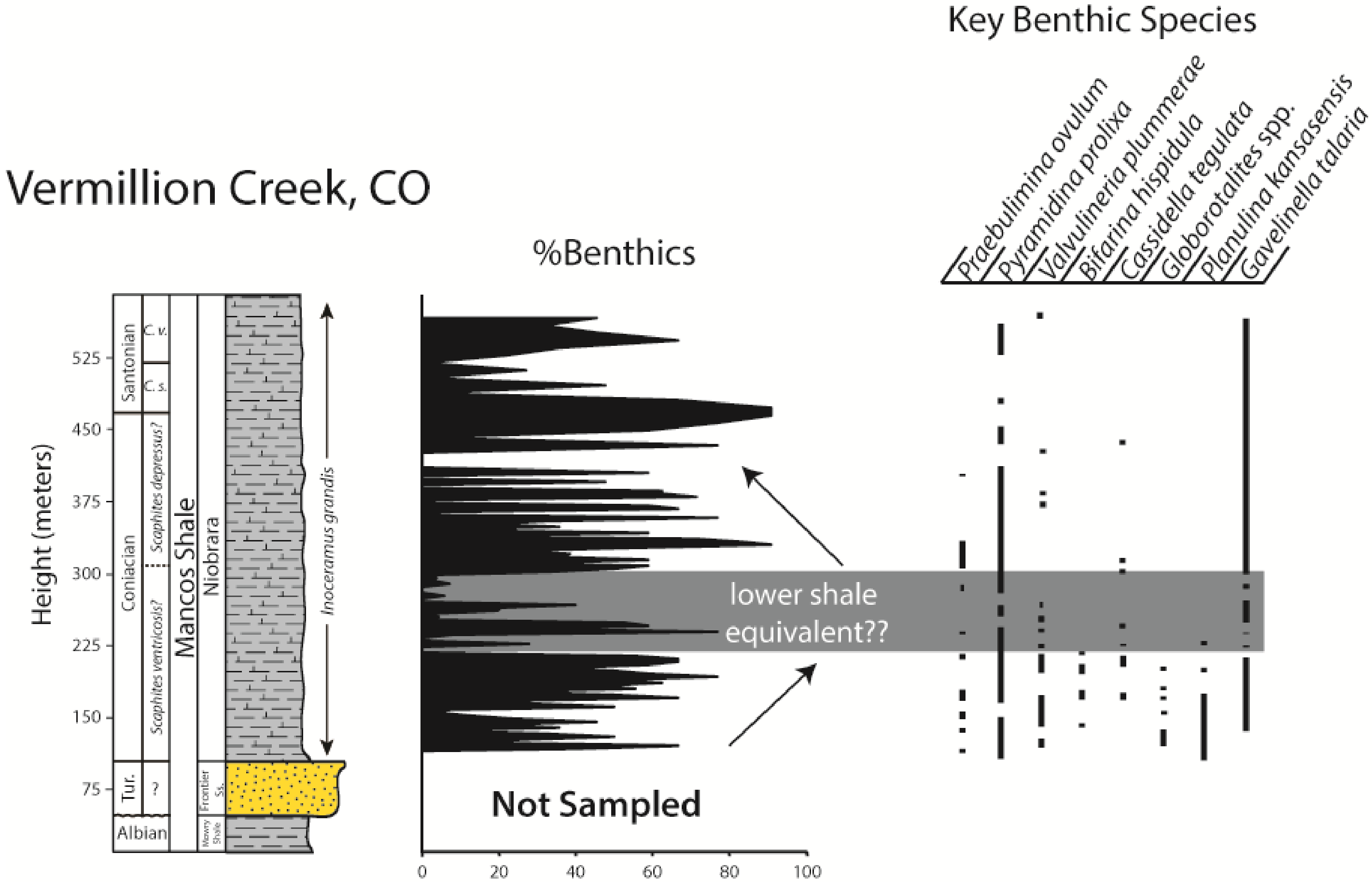

Figure 10. Summary of benthic foraminiferal abundance and the ranges of key species at Vermillion Creek, CO, after Kent (1968). %Benthics vs. total foraminifera. Gray bar shows low abundance interval assumed to be equivalent to lower shale unit on the Front Range. See Figure 2 for explanation of ammonite biozones.

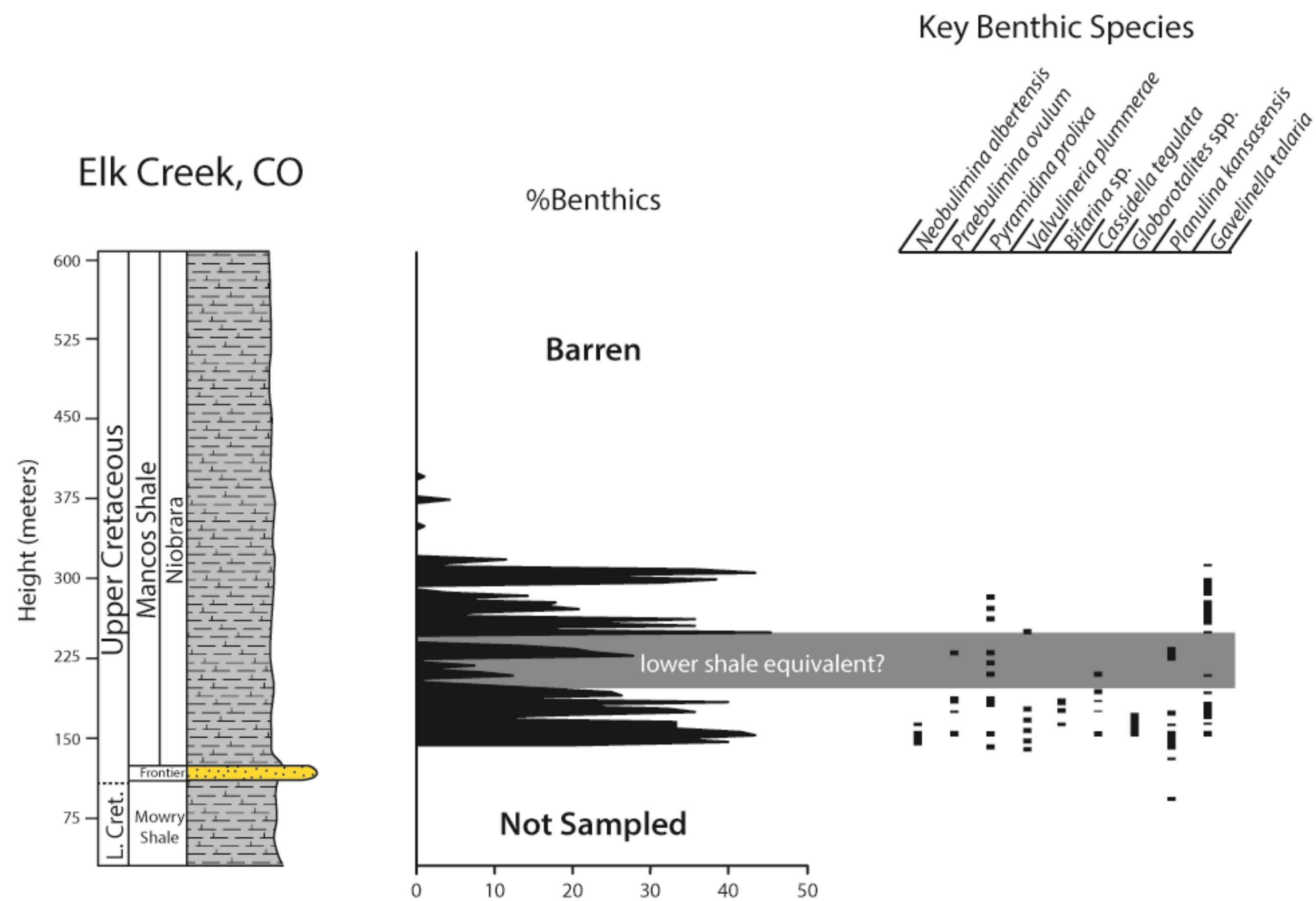

Figure 11. Summary of benthic foraminiferal abundance and the ranges of key species at Elk Creek, CO, after Kent (1968). %Benthics vs. total foraminifera. Gray bar shows low abundance interval assumed to be equivalent to lower shale unit on the Front Range.

Chlorite represents a large and increasing constituent of the clay assemblage at this level. Because of the lack of macrofossil biostratigraphy at Elk Creek, it is unclear if the recovery observed at Mesa Verde is equivalent to the top of the barren interval at Elk Creek, or if it might be found above the sampled section.

3.5.3 Northern Sea

The most striking feature of the record developed by Frerichs (1979) and Frerichs et al. (1975) at Centennial Valley is the difference in foraminiferal abundance between the Sage Breaks Shale and the Niobrara Formation (Figure 12). %Benthics increase from just above the Wall Creek Sandstone to an acme about 60 m above that level. Keeled planktic foraminifera are present throughout this interval, and are fairly diverse (up to 6 species, in the sample just above the Wall Creek) before sharply declining in parallel with the benthics. Foraminiferal number increases above this level, however, and remains high through the rest of the Sage Breaks Shale, while relatively low %benthics suggest that this increase is entirely driven by an abundant, thriving planktic community (Frerichs, 1979).

The *P. germari* zone, associated with the upper portion of the Sage Breaks Shale (Merewether et al., 2011), is equivalent to the Fort Hays Limestone in Pueblo, CO. It is tempting, then, to place the transition from high benthic abundance and keeled diversity to low benthic abundance and keeled diversity but very high foram numbers as equivalent to the lower Fort Hays. However, because the macrofossil biostratigraphy is correlated from another section (Rock River, ~50 mi north), it is impossible to precisely place these fossil occurrences in the stratigraphic section, making such correlations impossible.

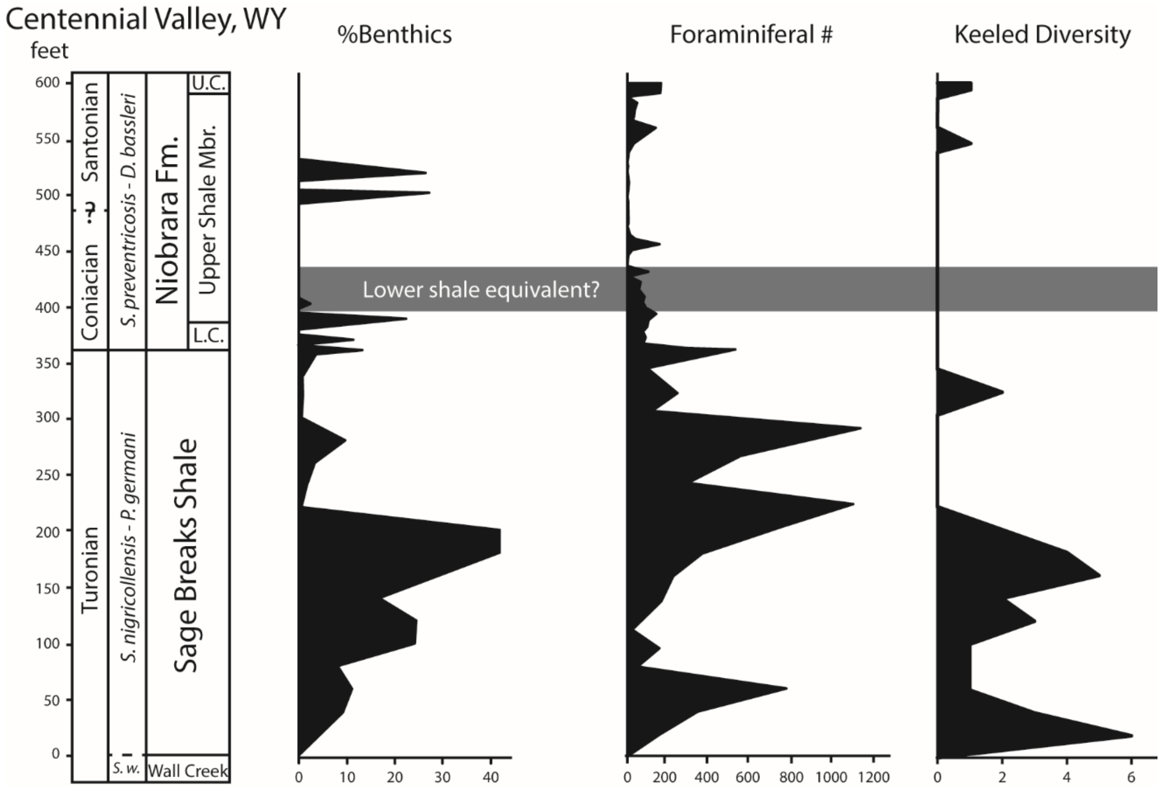

Figure 12. Summary of foraminiferal trends at Centennial Valley, after Frerichs et al. (1975) and Frerichs, (1979). Ammonite biozones after Merewether et al., 2011. %Benthics vs. total foraminifera; Foraminiferal Number reflects total individuals in each sample; Keeled Diversity represents number of keeled species present. Gray bar shows decline in abundance presumed to be equivalent to the lower shale unit on the Front Range. See Figure 2 for explanation of ammonite zones.

The unconformity between the Sage Breaks Shale and Niobrara Formation does make it possible to tie the lowermost Niobrara to the *S. preventricosus* zone, which ranges from the uppermost Fort Hays to the lowermost lower shale unit in the Colorado Front Range (Merewether et al., 2011). Benthic foraminifera make up no more than 15% of the overall assemblage in the Lower Chalk Member and briefly increase to 20% in the lowest sample in the Middle Shale Member before disappearing (two brief recoveries above this level are from samples with only a few foraminifera, and should not be considered significant) (Frerichs et al., 1975). Foraminiferal number is relatively low in the Lower Chalk Member, with < 200 foraminifera through the transition with the Middle Chalk Member, where foraminifera abundance eventually decreases to zero, before recovering to ~ Lower Chalk values just below the transition to the Upper Chalk. This level also records a minor recovery in keeled diversity, with several samples each containing one species of *Globotruncana* (Frerichs et al., 1975).

3.5.4 Southern Sea

The section at Wagon Mound, New Mexico starts in the lower, non-calcareous shale interval of the Juana Lopez Calcarenite (Figure 13). Lenses of sand-sized material are common and are composed primarily of inoceramid prisms. The coarse fraction of this shale is also dominated by inoceramid prisms, which outnumber foraminifera >10 to 1. This interval has the highest abundance of benthic foraminifera of the section, around 20%. The coarser upper unit of the Juana Lopez, like the Mesa Verde section, is barren of foraminifera, likely due dilution due the large numbers of foraminifera-sized shell fragments in the sediments. The boundary with the Montezuma Valley Member is in the upper Turonian *Scaphites whitifieldi* zone, and was not sampled due to deep weathering

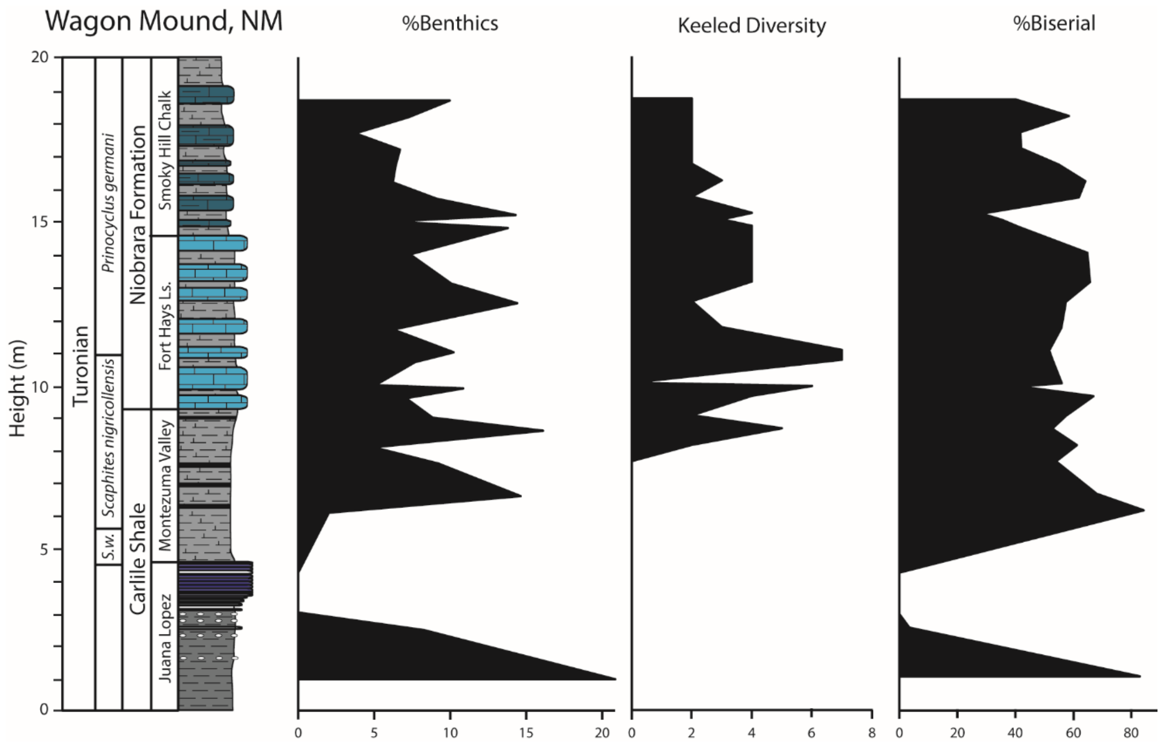

Figure 13. Summary of foraminiferal trends at Wagon Mound. %Benthics is vs. total foraminifera; %Biserial planktic foraminifera (vs. total planktics) and the simple diversity of keeled planktic foraminifera from the Kansas outcrop composite section. Ammonite biostratigraphy after Scott et al. (1986); see Figure 2 for explanation.

on a very shallow slope and vegetation on the outcrop. Few benthic foraminifers are found in the lower Montezuma Valley, but abundances quickly increase around 6 m and vary between 5 and 15% for the rest of the section. Keeled foraminifera make an appearance toward the top of the Montezuma Valley and, like in the Colorado Front Range, reach a peak in abundance above the base of the Fort Hays Limestone before decreasing gradually through the Fort Hays and lower chalk and shale unit of the Smoky Hill. Unfortunately, the transition to the lower shale unit is not preserved at this locality.

In west Texas, the middle/upper Turonian Langtry Member of the Eagle Ford Shale corresponds to the lowstand of the Greenhorn cycle (Lowery et al., 2014). The top of this unit contains sandy hummocks with the common occurrence of the echinoid *Hemisaster jacksoni* (Donovan et al., 2012), a common marine invertebrate of the Gulf Coast realm but missing from the Western Interior Sea. At the very top of the unit, just below the contact with the Austin Chalk (which is considered gradational in West Texas; Donovan et al., 2012), Lowery et al. (2014) identified a transgressive surface, based on an abrupt increase in benthic foraminifera and benthic diversity, decline in biserial planktic foraminifera, and a sudden increase in macrofossil debris (primarily inoceramid prisms), equivalent to a lag deposit at the base of the Austin Chalk near Austin, TX, which contains abundant fish bones and glauconite (the "Rubble Zone" of Lundquist, 2000). This transgressive surface is equivalent to the onset of Niobrara transgression in the WIS. While Western Interior lithofacies went through a succession of calcarenite (Juana Lopez), calcareous shale (Montezuma Valley and Sage Breaks), and finally limestone (Fort Hays) during this transgression, the lithofacies in Texas jumped from a thin transgressive lag overlying regressive calcareous shale/sandstone straight into the

high carbonate Austin Chalk, which records the oldest carbonates of the Niobrara Cycle (see discussion above). In the Austin, benthic foraminifera generally decrease toward the top of the section and are evenly divided between infaunal and epifaunal taxa throughout. This section contains the lower Coniacian *Cremnoceramus deformis erectus* inoceramid zone. The middle Coniacian ammonite *Peroniceras westphalicum* was identified approximately 38 m above the base of the Austin Chalk near Lozier canyon (Cobban et al., 2008), 10 m below the top of the measured section at Hwy 90, which would suggest that the Austin here upper Turonian-lower Coniacian in age and only equivalent to the lower Fort Hays in Colorado and Kansas.

3.6 Discussion/Interpretation

This discussion will synthesize data from all localities into time slices, based on ammonite zones, in order to illustrate regional paleoecological changes and suggest paleoceanographic drivers for them.

3.6.1 Middle to lower upper Turonian (*Prionocyclus macombi* to *Scaphites whitfieldi*)

The earliest phase of the Niobrara Cycle, equivalent to the Juana Lopez Calcarenite and Montezuma Valley Shale (and their associated unconformities in the center of the sea), represent rapid transgression of the Niobrara Sea. Restricted lowstand conditions gave way to continually improving oxygenation and normal marine waters as waters invaded the seaway from the north and south. Increasing import of Tethyan and Boreal waters with rising sea level likely invigorated circulation in the sea. Caballing is a process of mixing of two distinct water masses resulting in formation of a more dense third water mass that downwelled and may have exported “Western Interior Intermediate Water” out of the seaway (Fisher, 1991; Hay et al., 1993). Such a process suggests that

strengthening circulation would ventilate the seafloor. Indeed, increasing benthic foraminiferal abundance through the transgressive interval supports this hypothesis. Overall, the Niobrara transgression may be similar to the “Benthonic Zone” of Eicher and Worstell (1970), who described oxygenation of the seafloor during transgression of the Greenhorn Cycle at the base of the Bridge Creek Limestone. The staggered introduction of keeled planktic foraminifera show the progress of transgression, as gradually increasing water depths opened up habitat space for deeper planktic dwellers, and also suggests the middle water depths were well-ventilated.

In Texas, this interval is represented by a thin transgressive lag characterized by macrofossil debris (like the Juana Lopez), glauconite, and similar foraminiferal trends to those seen in the WIS proper, suggesting improved benthic ventilation but also condensation and winnowing on the seafloor. The early onset of carbonate deposition in Texas, which has been well-established (e.g., Walaszczyk and Cobban 2000), helps confirm the notion that carbonate deposition is tied to warm, southerly waters, and suggests that any pelagic limestone deposition in the WIS can be tied to a southern water mass (e.g., Longman et al., 1998).

3.6.2 Upper Turonian (*Scaphites nigricollensis to Scaphites mariasensis*)

The lower portion of the Fort Hays Limestone, which is late Turonian in age, records the late transgression of the Niobrara Cycle. It is missing in the western part of the study area, perhaps due to local subsidence or accommodation issues related to thrusting in the Sevier Highlands, as the early transgressive Juana Lopez and Montezuma Valley are well represented despite the fact that transgressive unconformities tend to expand in a proximal direction (Kauffman, 1984). In the central and southern sea,

however, the upper Turonian is well represented, and corresponds to a general continuation of the trends observed in the middle Turonian. Benthic foraminifera continue to be fairly abundant and diverse, and keeled foraminifera continue to diversify (increasing later in the S Colorado Portland Core than at the NE New Mexico Wagon Mound outcrop). Trace metal abundances in cores along the Front Range show a peak in manganese, which is generally, but not always, associated with oxic conditions. The abundance of benthic foraminifera at this level suggests that oxygen is, in this case, what is driving Mn abundance.

3.6.3 Lower Coniacian (*Scaphites preventricosus*)

Transgression slows and reaches a highstand in the upper portion of the Fort Hays Limestone (Kauffman, 1984). This is the second highest sea level in the history of the WIS, after the early Turonian Greenhorn highstand (Kauffman, 1984). As sea level rise begins to slow and reverse in the upper Fort Hays, trends in foraminifera, trace metals, circulation, and redox conditions also slow and begin to reverse. Benthic foraminiferal numbers decrease through the Fort Hays, and keeled planktics appear to follow the same trend in the Portland and Bounds cores, as well as in the Kansas outcrops. Black shale interbeds in the Fort Hays become thicker and, at least in the Bounds Core, are associated with higher organic carbon and trace metal markers for anoxia/euxinia (especially molybdenum, which indicates euxinia, or a state sulfide-reduction in the water column), as Mn decreases.

As sea level rise slows, so does the influx of Boreal and Tethyan water into the sea, resulting in a decrease in circulation and downwelling by caballing. Without this well-oxygenated bottom water mass, benthic conditions begin to deteriorate. The slowing

import of warm, carbonate-rich Tethyan water also decreases carbonate productivity in the sea, leading to a switch, particularly in the central and western sea from pure chalks and limestones, to marls and calcareous shales. This is what led to the change in lithology from the Fort Hays Limestone to the Smoky Hill Chalk, with the lower limestone and shale unit as a transitional interval.

The lower limestone and shale represents late highstand and early regression. Benthic foraminifera generally decline in the center of the sea, reaching values of 5-10%, which, on a well-oxygenated and reasonably productive margin, would represent upper bathyal water depths (500-1000 m; Culver, 1988; Leckie and Olson, 2003). Overall, the upper Fort Hays and lower limestone and shale unit and their equivalents correspond to the start of regression of the Niobrara Sea and a general transition from the well-oxygenated, normal marine conditions of the transgression of the Niobrara Sea to the anoxia and greater seaway restriction that followed.

3.6.4 Middle Coniacian (*Scaphites ventricosus*)

The transition recorded by the upper Fort Hays and lower shale and limestone unit abruptly ended in the lowermost part of the *S. ventricosus* zone, equivalent to the base of the lower shale unit of the Smoky Hill. Here, slowly decreasing oxygen suddenly crashed into strong euxinia, and total organic carbon preservation jumped from close to zero to >8 wt% in the Portland Core as benthic foraminifera disappear briefly in the Colorado Front Range. Mo abundance in the Berthoud State Core (Dean and Arthur, 1998b) and Bounds Core (Dean and Arthur, 1998b) sharply increases, as well. Northern (Frerichs et al., 1975) and northwestern (Kent, 1968) sites show an abrupt drop in %benthic foraminifera. The NW Colorado sites of Kent record fairly high %benthics through this interval, although

they fluctuate strongly and reach two short-lived nadirs in the *S. ventricosus* zone before quickly returning to previous values. These nadirs are not recorded at Mesa Verde, perhaps because they are not captured by the resolution of samples taken in this 550-m thick Niobrara Cycle section of the Mancos Shale. After the first nadir, benthic diversity does not recover, and the assemblages are dominated by only a few species. This suggests stressed conditions and continually deteriorating conditions, despite recovery in benthic abundance. Stressed benthic conditions are typically manifested as low diversity, high dominance benthic assemblages (Gooday, 2003). Benthic values also rebound, briefly, in the Front Range, in the basal portion of the overlying upper Coniacian *Scaphites depressus* zone. The benthic assemblages from the sections in southern Wyoming never recover.

In addition to the greater abundance of benthic foraminifera at the western sites in relation to localities in the center of the basin, %benthic values are progressively higher to the north. This suggests the continued influence of a coastal jet bringing cool, oxygen-rich Boreal waters down the western side of the sea, although steadily weakening based on declining benthic abundances (e.g., Kent, 1968; Hay et al., 1993; Slingerland, 1996; Leckie et al., 1998; DaGama et al., 2014). This interpretation is further supported by the highest discrete illite and lowest kaolinite abundances in this interval at Mesa Verde. Illite and chlorite (also high at this level) are generally formed through mechanical weathering (Dean and Arthur, 1998b), which suggests a dry, likely cool environment. Kaolinite, on the other hand, is formed by the chemical weathering of feldspar and suggests a humid, warm environment (1998b). Finklestein (1991) tied similar trends in the Bridge Creek Limestone Member of the Mancos Shale at Mesa Verde to the strength

of the northern-sourced water masses, and this appears to hold true for the Smoky Hill and Cortez Members as well.

If, on the other hand, these trends reflect changes in weathering rate instead of source area and current strength, low kaolinite suggests that the weathering rate is low and fairly steady throughout the Smoky Hill Member of the Mancos, despite the fact the center part of the seaway records declining carbonate content and increasing TOC well below this level. If this is caused by siliciclastic dilution, it is not coming from the western margin. The eastern margin is poorly understood at this time and is a possible candidate as a clay mineral source (e.g., Elderbak et al., 2014). However, if the eastern margin was a sediment source, it was not a large one, and certainly not large enough to affect the lithologic changes recorded in the carbonate-rich lower Niobrara Formation. Biserial planktic foraminifera also contradict a hypothesis of increasing clastic flux from the east diluting carbonate sedimentation and causing salinity-stratification. Biserial taxa live in the surface waters, and increase in abundance when surface waters differ from normal marine salinity (e.g., Leckie et al., 1998), so if freshwater flux was increasing during this time interval, biserial abundance would be expected to increase with it. The percentage of biserials at all sites does not show any discernable trends through the upper Fort Hays to lower limestone and shale and lower shale units even though carbonate content steadily decreases and TOC suddenly increases. Biserials tend to fluctuate in what appear to be 100-kyr cycles (perhaps reflecting real changes in precipitation and weathering flux) but do not track any of the observed, large-scale trends. Overall, biserial foraminifera show very poor correlation with either TOC or carbonate abundance (Figure 14), which is the opposite of what would be expected if freshwater input controlled these

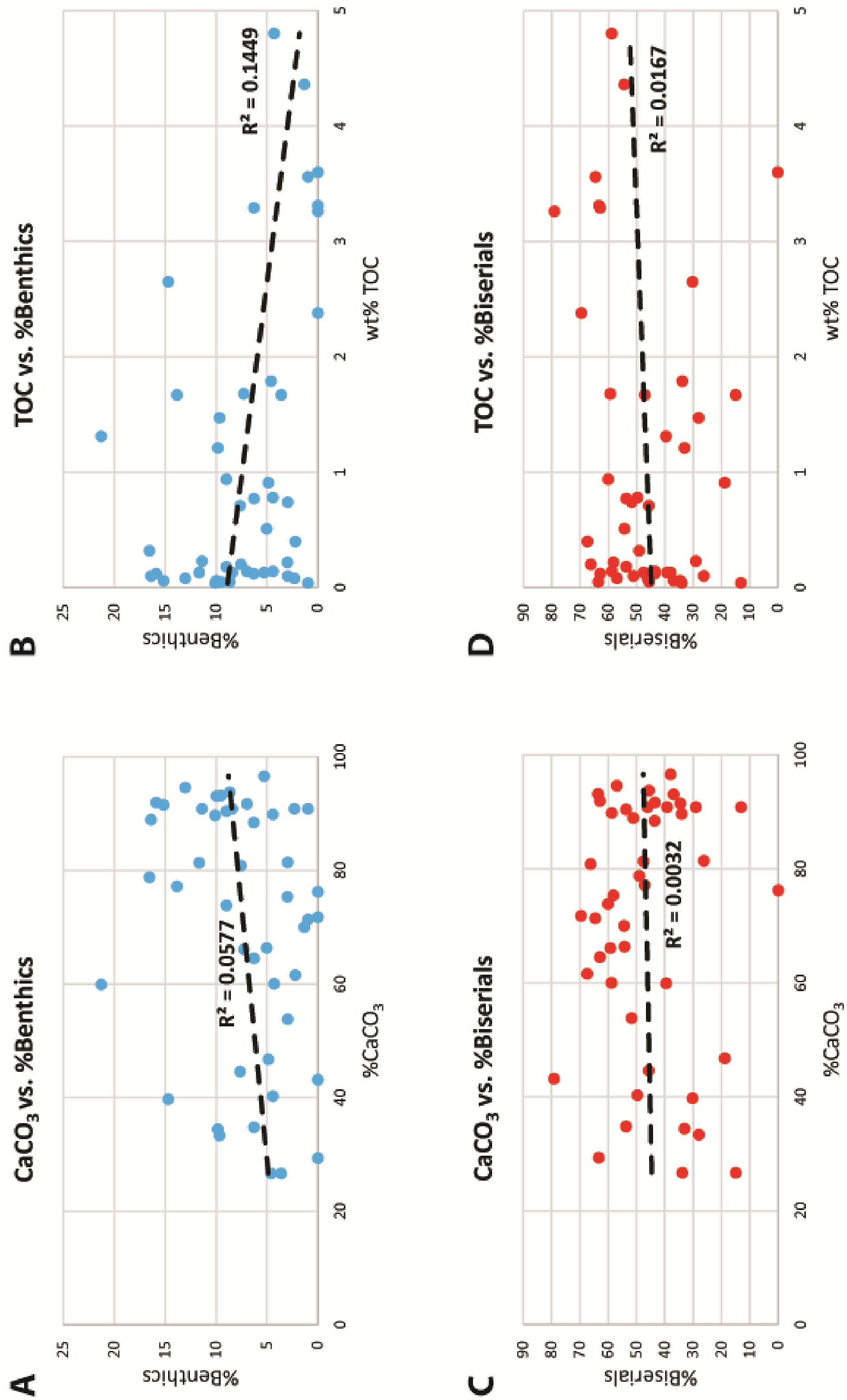

A
CaCO3 vs. %Benthics
R² = 0.0577
%Benthics
%CaCO3
B
TOC vs. %Benthics
R² = 0.1449
%Benthics
wt% TOC
C
CaCO3 vs. %Biserials
R² = 0.0032
%Biserials
%CaCO3
D
TOC vs. %Biserials
R² = 0.0167
%Biserials
wt% TOC

Figure 14 Cross plots of %benthic foraminifera and %carbonate (A), %benthics and TOC (B), %biserial planktic foraminifera and carbonate (C), and %biserials and TOC (D), with lines of best fit and R^2 values for each showing very low correlation. TOC and %carbonate data from Sageman et al., 2006.

mechanism the sea has to ventilate its deep waters: mixing and density-driven downwelling. Regression of the Niobrara Sea also compounded seaway constriction by supplying an abundance of river-borne nutrients, which sustained relatively high biological productivity and flux of organic matter to the seafloor.

3.6.6 Lower Santonian – lower Campanian (*Clioscaphites vermiformis – Scaphites leei* III)

For the benthos of the Western Interior Sea, the Santonian was a bleak time, with near zero benthic abundance along the Colorado Front Range, in Kansas, to the north in Wyoming, and even in their last refuge in the slowing suffocating waters of the western margin. Keeled planktic foraminifera are also absent, although this is possibly due to habitat loss driven by lowering sea level, rather than habitat loss driven by declining dissolved oxygen. Circulation slowed to a crawl, the sea became increasingly stratified, productivity increased in response to riverine runoff from all directions, and the seafloor became a soft, soupy mess colonized only by large flat clams (*Inoceramus platinus*).

Plankton in the mixed layer did fine, and occasionally, Tethyan water advanced into the seaway and supported calcareous nannofossil productivity and the deposition of chalks in the east, along the corridor where Tethyan water could minimally intrude. This time period corresponds to a sandy interval in the middle shale of the Smoky Hill. Known as a relatively thin interval in Colorado (Kauffman, 1985) and well-known as a significant middle sandy unit of the Smoky Hill in the Raton Basin (Scott et al., 1986), the progradation of this sandy facies, even as a minor constituent of an overall shaly interval, into the middle of the sea suggests sea levels were low indeed. Again, this was likely not caused by increased precipitation and riverine flux, as clay mineral trends at

Mesa Verde and in the Berthoud State Core do not show significant changes associated with this sandy interval.

3.6.7 Lower Campanian (*Scaphites hippocreppis* I-III)

Finally, at the end of the Niobrara Cycle, the upper chalky shale and upper chalk units of the Smoky Hill and their equivalents record some recovery from a 3-myr period of widespread anoxia. Keeled planktic foraminifera return to the center of the seaway, although benthics do not, while to the west benthic foraminifera return, especially agglutinated benthics. Agglutinated benthics have long been associated with Boreal waters in the WIS (Caldwell et al., 1993; West et al., 1998), suggesting a reinvigorated northern current moving south along the west side of the sea. The reversal of clay trends, with increasing chlorite at Mesa Verde, supports this hypothesis. The deposition of chalks to the east likewise signals an incursion of Tethyan waters. This (slightly) strengthened circulation and brought a modicum of oxygenation to the Niobrara Sea, at least its middle water depth.

3.6.8 Role of Sea Level

Sea Level appears to play a controlling role in the redox state of the Western Interior Sea. This influence likely goes beyond simple restriction and stratification, as periods of transgression and highstand are associated with increased proxies for Tethyan influence on the central and eastern side of the sea (higher carbonate, more Tethyan foraminifera, particularly keeled foraminifera) and increased proxies for Boreal water on the western side of the sea (more agglutinated foraminifera, detrital clays associated with cooler northern climates). To explain these trends and understand how they would impact the paleoceanography of the WIS, I propose a modified version of the caballing model

proposed by Hay et al. (1993) (Figure 15). The volume of water entering the sea from the north an south moderates the strength of mixing in the sea; the downwelling of this third water mass ventilates the sea floor, so the amount of mixing directly controls the amount of oxygen available to the benthos. If downwelling of oxygen-rich surface waters cannot keep pace with demand for oxygen on the seafloor, anoxia quickly sets in and organic carbon preservation is far more likely. This sets up threshold conditions for the development of anoxia within the WIS (Figure 16). As sea level falls, restriction of the basin reduces the amount of Tethyan and Boreal watermasses entering the sea, reducing mixing and downwelling of oxygen-rich waters, decreasing the amount of available oxygen. When this oxygen falls below a certain level, oxygen demand exceeds supply, and a rapid change occurs, as is seen in the *Scaphites ventricosus* zone. Rising sea level results in an opening of the basin, increasing the amount of Tethyan and Boreal waters entering the sea, increasing mixing and downwelling of oxygen-rich waters. At a certain point, the amount of oxygen downwelled exceeds demand, and a rapid change to well-oxygenated conditions occurs.

3.7 Conclusions

1. Foraminiferal records, sedimentation patterns, clay assemblages, and major and minor element geochemistry suggest that relative sea level change is the primary control on the paleoceanography of the Western Interior Sea during the third-order Niobrara Cycle. This control is exerted primarily through moderating the volume of outside (i.e., Tethyan and Boreal) waters entering the sea. This, in turn, controlled the strength of circulation, which drives mixing, caballing (e.g., Hay, 1993) and downwelling of a third, denser water mass. This denser water mass,

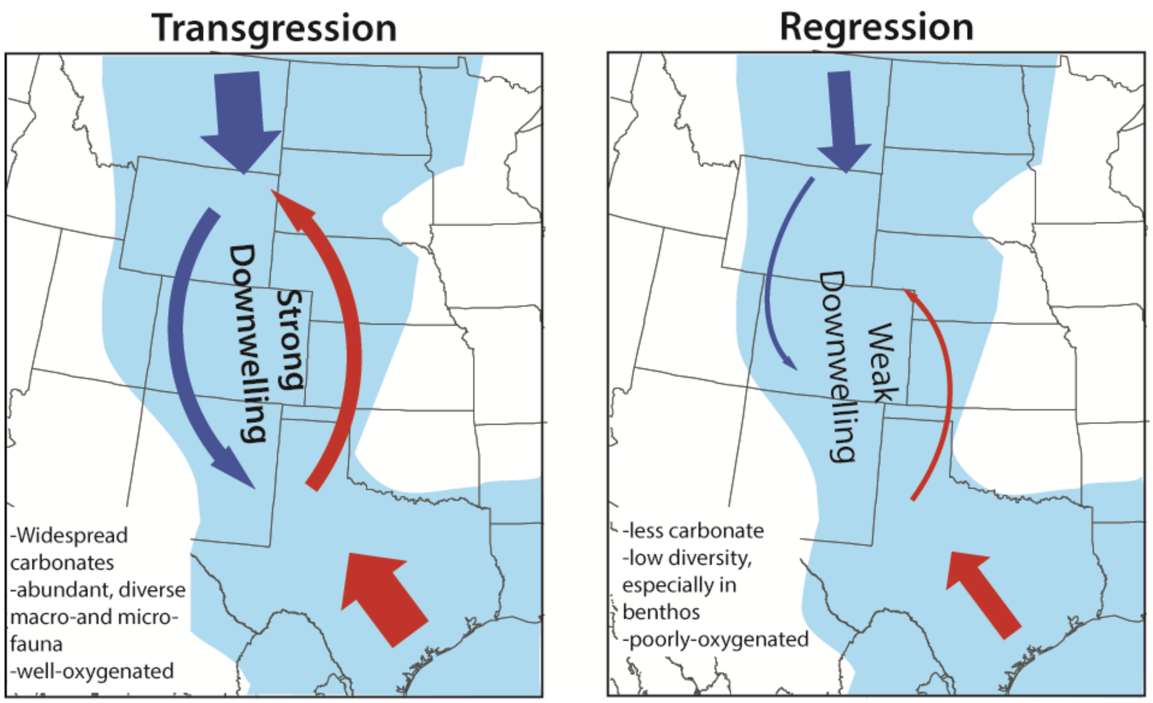

Figure 15. Diagram showing the effect of sea level on circulation in the WIS. Increasing import of Tethyan (southern) and Boreal (northern) into the seaway, leads to increased mixing and increased downwelling.

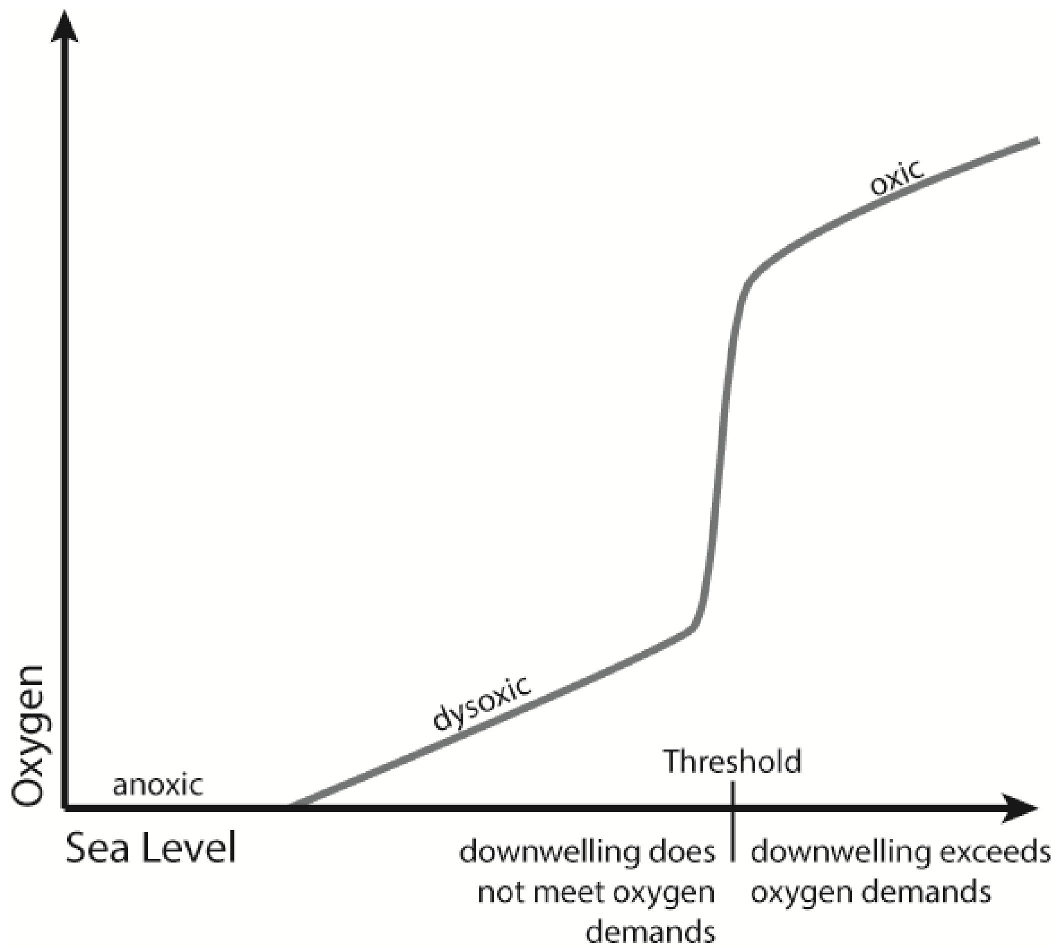

Figure 16. Simplified relationship between sea level and oxygen in the WIS. Falling sea level leads to decreased mixing and downwelling, which slowly decreases oxygen export to the sea floor until a critical threshold is crossed where oxygen demand exceeds oxygen supply and a rapid shift to anoxia occurs. Rising sea level causes the opposite trend.

Western Interior Intermediate Water, is exported oxygen to the sea floor, allowing the growth of a thriving, diverse benthic community during times of transgression in the seaway and vigorous mixing of Tethyan and Boreal water masses.

2. Following the lowstand of the Cenomanian-Turonian Greenhorn Cycle during the middle Turonian, early transgression of the Niobrara Cycle brought gradually improving conditions to the Western Interior Sea. Carbonate deposition, associated with southern, Tethyan water, began earlier in Texas and spread northwards, particularly on the eastern side of the sea. As sea level rise slowed and reversed, so did these trends, with decreasing dissolved oxygen and increasing organic carbon deposition at and above the early Coniacian highstand. These trends proceeded gradually until the middle Coniacian *Scaphites ventricosus* zone, equivalent to the lower shale on the Colorado Front Range, when falling sea level crossed a threshold and the sea quickly stratified, bringing euxinic conditions across the deep central axis. Circulation briefly resumed above this level, bringing a brief recovery in the benthic community, but falling sea level caused continued decline and a long interval in the middle of the Smoky Hill Chalk (upper Coniacian-Santonian) of no benthic and few to no deep-dwelling planktic foraminifera. Strengthening circulation in the basal Campanian upper chalky shale and upper chalk units and their equivalents brought a mild recovery, with keeled planktics reappearing in the central sea, and benthic foraminifera, chiefly agglutinated benthics associated with northern waters, returning to the Mesa Verde area.

3. Clay mineralogy and surface-dwelling planktic foraminifera, particularly biserial taxa, do not show any correspondence to trends in oxygenation and organic carbon production/preservation or lithology. This suggests that wet/dry climate cycles did not drive biological productivity in the sea, changes in circulation, or, by extension, changes in lithology in the Western Interior Sea during the Niobrara Cycle. Relative changes in sea level, likely driven by episodic tectonic loading and increased accommodation space, was the principle driver of seaway paleoceanography, water mass mixing, and organic carbon production and burial.
4. The diachronous onset of low-oxygen across the Western Interior Sea during OAE3 demonstrates that even in regions prone to anoxia during this interval, OAE3 does not represent an event. This supports the argument that “OAE3” is not a true, global event (e.g., Wagreich, 2012).

CONCLUSION

Sea level is the primary control on the development of anoxia in the Western Interior Sea during the Cenomanian-Campanian. The restricted nature of the sea and its dependence on outside water masses to drive circulation meant that the local sea level forcing greatly overwhelmed any global trends toward increasing or decreasing dissolved oxygen. During the late Cenomanian OAE2, rising sea level ventilated the sea during a time when large parts of the open ocean were anoxic and even euxinic. During the Coniacian-Campanian OAE3, falling sea level choked off circulation, driving increased stratification and an expanding oxygen minimum zone, during a time when large parts of the open ocean, particularly the eastern Tethys, were experiencing increasing oxygenation. Organic carbon accumulation rate during both events show a great disparity in the WIS, with organic carbon burial during OAE3 in the Niobrara vastly exceeding rates associated with OAE2 in the Bridge Creek (Locklair et al., 2011). Likewise, anoxia does not develop in the sea during OAE2 until later in the event, and the lack of associated organic carbon enrichment lead many authors to assume that the anoxia was driven by the incursion of a low-oxygen water mass from the open ocean (e.g., Eicher and Worstell, 1970). The Niobrara, meanwhile, is associated with multiple proxies for sustained anoxia and euxinia.

During both the Cenomanian-Turonian Greenhorn Cycle and the Turonian-Campanian Niobrara Cycle, rising sea level is associated with increasing ventilation, an abundant, diverse benthic community, and the deposition of carbonate facies, particularly

in the central and eastern parts of the sea. Falling sea level is associated with increasing stratification, declining benthic population and diversity, and the deposition of organic-rich facies. During both these sea level trends, the sea exhibits threshold behavior: during transgression, conditions (salinity and oxygenation, primarily) improve gradually until sea level rise passes some critical threshold to allow an ideal volume of open ocean water into the sea and geologically instantaneous improvement occurs. This is exemplified by the base of the Bridge Creek Limestone in Colorado ("Bed 63") and its equivalent, the base of the Scott Ranch Member of the Eagle Ford Shale in west Texas in the sudden abundance of benthic foraminifera (the "Benthonic Zone" of Eicher and Worstell, 1970) and the change in lithology from organic rich dark shale to organic poor limestone and marl. Multiple transgressive unconformities in the central sea make a similar horizon more difficult to pinpoint during the transgression of the Niobrara, although the Ft. Hays Limestone Member represents peak transgression and the best ventilated conditions of the Niobrara cycle. During regression and deposition of the Smoky Hill Member, the same trend occurs in reverse: conditions deteriorate gradually until sea level fall passes some critical threshold restricting the inflow of open ocean water, and conditions almost instantaneously deteriorate. This is exemplified at the base of the lower shale unit of the Smoky Hill Chalk Member of the Niobrara Formation in Colorado with a sudden increase in TOC and trace metal markers for euxinia and the sudden disappearance of benthic and deeper-dwelling planktic foraminifera.

Orbitally-forced wet/dry climate cycles have long been invoked to explain some or all of the paleoceanographic change in the Western Interior Sea (Gilbert, 1895; Fischer et al., 1991; Hay et al., 1993; Pratt et al., 1993; Slingerland et al., 1996; Dean and Arthur

1998b). There is certainly an orbitally-derived signal recorded in the rocks of the Greenhorn and Niobrara Formations (e.g., Meyers et al., 2001; Locklair and Sageman, 2008; Sageman et al., 2014), and in an ice-free world like the Cretaceous, insolation changes were most likely expressed as changes in precipitation. However, these changes appear to be limited to higher-frequency cycles overprinted on the 4-5 myr 2^{nd}-order and 1-2 myr 3^{rd}-order tectonically driven sea level cycles. Shallow-dwelling planktic foraminifera should show a strong response to changes in surface salinity that would accompany increased precipitation and runoff. These taxa do vary, but at a high-resolution and low-amplitude, and do not track observed changes in benthic conditions or lithology, suggesting that while regional precipitation did fluctuate enough to imprint on the rock record, it was not the driver of the major observed changes. This interpretation is supported by clay mineralogy, which appears to track changes in the strength of circulation and not freshwater runoff.

So What?

The expression of both OAEs preserved in the Western Interior differ significantly from their “global” or “typical” expression. This is not a novel idea – it’s been around at least since Pratt and Threkeld (1984) showed that organic matter enrichment occurs prior to the onset of OAE2 – although hopefully the preceding 142 pages render it more robust. But, *of course* local records differ from a global ideal; it should not come as a surprise that the geochemical, biologic, and lithologic records of a particular outcrop or region are primarily affected by the local environment. One might as well complain that lithology varies from basin to basin during a particular interval of time. Hopefully it goes without saying that *all* geochemical, biologic, and lithologic

records are primarily a product of their local environment, and any global climatic event is going to be filtered through the lens of that local environment. Or, to take look at the opposite side of the same coin: all global records are the sum of local trends. So the mere fact that sections containing records of OAE2 or OAE3 in the WIS differ from equivalent "classic" sections in Europe or the South Atlantic does not automatically disqualify them as important records of those intervals.

Indeed, the similarities and differences between these regions highlight important mechanisms controlling the development of anoxia and the deposition of black shales. One example of this may be the importance of sea level change and oceanographic restriction to the development of anoxia. For example, although van Helmond et al. (2015) convincingly invoke runoff-induced stratification for the development of Cenomanian-Turonian TOC-rich black shales at Wunstorf, Germany, the restricted nature of that basin certainly played an important role. More generally, most "classic" OAE2 intervals are in the North Atlantic and eastern Tethyan region, which was a restricted ocean basin before the opening of the South Atlantic resulted in a new global circulation pattern and a general ventilation of the region, which prevented the development of black shales during OAE3 time (e.g., Wang et al., 2011; Wagreich, 2012). The WIS did not experience this ventilation, and saw the opposite trend as falling sea level restricted the basin; as a result, sediments there are enriched in TOC and record evidence of anoxia.

Globally, both the Cenomanian-Turonian and Coniacian-Campanian are periods of the enhanced development of black shales and anoxia. By emphasizing the role local conditions play in their development, the results presented in this dissertation reinforce the fact that these perturbations require more than just globally enhanced nutrient

delivery to develop. These local conditions are important, and the unique regional factors add up to a globally important event.

In the case of the Coniacian-Campanian OAE3, the local biotic response to anoxia across the WIS suggests that the onset of anoxia was diachronous even within the Western Interior basin. This diachronaitity supports the argument made by others (e.g., Wagreich, 2012) that OAE3 is not an "event" in the sense of other OAEs, but "merely" an interval of enhanced production/preservation of organic matter and anoxia development in regions prone to it. A new nomenclatural designation for this interval would be useful, as it would allow researchers to stop thinking of it as an easy-to-ignore lesser OAE, and focus attention on a long-term period of black shale formation that played an important role in the cooling of the Santonian-Campanian.

WORKS CITED

Ando, A., Huber, B.T., MacLeod, K.G., 2010. Depth-habitat reorganization of planktonic foraminifera across the Albian/Cenomanian boundary. Paleobiology 36, 357—373, doi: 10.1666/09027.1

Arthur, M.A., Schlanger, S.O., 1979. Cretaceous “oceanic anoxic events” as causal factors in development of reef-reservoired giant oil fields. AAPG Bulletin 63, 870—885

Arthur, M.A., Zachos, J.C., Jones, D.S., 1987. Primary productivity and the Cretaceous/Tertiary boundary event in the oceans. Cretaceous Research 8, 43—45

Arthur, M.A., Brumsack, H.J., Jenkyns, H.C., Schlanger, S.O., 1990. Stratigraphy, geochemistry, and paleoceanography of organic carbon-rich Cretaceous sequences, in: Ginsburg, R.N., Beaudoin, B. (Eds.), Cretaceous Resources, Events, and Rhythms: Dordrecht (Kluwer), 75-119.

Arthur, M.A., Sageman, B.B., 2005. Sea level control on source rock development: Perspectives from the Holocene Black Sea, the mid-Cretaceous Western Interior Basin of North America, and the Late Devonian Appalachian Basin, in: Harris, N.B. (Ed.), The Deposition of Organic Carbon-Rich Sediments: Models, Mechanisms and Consequences. Society for Sedimentary Geology, Tulsa, pp. 35—59

Barclay, R.S., McElwain, J.C., Sageman, B.B., 2010. Carbon sequestration activated by a volcanic CO_2 pulse during Oceanic Anoxic Event 2. Nature Geoscience 3, 205—208

Bralower, T.J., 1988. Calcareous nannofossil biostratigraphy and assemblages of the Cenomanian-Turonian boundary interval: implications for the origin and timing of oceanic anoxia. Paleoceanography 3, 275—316

Bralower, T.J., Bergen, J.A., 1998. Cenomanian-Santonian calcareous nannofossil biostratigraphy of a transect of cores drilled across the Western Interior Seaway, in: Dean, W.E., Arthur, M.A. (Eds.), Stratigraphy and paleoenvironments of the Cretaceous Western Interior Seaway, USA. SEPM Concepts of Sedimentology and Paleontology 6, 59—77

Burns, C.E., Bralower, T.J., 1998. Upper Cretaceous nannofossil assemblages across the Western Interior Seaway: implications for the origins of lithologic cycles in the Greenhorn and Niobrara Formations, in: Berggren, W.A., Kent, D.V., Aubry, M.-P., Harbendol, J. (Eds.), Geochronology Times Scales and Global Stratigraphic Correlation SEPM Special Publication 54, 35—58

Caron, M., 1985. Cretaceous planktic foraminifera, in: Bolli, H.M., Saunders, J.B., Perch-Nielsen, K. (Eds.), Plankton Stratigraphy. Cambridge University Press, 17—86.

Caron, M., Dall'Agnolo, S., Accarie, H., Barrera, E., Kauffman, E.G., Amédro, D., Robaszynski, F., 2006. High-resolution stratigraphy of the Cenomanian-Turonian boundary interval at Pueblo (USA) and Wadi Bahloul (Tunisia): stable isotope and bio-events correlation. Géobios 39, 171—200

Cobban, W.A., Scott, G.R., 1972. Stratigraphy and ammonite fauna of the Graneros Shale and Greenhorn Limestone near Pueblo, Colorado. Washington, D.C., U.S. Geological Survey Professional Paper 645, 108 p.

Cobban, W.A., Hook, S.C., McKinney, K.C., 2008. Upper Cretaceous molluscan record along a transect from Virden, New Mexico, to Del Rio, Texas. New Mexico Geology 30, 75—92.

Corbett, M.J., Watkins, D.K., 2013, Calcareous nannofossil paleoecology of the mid-Cretaceous Western Interior Seaway and evidence of oligotrophic surface waters during OAE2, Palaeogeography, Palaeoclimatology, Palaeoecology 392, 510—523

Corbett, M.J., Watkins, D.K., Popspichal, J.J., 2014, A quantitative analysis of calcareous nannofossil bioevents of the Late Cretaceous (Late Cenomanian-Coniacian) Western Interior Seaway and their reliability in established zonation schemes, Marine Micropaleontology 109, 30—45

Da Gama, R.O.B.P., Lutz, B., Desjardins, P., Thompson, M., Prince, I., Espejo, I., 2014. Integrated paleoenvironmental analysis of the Niobrara Formation: Cretaceous Western Interior Seaway, northern Colorado. Palaeogeography, Palaeoclimatology, Palaeoecology 413, 66 — 80

Dane, C.H., Cobban, W.A., Kauffman, E.G., 1966. Stratigraphy and regional relationships of a reference section for the Juana Lopez Member, Mancos Shale, in the San Juan Basin, New Mexico. US Geological Survey Bulletin 1224-H, H1—H15

Dean, W.E., Arthur, M.A., 1998a.Cretaceous Western Interior Seaway Drilling Project: an overview in: Dean,W.E., Arthur, M.A. (Eds..), Stratigraphy and paleoenvironments of the Cretaceous Western Interior Seaway, U.S.A: SEPM Concepts in Sedimentology and Paleontology 6, 1—10

Denne, R.A., Hinote, R.E., Breyer, J.A., Kosanke, T.H., Lees, J.A., Engelhardt-Moore, N., Spaw, J.M.,Tur, N.0 2014. The Cenomanian-Turonian Eagle Ford Group of South Texas: Insights on timing and paleoceanographic conditions from geochemistry and micropaleontologic analyses, Palaeogeography, Palaeoclimatology, Palaeoecology (2014), doi:10.1016/j.palaeo.2014.05.029

Desmares, D., Grosheny, D., Beaudoin, B., Gardin, S., Gauthier-Lafaye, F., 2007. High-resolution stratigraphic record constrained by volcanic ash beds at the Cenomanian-Turonian boundary in the Western Interior Basin, USA. Cretaceous Research 28, 561—582

Donovan, A. D., Staerker, T.S., 2010. Sequence stratigraphy of the Eagle Ford (Boquillas) formation in the subsurface of south Texas and the outcrops of west Texas. Gulf Coast Association of Geologic Societies Transactions 60, 861–899

Donovan, A.D., Staerker, T.S., Pramudito, A., Li, W., Corbett, M.J., Lowery, C.M. Miceli Romero, A., Gardner, R.D., 2012. The Eagle Ford outcrops of west Texas: a laboratory for understanding heterogeneities within unconventional mudstone reservoirs. Gulf Coast Association of Geologic Societies Journal 1, 162—185

Eicher, D.L., 1965. Foraminifera and biostratigraphy of the Graneros Shale. Journal of Paleontology 39, 875—909

Eicher, D.L., 1966. Foraminifera of the Cretaceous Carlile Shale of Colorado. Cushman Foundation for Foraminiferal Research Contributions 17, 16—31

Eicher, D.L., 1969. Cenomanian Turonian planktonic foraminifera from the Western Interior of the United States, in: Bronnimann, P., Renz, H.H. (Eds.), Proceedings of the first international conference on planktonic microfossils. Leiden, E.J. Brill 2, 163—174

Eicher, D.L., Worstell, P., 1970. Cenomanian and Turonian foraminifera from the Great Plains, United States. Micropaleontology 16, 269—324

Eicher, D.L., Diner, R., 1985. Foraminifera as indicators of water mass in the Cretaceous Greenhorn Sea, Western Interior, in: Pratt, L., Kauffman, E.G., Zelt, F.B. (Eds.), Fine-grained deposits and biofacies of the Cretaceous Western Interior Seaway: evidence of cyclic depositional processes. SEPM Annual Mid-Year Meeting, Field Trip No. 4, 122—134

Eicher, D.L., Diner, R., 1989. Origin of the Cretaceous Bridge Creek cycles in the Western Interior, United States. Palaeogeography, Palaeoclimatology, Palaeoecology 74, 127—146

Elder, W.P., 1985. Biotic patterns across the Cenomanian-Turonian boundary near Pueblo, Colorado, in: Pratt, L., Kauffman, E.G., Zelt, F.B. (Eds.), Fine-grained deposits and biofacies of the Cretaceous Western Interior Seaway: evidence of cyclic depositional processes. SEPM Annual Mid-Year Meeting, Field Trip No. 4, 157—169

Elder, W.P., 1989. Molluscan extinction patterns across the Cenomanian-Turonian stage boundary in the western interior of the United States. Paleobiology 15, 299—320

Elder, W.P., 1991. Molluscan paleoecology and sedimentation patterns of the Cenomanian-Turonian extinction interval in the southern Colorado Plateau region, in: Nations, J. D., Eaton, J. G. (Eds.), Stratigraphy, depositional environments, and sedimentary tectonics of the Western Margin, Cretaceous Western Interior Seaway. Geological Society of America, Boulder, Special Paper 260, 113—137

Elder, W.P., Kirkland, J.I., 1985. Stratigraphy and depositional environments of the Bridge Creek Limestone Member of the Greenhorn Limestone at Rock Canyon Anticline near Pueblo, Colorado, in: Pratt, L., Kauffman, E.G., Zelt, F.B. (Eds.), Fine-grained deposits and biofacies of the Cretaceous Western Interior Seaway: evidence of cyclic depositional processes. SEPM Annual Mid-Year Meeting, Field Trip No. 9, 122—134

Elder, W.P., Gustason, E.R., and Sageman, B.B., 1994. Correlation of basinal carbonate cycles to nearshore parasequences in the Late Cretaceous Greenhorn seaway, Western Interior U.S.A. Geological Society of America Bulletin 106, 892—902

Elderbak, K., Leckie, R.M., Tibert, N.E., this volume. Paleoenvironmental and paleoceanographic changes across the Cenomanian-Turonian Boundary Event (Oceanic Anoxic Event 2) as indicated by foraminiferal assemblages from the eastern margin of the Cretaceous Western Interior Seaway. Palaeogeography, Palaeoclimatology, Palaeoecology

Eldrett, J.S., Minisini, D., Bergman, S.C., 2014. Decoupling of the carbon cycle during Oceanic Anoxic Event 2. Geology doi:10.1130/G35520.1.

Eleson, J.W., Bralower, T.J., 2005. Evidence of changes in surface water temperature and productivity at the Cenomanian/Turonian Boundary. Micropaleontology 51, 319—322

Erba, E., 1992. Middle Cretaceous nannofossils from the Western Pacific (ODP Left 129): evidence for paleoequatorial crossings, in: Lawson, R.L., Lancelot, Y., (Eds.), Proceedings of the Ocean Drilling Program Scientific Results 129, 189—201

Erba, E., 2004. Calcareous nannofossils and Mesozoic oceanic anoxic events. Marine Micropaleontology 52, 85—106

Erba, E., Castradori, G., Guasti, G., Ripepe, M., 1992. Calcareous nannofossils and Milankovitch cycles: The example of the Albian Gault Clay Formation (southern England). Palaeogeography, Palaeoclimatology, Palaeoecology 93, 47-69. doi:10.1016/0031-0182(92)90183-6.

Erbacher, J., Thurow, J., Littke, R., 1996. Evolution patterns of radiolaria and organic matter variations: a new approach to identify sea-level changes in mid-Cretaceous pelagic environments. Geology 24, 499—502

Erbacher, J., and Thurow, J., 1997. Influence of oceanic anoxic events on the evolution of mid-Cretaceous radiolaria in the North Atlantic and western Tethys. Marine Micropaleontology 30, 139—158

Fisher, C.G., Hay, W.W., and Eicher, D.L., 1994. Oceanic front in the Greenhorn Sea (late middle through late Cenomanian). Paleoceanography 9, 879—892

Friedrich, O., Erbacher, J., Mutterlose, J., 2006. Paleoenvironmental changes across the Cenomanian/Turonian boundary event (Oceanic Anoxic Event 2) as indicated by benthic foraminifera from the Demerara Rise (ODP Leg 207). Revue de Micropaléontologie 49, 121—139

Friedrich, O., 2010. Benthic foraminifera and their role to decipher paleoenvironment during mid-Cretaceous Oceanic Anoxic Events – the "anoxic benthic foraminifera" paradox. Revue de Micropaléontologie 53, 175—192

Friedrich, O., Norris, R.D., Erbacher, J., 2012. Evolution of Late Cretaceous oceans – A 55 m.y. record of Earth's temperature and carbon cycle. Geology 40, 107—110

Frerichs, W.E. and Dring, N.B., 1981. Planktonic foraminifera from the Smoky Hill Shale of West central Kansas. Journal of Foraminiferal Research 11, 47-69.

Frush, M.P., Eicher, D.L., 1975. Cenomanian and Turonian foraminifera and paleoenvironments in the Big Bend region of Texas and Mexico, in: Caldwell, W.G.E. (Ed.), The Cretaceous System in the Western Interior of North America. The Geological Society of Canada Special Paper 13, 277—301

Gale, A.S., Smith, A.B., Monks, N.A.E., Young, J.A., Howard, A., Wray, D.S., Huggett, J.M., 2000. Marine biodiversity through the Late Cenomanian-Early Turonian: paleoceanographic controls and sequence stratigraphy biases. Journal of the Geological Society 157, 745—757

Gale, A.S., Kennedy, W.J., Voight, S., Walaszczyk, I., 2005. Stratigraphy of the Upper Cenomanian-Lower Turonian chalk succession at Eastbourne, Sussex, UK: ammonites, inoceramid bivalves, and stable carbon isotopes. Cretaceous Research 26, 460—487

Gale, A.S., Voigt, S., Sageman, B.B., Kennedy, W.J., 2008. Eustatic sea-level record for the Cenomanian (Late Cretaceous) – extension to the Western Interior Basin, USA. Geology 36, 859—862

Geisen, M., Bollman, J., Herrle, J.O., Mutterlose, J., Young, J.R., 1999. Calibration of the random settling technique for calculation of absolute abundances of calcareous nannoplankton. Micropaleontology 45, 437—442

Gibson, T. G., 1989. Planktonic: benthonic foraminiferal ratios: modern patterns and Tertiary applicability. Marine Micropaleontology 15, 29—52

Gooday, A.J., 2003. Benthic Foraminifera (Protista) as tools in deep-water palaeoceanography: environmental influences on faunal characteristics. Advances in Marine Biology 46, 1—90

Gradstein, F.M., Ogg, J.G., Schmitz, M., Ogg, G. 2012. The Geologic Time Scale. Elsevier, Amsterdam, The Netherlands

Hancock, J.M., Kauffman, E.G., 1979. The great transgressions of the Late Cretaceous. Geological Society of London Journal 136, 175—186

Hancock, J.M., Walaszczyk, I., 2004. Mid-Turonian to Coniacian changes of sea level around Dallas, Texas. Cretaceous Research 25, 459—471

Hattin, D.E. and Cobban, W.A., 1977. Fourth and fifth days: Upper Cretaceous stratigraphy, paleontology and paleoecology of western Kansas. The Mountain Geologist 14, 175—215.

Hattin, D.E., 1982. Stratigraphy and depositional environment of Smoky Hill Chalk Member, Niobrara Chalk (Upper Cretaceous) of the type area, western Kansas. Bulletin-Kansas State Geological Survey, vol. 225. 108 pp.

Haq, B.V., Harbendol, J., Vail, P.R., 1987. Chronology of fluctuating sea levels since the Triassic (250 million years ago to present). Science 235, 1159—1167

Haq, B.U., 2014. Cretaceous eustasy revisited. Global Planetary Change 113, 44—58

Hardenbol, J., J. Thierry, M.B. Farley, T. Jacquin, P.C. de Graciansky, and P. Vail, 1998, Mesozoic and Cenozoic sequence chronostratigraphic framework of European basins, in P.C. Graciansky, et al. (eds) Mesozoic and Cenozoic Sequence Stratigraphy of European Basins: SEPM Special Publication 60, 3—13

Hardas, P., Mutterlose, J., 2007. Calcareous nannofossil assemblages of Oceanic Anoxic Event 2 in the equatorial Atlantic: Evidence of an eutrophication event. Marine Micropaleontology 66, 52—69

Hattin, D.E., 1971. Widespread, synchronously deposited, burrow-mottled limestone beds in Greenhorn Limestone (Upper Cretaceous) of Kansas and central Colorado. American Association of Petroleum Geologists Bulletin 55, 412—431

Hattin, D.E., 1975. Stratigraphy and depositional environment of Greenhorn Limestone (Upper Cretaceous) of Kansas. Kansas Geological Survey Bulletin 209, 128 p.

Hayden Scott, C.C., 1992. Clay mineralogy of the Upper Cretaceous Mancos Shale near Mesa Verde National Park, southwestern Colorado: Clues to the paleoceanography of the Western Interior Seaway. MS Thesis, University of Massachusetts, 225 p.

Hayward, B.W., 1990. Use of foraminiferal data in analysis of Taranaki basin, New Zealand. Journal of Foraminiferal Research 20, 71—83

Hazzard, R.T., 1959. Measured section, in: Cannon, R.L., Hazzard, R.T., Young, A., Young, K.P. (Eds.), Geology of the Val Verde Basin. West Texas Geological Society Guidebook, November 5—8, Midland, 118 p.

Hentz, T.F., Ruppel. S.C., 2010. Regional lithostratigraphy of the Eagle Ford Shale: Maverick Basin to East Texas Basin. Gulf Coast Association of Geological Societies Transaction 60, 325—337

Herrle, J.O., 2002. Paleoceanographic and paleoclimatic implications on mid-Cretaceous black shale formation in the Vocontian Basin and the Atlantic: Evidence from calcareous nannofossils and stable isotopes. Tübinger Mikropaläontologische Mitteilungen 27, 1—114

Herrle, J.O., 2003. Reconstructing nitricline dynamics of mid-Cretaceous oceans; evidence from calcareous nannofossils from the Niveau Paquier black shale (SE France). Marine Micropaleontology 47, 307—321. doi:10.1016/S0377-8398(02)00133-0.

Hill, R.T., 1887a. The topography and geology of the Cross Timbers and surrounding regions in northern Texas. American Journal of Science, 3rd Series 33, 291—303

Hill, R.T., 1887b. The Texas section of the American Cretaceous. American Journal of Science, 3rd Series 34, 287—309

Huber, B.T., Petrizzo, M.R., 2014. Evolution and taxonomic study of the Cretaceous planktic foraminiferal genus *Helvetoglobotruncana* Reiss, 1957. Journal of Foraminiferal Research 44, 40—57

Jarvis, I., Gale, A.S., Jenkyns, H.C., Pearce, M.A., 2006. Secular variation in Late Cretaceous carbon isotopes: a new $\delta^{13}C$ carbonate reference curve for the Cenomanian–Campanian (99.6-70.6 Ma). Geology Magazine 143, 561—608

Jenkyns, H.C., 1980. Cretaceous anoxic events: from continents to oceans. Journal of the Geological Society 137, 171—188, doi:10.1144/gsjgs.137.2.0171

Jenkyns, H.C., 2010. Geochemistry of oceanic anoxic events. Geochemistry, Geophysics, Geosystems, 11, 30 p.

Jiang, M.J., 1989. Biostratigraphy and geochronology of the Eagle Ford Shale, Austin Chalk, and lower Taylor Marl in Texas based on calcareous nannofossils. Ph.D. dissertation, Texas A&M University, 496 p.

Joo, Y.I., Sageman, B.B., 2014. Cenomanian to Campanian carbon isotope chemostratigraphy from the Western Interior Basin, U.S.A. Journal of Sedimentary Research, 84, 529—542

Jorissen, F.J., 1999. Benthic foraminiferal microhabitats below the sediment-water interface. In: Sen Gupta, B.K. (Ed.), Modern Foraminifera. Kluwer Academic Publishers, Dordrecht, 161—179

Kaiho, K., Hasegawa, T., 1994. Cenomanian benthic foraminiferal extinctions and dysoxic events in the northwestern Pacific Ocean margin. Palaeogeography, Palaeoclimatology, Palaeoecology 111, 29—43

Kauffman, E.G., 1977a. Geological and biological overview: Western Interior Cretaceous Basin, in: Kauffman, E.G. (Ed.), Cretaceous facies, faunas and paleoenvironments across the Western Interior Basin. Mountain Geologist 14, 75—99

Kauffman, E.G., 1977b. Upper Cretaceous cyclothems, biotas, and environments, Rock Canyon Anticline, Pueblo, Colorado, in: Kauffman, E.G. (Ed.), Cretaceous facies, faunas, and paleoenvironments across the Western Interior Basin: Mountain Geologist 14, 129—152

Kauffman, E.G., 1984. Paleobiogeography and evolutionary response dynamic in the Cretaceous Western Interior Seaway of North America, in: Westermann, G.E.G. (Ed.), Jurassic-Cretaceous biochronology and paleogeography of North America. Geological Association of Canada Special Paper 27, 273—306

Kauffman, E.G., Pratt, L.M., 1985. A field guide to the stratigraphy, geochemistry, and depositional environments of the Kiowa-Skull Creek, Greenhorn, and Niobrara marine cycles in the Pueblo-Canon City Area, Colorado, in : L.M. Pratt, E.G. Kauffman, & F.B. Zelt (Eds.), Fine-grained Deposits and Biofacies of the Cretaceous Western Interior Seaway: Evidence of Cyclic Sedimentary Processes. Society of Economic Paleontologists and Mineralogists, Tulsa, 250—276.

Kauffman, E.G., Caldwell, W.G.E., 1993. The Western Interior Basin in space and time. in: Kauffman, E.G. Caldwell, W.G.E. (Ed.), Evolution of the Western Interior Basin. Geological Association of Canada Special Paper 39, 1—30

Kennedy, W.J., Walaszczyk, I., Cobban, W.A., 2005. The global boundary stratotype section and point for the base of the Turonian Stage of the Cretaceous: Pueblo, Colorado, U.S.A: Episodes 28, 93—104

Kent, H.C., 1968. Biostratigraphy of Niobrara-Equivalent Part of Mancos Shale (Cretaceous) in Northwestern Colorado. AAPG Bulletin 52, 2098—2115

Laferriere, A.P., 1987. Cyclic sedimentation in the Fort Hays Limestone Member, Niobrara Formation (Upper Cretaceous) in northeastern New Mexico and southeastern Colorado. New Mexico Geological Society 38th Field Conference, Northeastern New Mexico, Guidebook, 249—254

Laferriere, A.P., 1992. Regional isotopic variations in the Fort Hays Member of the Niobrara Formation, United States Western Interior: Primary signals and diagenetic overprinting in a Cretaceous pelagic rhythmite. Geological Society of America Bulletin 104, 980—992.

Leckie, R.M., 1985. Foraminifera of the Cenomanian-Turonian boundary interval, Greenhorn Formation, Rock Canyon Anticline, Pueblo, Colorado, in: Pratt, L., Kauffman, E.G., Zelt, F.B. (Eds.), Fine-grained deposits and biofacies of the Cretaceous Western Interior Seaway: evidence of cyclic depositional processes: SEPM Annual Mid-Year Meeting, Field Trip No. 4, 139—149

Leckie, R.M., 1987. Paleoecology of mid-Cretaceous planktonic foraminifera: a comparison of open ocean and epicontinental sea assemblages. Micropaleontology 33 (2), 164—176

Leckie, R.M., Schmidt, M., Finkelstein, D., Yuretich, R., 1991. Paleoceaographic and paleoclimatic interpretations of the Mancos Shale (Upper Cretaceous), Black Mesa Basin, Arizona, in: Nations, D., and Eaton, J. (Eds.), Stratigraphy, Depositional Environments and Sedimentary Tectonics of the Southwestern Margin, Cretaceous Western Interior Seaway. Geological Society of America Special Paper 260, 139—152.

Leckie, R.M., Kirkland, J.I., Elder, W.P., 1997. Stratigraphic framework and correlation of a principal reference section of the Mancos Shale (Upper Cretaceous), Mesa Verde, Colorado. New Mexico Geological Society Guidebook, 48th Field Conference, Mesozoic Geology and Paleontology of the Four Corners Region. 163—216

Leckie, R.M., Yuretich, R.F., West, O.L.O, Finkelstein, D., Schmidt, M., 1998. Paleoceanography of the southwestern Western Interior Sea during the time of the Cenomanian-Turonian boundary (Late Cretaceous), in: Dean,W.E., Arthur, M.A. (Eds..), Stratigraphy and paleoenvironments of the Cretaceous Western Interior Seaway, U.S.A: SEPM Concepts in Sedimentology and Paleontology 6, 101—126

Leckie, R.M., Bralower, T.J., Cashman, R., 2002. Oceanic anoxic events and plankton evolution: biotic response to tectonic forcing during the mid-Cretaceous: Paleoceanography 17, 10.1029/2001PA000623.

Leckie, R.M., Olson, H.C., 2003. Foraminifera as proxies for sea-level change on siliciclastic margins, in: Leckie, R.M., Olson, H.C. (Eds.), Micropaleontologic proxies for sea-level change and stratigraphic discontinuities: SEPM Special Publication No. 75, 5—19

Linnert, C., Mutterlose, J. Erbacher, 2010, Calcareous nannofossils of the Cenomanian/Turonian boundary interval from the Boreal Realm (Wunstorf, northwest Germany): Marine Micropaleontology 74, 38—58

Linnert, C., Mutterlose, J., Herrle, J.O., 2011. Late Cretaceous (Cenomanian-Maastrichtian) calcareous nannofossils from Goban Spur (DSDP Sites 549). Palaeoclimatology, Palaeoecology 299, 507—528

Lock, B. E., Peschier, L., Whitcomb, N., 2010. The Eagle Ford (Boquillas Formation) of Val Verde County, Texas—A window on the South Texas play. Gulf Coast Association of Geological Societies Transactions 60, 419—434

Locklair, R., Sageman, B.B., and Lerman, A., 2011. Marine carbon burial flux and the carbon isotope record of Late Cretaceous (Coniacian–Santonian) Oceanic Anoxic Event III. Sedimentary Geology 235, 38—49.

Lowery, C.M., Corbett, M.J., Leckie, R.M., Watkins, D., Staerker, T.S., Donovan, A.D., Miceli Romero, A., Pramudito, A., 2014. Foraminiferal and nannofossil paleoecology and paleoceanography and the Cenomanian-Turonian Eagle Ford Shale across southern Texas. Palaeogeography, Palaeoclimatology, Palaeoecology 413, 49—65 http://dx.doi.org/10.1016/j.palaeo.2014.07.025

Lundquist, J.J., 2000. Foraminiferal biostratigraphic and paleoceanographic analysis of the Eagle Ford, Austin, and Lower Taylor Groups (middle Cenomanian through lower Campanian) of Central Texas. Ph.D. dissertation, University of Texas at Austin. 545 p.

Martinson, V.S., Heller, P.L., Frerichs, W.E., 1998. Distinguishing middle Late Cretaceous tectonic events from regional sea-level change using foraminiferal data from the U.S. Western Interior. GSA Bulletin 110, 259—268

McNeil, D.H., Caldwell, W.G.E., 1981. Cretaceous rocks and their foraminifera in the Manitoba Escarpment. Geological Association of Canada Special Paper 21, 439 p.

Meyers, S., Sageman, B.B., Hinnov, L., 2001. Integrated quantitative stratigraphy of Cenomanian-Turonian Bridge Creek Limestone Member using evolutive harmonic analysis and stratigraphic modeling. Journal of Sedimentary Research 71, 628—644

Meyers, S.R., and Sageman, B.B., 2004. Detection, quantification, and significance of hiatuses in pelagic and hemipelagic strata. Earth and Planetary Science Letters 224, 55–72

Meyers, S.R., Sageman, B.B., Lyons, T.W., 2005. Organic carbon burial rate and the molybdenum proxy: theoretical framework and application to Cenomanian-Turonian Oceanic Anoxic Event 2, Paleoceanography 20, PA2002, doi:10.1029/2004PA001068

Molenaar, C.M., Cobban, W.A., Mereweather, E.A., Pillmore, C.L., Wolfe, D.G., Holbrook, J.M., 2002. Regional stratigraphic cross sections of Cretaceous rocks from east-central Arizona to the Oklahoma panhandle. USGS Miscellaneous Field Studies Map MF-2382.

Monteiro, F.M., Pancost, R.D., Ridgwell, A., Donnadieu, Y., 2012. Nutrients as the dominant control on the spread of anoxia and euxinia across the Cenomanian-Turonian ocean anoxic event (OAE2): model-data comparison. Paleoceanography 27 PA4209, doi:10.1029/2012PA002351

Murray, J.W., 1976. A method of determining proximity of marginal seas to an ocean. Marine Geology 22, 103—119

Norris, R.D., Wilson, P.A., 1998. Low-latitude sea-surface temperatures for the mid-Cretaceous and the evolution of planktic foraminifera. Geology 26, 823—826

Nielsen, K.S., Schröder-Adams, C.J., Leckie, D.A., Haggart, J.W., Elberdak, K., 2008. Turonian to Santonian paleoenvironmental changes in the Cretaceous Western Interior Sea: The Carlile and Niobrara Formations in southern Alberta and southwestern Saskatchewan, Canada. Palaeoceanography, Palaeoclimatology, Palaeoecology 270, 64—91

Owens, J.D., Lyons, T.W., Li, X., MacLeod, K.G., Gordon, G., Kuypers, M.M.M., Anbar, A., Kuhnt, W., Severmann, S., 2012. Iron isotope and trace metal records of iron cycling in the proto-North Atlantic during the Cenomanian-Turonian oceanic anoxic event (OAE-2). Paleoceanography 27, PA3223, doi:10.1029/2012PA002328.

Paul, C.R.C., Lamolda, M.A., Mitchell, S.F., Vaziri, M.R., Gorostidi, A., Marshall, J.D., 1999. The Cenomanian-Turonian boundary at Eastbourne (Sussex, UK): a proposed European reference section. Palaeogeography, Palaeoclimatology, Palaeoecology, 150, 83—121

Pessagno, E., 1969. GSA Memoir 111, Upper Cretaceous Stratigraphy of the Western Gulf Coast Area of Mexico, Texas, and Arkansas, 139 p.

Petrizzo, M.R., Huber, B.T., Wilson, P.A., MacLeod, K.G., 2008, Late Albian paleoceanography of the western subtropical North Atlantic. Paleoceanography, PA1213, doi:10.1029/2007PA001517

Pratt, L.M., Threlkeld, C.N., 1984. Stratigraphic significance of $^{13}C/^{12}C$ ratios in mid-Cretaceous rocks of the Western Interior, U.S.A., in: Stott, D.F., Glass, D.J. (Eds.), The Mesozoic of Middle North America. Canadian Society of Petroleum Geologists Memoir 9, 305—312

Pratt, L.M., 1985. Isotopic studies of organic matter and carbonate in rocks of the Greenhorn marine cycle, in: L.M. Pratt, E.G. Kauffman, & F.B. Zelt (Eds.), Fine-grained Deposits and Biofacies of the Cretaceous Western Interior Seaway: Evidence of Cyclic Sedimentary Processes. Society of Economic Paleontologists and Mineralogists, Tulsa, 38—59

Pratt, L.M., Arthur, M.A., Dean, W.E., and Scholle, P.A., 1993. Paleo-oceanographic cycles and events during the Late Cretaceous in the Western Interior seaway of North America, in: W.G.E. Caldwell & Kauffman, E.G. (Eds.), Evolution of the Western Interior Basin Geological Association of Canada Special Paper 39, 333—353

Premoli-Silva, I., Erba, E., Tornaghi, M.E., 1989. Paleoenvironmental signals and changes in surface fertility in Mid Cretaceous C_{org}-rich pelagic of the Fucoid Marls (central Italy). Geobios 22, 225—236. doi:10.1016/S0016-6995(89)80059-2

Premoli-Silva, I., Sliter, W.V., 1999. Cretaceous paleoceanography: Evidence from planktonic foraminiferal evolution. In: Barrera, E., Johnson, C. (Eds.) Evolution of the Cretaceous ocean-climate system, Geological Society of America Special Paper 332, 301—328

Rangel, A., Parra, P., Niño, C., 2000. The La Luna formation: chemostratigraphy and organic facies in the Middle Magdalena Basin, Organic Geochemistry 31, 1267—1284

Roth, P.H., 1981. Mid-Cretaceous calcareous nannoplankton from the central Pacific: Implications for paleoceanography. Initial Reports of the Deep Sea Drilling Project 62, 471—489

Roth, P.H., and Bowdler, J., 1981. Middle Cretaceous calcareous nannoplankton biogeography and oceanography of the Atlantic Ocean, in: Warme, J.E., Douglas, R.G., and Winterer, E.L. (Eds.), The Deep Sea Drilling Project: a Decade of Progress. SEPM Special Publication 32, 517—546

Roth, P.H., 1986. Mesozoic paleoceanography of the North Atlantic Tethys oceans,, in: Summerhays, C.P., Shackelton, N.J. (Eds.), Geological Society of America Special Publication 21, 299—320

Roth, P.H., 1989. Ocean circulation and calcareous nannoplankton evolution during the Jurassic and Cretaceous. Palaeogeography, Palaeoclimatology, Palaeoecology 74, 111—126 doi:10.1016/0031-0182(89)90022-9

Roth, P.H., Krumback, K.R., 1986. Middle Cretaceous calcareous nannofossil biogeography and preservation in the Atlantic and Indian Oceans: implications for paleoceanography. Marine Micropaleontology 10, 235—266. doi:10.1016/0377-8398(86)90031-9

Rubey, W.W., 1930. Lithologic studies of the fine grained Upper Cretaceous rocks of the Black Hills region: United States Geological Survey Professional Paper 165-A, 1—54

Ryer, T.A., Lovekin, J.R., 1986. The Upper Cretaceous Vernal Delta of Utah – depositional or paleotectonic feature? in: Paleotectonics and Sedimentation in the Rocky Mountain Region, Untied States, American Association of Petroleum Geologists Memoir 41, 497—510

Sageman, B.B., 1985. High-resolution stratigraphy and paleobiology of the Hartland Shale Member: analysis of an oxygen-deficient epicontinental sea, in: Pratt, L.M., Kauffman, E.G., Zelt , F.B. (Eds.), Fine-grained deposits and biofacies of the Cretaceous Western Interior Seaway: evidence of cyclic sedimentary processes. SEPM Mid-Year Annual Meeting, Field Trip No. 4, 110—121

Sageman, B.B., Arthur, M.A., 1994. Early Turonian paleogeographic/paleobathymetric map, Western Interior, US., in: Caputo, M., Peterson, J. (Eds..), Mesozoic systems of the Rocky Mountain region, U.S. Society of Economic Paleontologists and Mineralogists Special Publication, Rocky Mountain Section, 457—470

Sageman, B.B., Rich, J., Arthur, M.A., Dean, W.E., Savrda, C.E., Bralower, T.J., 1998. Multiple Milankovitch cycles in the Bridge Creek Limestone (Cenomanian-Turonian), Western Interior Basin. Concepts in Sedimentology and Paleontology 6, 153—171

Sageman, B.B., Meyers, S.R., Arthur, M.A., 2006. Orbital time scale and new C-isotope record for Cenomanian-Turonian boundary stratotype. Geology 34, 125—128

Savrda, C.E., Bottjer, D.J., 1993. Trace fossil assemblages in fine-grained strata of the Cretaceous western interior, in: Caldwell, W.G.E., Kauffman, E.G. (Eds.), Evolution of the Western Interior Basin. Geological Association of Canada Special Paper 39, 621—639

Schlanger, S.O., Jenkyns, H.C. 1976. Cretaceous oceanic anoxic events: causes and consequences. Geologie En Mijnbouw 55, 179—184

Schlanger, S.O., Arthur, M.A., Jenkyns, H.C., Scholle, P.A., 1987. The Cenomanian-Turonian Oceanic Anoxic Event I. Stratigraphy and distribution of organic carbon-rich beds and the marine δ C excursion, in: Brooks, J., Fleet , A.J. (Eds.), Marine Petroleum Source Rocks. Geological Society Special Publication 26, 371—399

Scholle P.A., Arthur, M.A., 1980. Carbon isotope fluctuations in Cretaceous pelagic limestones: potential stratigraphic and petroleum exploration tool. AAPG Bulletin 64, 67—87

Schröder-Adams, C.J., Adams, P.J., Haggart, J., Leckie, D.A., Bloch, J., Craig, J. and McIntyre, D.J., 1998. An integrated paleontological approach to reservoir problems: Upper Cretaceous Medicine Hat Formation and First White Speckled Shale in Southern Alberta, Canada. Palaios 13, 361—375.

Schröder-Adams, C.J., Herrle, J.O., Embry, A.F., Haggart, J.W., Galloway, J.M., Pugh, A.T., Harwood, D.M., 2014. Aptian to Santonian foraminiferal biostratigraphy and paleoenvironmental change as revealed at Glacier Ford, Axel Heiberg Island, Canadian Arctic Archipelago. Palaeogeography, Palaeoclimatology, Palaeoecology 413. 81—100

Scott, G.R., Cobban, W.A., 1964. Stratigraphy of the Niobrara Formation at Pueblo, Colorado. U.S. Geological Survey Professional Paper, Report P 0454-L, p. L1-L30.

Scott, G.R., Cobban, W.A., Merewether, E.A., 1986. Stratigraphy of the Upper Cretaceous Niobrara Formation in the Raton Basin, New Mexico. New Mexico Bureau of Mines and Mineral Resources Bulletin 115, 34 p.

Slatt, R.M., O'Brien, N.R., Romero, A.M., Rodriguez, H.H., 2012. Eagle Ford condensed section and its oil and gas storage and flow potential. AAPG Search and Discovery Article 80245

Sloss, L., 1963. Sequences of the cratonic interior of North America. Geological Society of America Bulletin 74, 93—114

Smith, C.C., 1981. Calcareous nannoplankton and stratigraphy of late Turonian, Coniacian, and early Santonian age of the Eagle Ford and Austin groups of Texas. U.S. Geological Society Professional Paper 1075, 96 p.

Snow, L.J., Duncan, R.A., Bralower, T.J., 2005. Trace element abundances in the Rock Canyon Anticline, Pueblo, Colorado, marine sedimentary section and their relationship to Caribbean plateau construction and Oxygen Anoxic Event 2. Paleoceanography 20, PA3005, doi:10.1029/2004PA001093

Sohl, N.F., Martinez, E. R., Salmerón-Ureña, P., Soto-Jaramillo, F. 1991. Upper Cretaceous, in: Salvador, A. (Ed.), The Geology of North America Volume J: Gulf of Mexico Basin. Geological Society of America, Boulder, CO

Stephenson, 1929. Unconformities in the Upper Cretaceous series of Texas: AAPG Bulletin 13, 1323—1334

Sterzinar, E., 2005. Benthic and Planktic Foraminiferal Biostratigraphy and Paleoecology of the Turonian-Campanian Niobrara Cycle of the Mancos Shale, Mesa Verde, Colorado. MS Thesis, University of Massachusetts

Tantawy, A.A., 2008, Calcareous nannofossil biostratigraphy and paleoecology of the Cenomanian-Turonian transition in the central desert of Egypt. Marine Microplaeontology 47, 323—356

Thierstein, H.R., 1981. Late Cretaceous nannoplankton and the change at the Cretaceous-Tertiary boundary, in: Douglas R.C., Winterer, E.L., (Eds.) The Deep Sea Drilling Project: A Decade of Progress. SEPM Special Publication 32, 355—394

Tibert, N.E., Leckie, R.M., Eaton, J.G., Kirkland, J.I., Colin, J.P., Leithold, E.L., and McCormic, M., 2003. Recognition of relative sea level change in Upper Cretaceous coal-bearing strata: A paleoecological approach using agglutined foraminifera and ostracodes to detect key stratigraphic surfaces, in: Olson, H., & Leckie, R.M. (Eds.), Microfossils as a proxy for sea level changes and stratigraphic discontinuities. Society for Sedimentary Geology (SEPM) Special Publication, 263—299

Tribovillard, N., Algeo, T.J., Lyons, T., Riboulleau, A., 2006. Trace metals as paleoredox and paleoproductivity proxies: An update. Chemical Geology 232, 12—32

Tsikos, H., Jenkyns, H., Walsworth-Bell, B., Petrizzo, M.R., Forster, A., Kolonic, S., Erba, E., Premoli Silva, I., Baas, M., Wagner, T., Sinninghe Damsté, J.S., 2004. Carbon-isotope stratigraphy recorded by the Cenomanian-Turonian oceanic anoxic event: correlation and implications based on three key localities. Journal of the Geological Society of London 161, 711—720

Udden, J.A., 1907. A sketch of the geology of the Chisos country, Brewster County, Texas. University of Texas Bulletin 93, Austin, 29—33

Van Bentum, E.C., Reichart, G.-J., Forster, A., Sinninghe Damasté, J.S., 2012. Latitudinal differences in the amplitude of the OAE-2 carbon isotopic excursion: pCO_2 and paleoproductivity. Biogeosciences 9, 717—731

Van der Zwaan, G.J., Jorissen, F.J., Stitger, H.C., 1990. The depth dependency of planktonic/benthic foraminiferal ratios: constraints and applications. Marine Geology 95, 1—16

Van Helmond, N.A.G.M., Sluijs, A., Sinnighe Damasté, J.S., Reichart, G.-J., Voight, S., Erbacher, J., Pross, J., Brinkhuis, H., 2015. Freshwater discharge controlled deposition of Cenomanian-Turonian black shales on the NW European epicontinental shelf (Wunstorf, northern Germany). Climate of the Past 11, 495—508

Van Hinsbergen, D.J.J., Kouwenhoven, T.J., Van der Zwaan, G.J., 2005. Paleobathymetry in the backstripping procedure: correction of oxygenation effects on depth estimates. Palaeogeography, Palaeoclimatology, Palaeoceology 21, 245—265

Voigt, S., 2000. Cenomanian-Turonian composite $\delta^{13}C$ for Western and Central Europe: the role of organic and inorganic carbon fluxes. Palaeogeography, Palaeoclimatology, Palaeoecology 160, 91—104

Wagreich, M., 2009. Coniacian-Santonian oceanic red beds and their link to Oceanic Anoxic Event 3, in: Hu, X., Wang, C., Scott, R., Wagreich, M., Jansa, L., (Eds.), Cretaceous Oceanic Red Beds: Stratigraphy, Composition, Origins, and Paleoceanographic and Paleoclimatic Significance. SEPM Special Publication 91, 235—242

Wagriech, M., 2012. "OAE3" – regional Atlantic organic carbon burial during the Coniacian-Santonian. Climate of the Past 8, 1447—1455.

Wang, C.S., Hu, X., Huang, Y., Wagreich, M., Scott, R., Hay, W., 2011. Cretaceous oceanic red beds as possible consequences of oceanic anoxic events. Sedimentary Geology 235, 27—37

Watkins, D.K., 1985. Biostratigraphy and paleoecology of calcareous nannofossils in the Greenhorn marine cycle in: Pratt, L.M., Kauffman, E.G., Zelt , F.B. (Eds.), Fine-grained deposits and biofacies of the Cretaceous Western Interior Seaway: evidence of cyclic sedimentary processes. SEPM Mid-Year Annual Meeting, Field Trip No. 4 151—156

Watkins, D.K., 1986. Calcareous nannofossil paleoceanography of the Cretaceous Greenhorn Sea. Geological Society of America Bulletin 97, 1239—1249

Watkins, D.K., Bergen, J.A., 2003. Late Albian adaptive radiation in the calcareous nannofossil genus *Eiffellithus*. Micropaleontology 49, 231—252

Watkins, D.K., Cooper, M.J., Wilson, P.A., 2005. Calcareous nannoplankton response to late Albian oceanic anoxic event in the western North Atlantic. Paleoceanography 20, PA2010, doi:10.1029/2004PA001097

Weimer, R.J., 1978. Influence of Transcontinental Arch on Cretaceous marine sedimentation: a preliminary report, in: Pruitt, J.D., Coffin, P.E. (Eds.) Energy Resources of the Denver Basin. Rocky Mountain Association of Geologists 1978 Symposium, 124—130

West, O.L.O., Leckie, R.M., Schmidt, M., 1998. Paleoceanography of the southwestern Western Interior Sea during the time of the Cenomanian-Turonian boundary (Late Cretaceous), in: Dean, W., and Arthur, M.A. (Eds.), Stratigraphy and Paleoenvironments of the Western Interior Seaway, USA, SEPM Concepts in Sedimentology and Paleontology 6, 79—99

White, T., Furlong, K., Arthur, M., 2002. Forebulge migration in the Cretaceous Western Interior basin of the central United States. Basin Research 14, 43—54

Williams, J.R., Bralower, T.J., 1995. Nannofossil assemblages, fine fraction stable isotopes, and the paleoceanography of the Valanginian-Barremian (Early Cretaceous) North Sea Basin. Paleoceanography 10, 815—839